The kinesin-3 family motor KLP-4 regulates anterograde trafficking of GLR-1 glutamate receptors in the ventral nerve cord of *C. elegans*

A dissertation

submitted by

Michael Inacio Monteiro

In partial fulfillment of the requirements for the degree of

Doctor of Philosophy

in

Cellular and Molecular Physiology

TUFTS UNIVERSITY

Sackler School of Graduate Biomedical Sciences

February, 2013

Advisor: Peter Juo, Ph.D.

Abstract

Glutamate is the major excitatory neurotransmitter in the mammalian brain. Changes in the strength of glutamatergic synapses are thought to underlie learning and memory and to contribute to the pathology of numerous neurological diseases. The transport of glutamate receptors from the cell body to synapses contributes to the regulation of synaptic strength. We previously showed that cyclin-dependent kinase-5 (CDK-5) positively regulates the abundance of fluorescently-tagged GLR-1 glutamate receptors at synapses in the ventral nerve cord (VNC) of *C. elegans*. In this thesis I investigate the roles of novel regulators of GLR-1 abundance in the VNC. In Chapter 2, I generate genetic mutants that suppress the effects of *cdk*-5 overexpression on GLR-1 abundance at synapses to identify genes that regulate GLR-1 abundance in the VNC and that may function in the same cellular pathway as CDK-5. I identify a mutation in *klp-4/*KIF13, which encodes a kinesin-3 family motor as a strong suppressor of increased GLR-1 abundance in animals that overexpress *cdk-5*. In Chapter 3, I characterize the novel kinesin motor KLP-4 and its role in GLR-1 trafficking. I find that *klp-4* mutants have decreased abundance of GLR-1 at synapses in the VNC. Time-lapse microscopy indicates that *klp-4* and *cdk-5* mutants exhibit decreased anterograde trafficking of GLR-1. I conduct genetic analyses on *klp-4* mutants with loss and gain of function of *cdk-5* and find that KLP-4 and CDK-5 function in the same pathway to regulate GLR-1 in the VNC. Interestingly, I find that loss of function of KLP-4 affects GLR-1 levels in the cell body differently than loss of function of CDK-5. GLR-1 abundance increases in cell bodies of *cdk-5* mutants but is unchanged in *klp-4* mutants. However, GLR-1 does accumulate in *klp-4* mutant cell bodies if receptor degradation in the MVB/lysosome pathway is blocked, suggesting that in the absence of its KLP-4 motor, GLR-1 is degraded. Finally, in Chapter 4, I investigate potential mechanisms for control of KLP-4 activity and identify a microRNA family, *mir-75/mir-79* and the kinesin-1 motor, *unc-116/*Kif5 as novel regulators of GLR-1 abundance in the VNC.

Acknowledgements

I would like to thank first of all my mentor, Peter Juo, for always making the training and advancement of the people in his lab his first priority. I'm very fortunate to have spent my time in graduate school training with someone so dedicated to the pursuit of excellence, and yet so patient and good-natured during the times when my own pursuit fell short. I would also like to thank the members of the Juo lab, past and present: Jennifer Kowalksi, Emily Malkin, Patricia Goodwin, Steven Garafalo, Caroline Dahlberg, Annette McGehee and Benjamin Moss. Thank you for all of the help that you've given me and for making every day in the lab fun and comfortable. Also, thank you for bringing delicious homemade snacks to lab meetings and teas. I'm sorry I was only ever good for bagels and plastic forks.

Thank you to my thesis committee, Dan Jay, Laura Liscum, and Brent Cochran for your guidance with my project and my passage through the program and to Josh Kaplan for your time and effort. Thank you to the rest of the Physiology faculty, students and staff for making the Physiology department a friendly and enjoyable place to spend time.

I would like to thank my parents, Rita and Alex, for a lifetime of love and support, Tereza, Joe, and Theresa for never sounding surprised when I still had one more year of school left and Luke, Charlie, Amelia and Rae, for occasionally thinking it was interesting that I work with worms.

Finally, I'd like to thank Leah, Caroline and Declan. Leah, without your daily support and understanding I could not have done this. Caroline and Declan, thank you for serving as a source of happiness, every day, no matter what. It's my hope that one day, in the not too distant future, you'll flip through this thesis, and be smart enough to see all the things I should have done differently, but you'll be kind enough to not make a whole big thing out of it.

Table of contents

List of Tables and Figures

Tables

Chapter 2

Figures

Chapter 1

Chapter 2

Chapter 3

Appendix

The kinesin-3 family motor KLP-4 regulates anterograde trafficking of GLR-1 glutamate receptors in the ventral nerve cord of C. elegans

Chapter 1

Introduction

Glutamate Signaling

Importance of glutamate signaling to health and function of the brain

The neuron is the functional unit of the nervous system and efficient communication between neurons is essential for proper brain function. For many neurons communication occurs at chemical synapses, a process that requires neurotransmitters to be released by the presynaptic axon and received by the postsynaptic dendrite. The majority of excitatory activity in the mammalian brain is mediated by the neurotransmitter glutamate. It is not surprising then, that precise regulation of glutamate signaling is required for proper brain function. In fact, it is believed that changes in the strength of glutamate signaling are the cellular bases of memory formation and storage (Bredt and Nicoll, 2003; Collingridge et al., 2004; Martin et al., 2000; Shepherd and Huganir, 2007).

The first experiments to reveal a link between glutamate signaling and the process of learning and memory were performed on cultured neurons from the hippocampus, a center of learning and memory storage in the brain. Application of glutamate to these neurons led to lasting changes in their subsequent postsynaptic responses to stimuli (Collingridge et al., 2004; Bredt and Nicoll, 2003; Bliss and Lomo, 1970; Bliss and Lomo, 1973; Dunwiddie and Lynch, 1978). The ability of a synapse to exhibit long-lasting, activity-dependent changes in the magnitude of a post synaptic response is referred to as synaptic plasticity. Two examples of plasticity, long-term potentiation (LTP) and long-term depression (LTD), describe sustained increases and decreases, respectively, in the magnitude of postsynaptic responses.

Not surprisingly given the central role of glutamate signaling in learning and memory, aberrant glutamate signaling is implicated in several neurological diseases in which cognition is affected, such as Alzheimer's disease and Fragile X Mental Retardation. Decreased glutamate signaling may play an important role in the pathology of each of these

two disorders (Bowie, 2008; Shepherd and Huganir, 2007). In addition to learning and memory, the regulation of glutamate signaling is important for neuronal viability. One immediate effect of glutamate signaling is increased intracellular calcium levels. While some amount of variation in intracellular calcium levels is an important component of normal signaling pathways, excess intracellular calcium can result in cytotoxicity (Kwak and Weiss, 2006). Excess glutamate signaling is thought to contribute to the excitotoxicity and cell death that occur in the brain of stroke victims and in motor neurons of patients with amyotrophic lateral sclerosis (Bowie, 2008; Kwak and Weiss, 2006; Van Den Bosch et al., 2006). The central role of glutamate signaling in the health and function has been the motivation behind much work aimed at understanding the mechanisms by which glutamate signaling can be regulated.

Synaptic cycling of glutamate receptors regulates synaptic transmission

Ionotropic glutamate receptors (GluRs) are heteromeric protein complexes that function as glutamate-activated ion channels. A functional channel consists of four like subunits assembled into a single channel complex. The opening of such a channel allows for ion flow that changes the local intracellular electrochemical milieu. GluRs can be divided into two major types based on their responses to pharmacological agents, N-Methyl-D-aspartate receptors (NMDARs) and non-NMDA receptors, which include kainate receptors and α-amino-3-hydroxy-5-methyl-4-isoxazolepropionic acid receptors (AMPARs). AMPARs mediate fast, transient excitatory activity when stimulated by glutamate. In contrast, stimulation of NMDARs, which requires membrane depolarization in addition to glutamate, causes smaller, longer lasting postsynaptic responses (Scannevin and Huganir, 2000).

One source of the variation in strength of a given glutamatergic synapse is the number of AMPARs that are present in the postsynaptic membrane at any one time. This

was first demonstrated in cultured hippocampal neurons that were stimulated with exogenous glutamate. Using electrophysiology and immunohistochemistry, it was shown that glutamate treatment paradigms that had previously been shown to induce increased synaptic strength, or LTP, also increased the number of AMPARs at synapses. Similarly, decreased synaptic strength, or LTD was correlated with decreased synaptic AMPAR levels (Bredt and Nicoll, 2003; Carroll et al., 1999; Collingridge et al., 2004; Durand et al., 1996; Isaac et al., 1995; Liao et al., 1995; Shepherd and Huganir, 2007; Shi et al., 1999). It has since been demonstrated that changes in receptor conductance also contribute to synaptic plasticity (Barria et al., 1997; Benke et al., 1998; Derkach et al., 2007). The discovery that the number of AMPARs at the synapse can change in response to neuronal activity, and that altered levels of synaptic AMPARs can cause long-lasting changes in synaptic strength, has lead to a great deal of research into how the number of synaptic AMPARs is regulated.

The immediate source of AMPARs that are readily inserted into the postsynaptic membrane upon neuronal activity is the recycling endosome located just below the synaptic membrane (Park et al., 2004; Park et al., 2006). Generally, trafficking of AMPARs begins in the cell body where they are translated, assembled and packaged into vesicles. While much remains to be learned about the early trafficking of GluRs, it is clear that events within the cell body contribute to regulating the number of receptors present at the synapse and in the synaptic membrane.

Events in the cell body regulate synaptic GluR levels

All GluRs consist of multiple subunits that are assembled in the endoplasmic reticulum (ER). The ER serves as a point of quality control in the biosynthetic pathway for many proteins, including GluRs (Shim et al., 2004; Vandenberghe et al., 2005). Exit of newly synthesized glutamate receptors from the ER is a tightly controlled process, which

regulates the number of synaptic GluRs.

ER retention signals

One major factor that controls exit of glutamate receptors from the ER is the presence of ER retention signals on receptor subunits. In the absence of these retention signals, receptors are released more readily from the ER and the number of receptors at the cell membrane increases (Xia et al., 2001) (Figure 1-1). Proper assembly of the receptor complex masks these retention sites from the ER machinery allowing ER exit of assembled receptor complexes. Improper assembly of receptor complexes can expose ER retention signals to the ER machinery, resulting in ER retention. This process prevents potentially nonfunctional receptors from reaching the synapse. The Ehlers laboratory has shown that the coordinated actions of protein kinase C and protein kinase A regulate the masking of ER rention signals on NMDAR subunits (Scott et al., 2001; Scott et al., 2003). Interestingly they have also shown that an activity-induced splicing event regulates trafficking out of the ER for these receptors (Mu et al., 2003). The proportion of a splice isoform that exits the ER quickly is increased when neuronal activity is blocked, whereas a splice variant that exits the ER more slowly is predominant under conditions of high neuronal activity (Mu et al., 2003). This work established a mechanism for neuronal activity controlling the early biosynthetic trafficking of NMDARs.

Functionally relevant sequence variations affect receptor exit from the ER

Sequence variations that change receptor function can also affect the level of receptors at the synapse by regulating the early biosynthetic trafficking pathway. Variations in RNA editing or splicing and function-blocking point mutations can affect how readily GluRs are released from the ER. In mammalian neuronal cultures, certain splice isoforms of

GluR subunits differ in their ability to bind ligand or in their potential gating properties. Different splice variants have dramatically different ER exit capabilities (Coleman et al., 2006; Coleman et al., 2010) (Figure 1-1). The AMPA receptor subunit GluA2 contains RNA editing sites (Glu/Arg 607 and Val/Leu 758) that affect the gating properties of the receptor channel (Greger et al., 2002; Penn et al., 2008). These residues, which have significant functional importance for the receptor at the synapse also control exit from the ER (Greger et al., 2002). Receptor subunits containing single residue changes of L758V or R607Q undergo a more rapid transport from the ER to the cell surface in cultured hippocampal neurons.

Genetic mutations in the ligand binding-domains of kainate-type GluRs, which render the channel non-functional but do not inhibit complex formation, cause retention of the receptors in the ER (Fleck et al., 2003; Gill et al., 2009; Mah et al., 2005) (Figure 1-1). Similarly, point mutations in the channel pore region or in the ligand-binding domain of the *C. elegans* glutamate receptor, GLR-1, result in retention of the receptor in the ER and decreased abundance of receptor at the synapse (Grunwald and Kaplan, 2003).

Synaptic levels of GluRs in *C. elegans* can also be regulated pre-translationally. The splicing factor GRLD-1 promotes a *glr-1* splicing event that results in increased overall GLR-1 levels and increased GLR-1 at synapses in some *glr-1* expressing neurons (Wang et al., 2010). Therefore, in neurons *in vitro* and *in vivo*, RNA editing, splicing and genetic mutations that alter receptor function can interfere with early steps of the GluR biosynthetic pathway. The fact that these events affect synaptic GluR levels, demonstrates that early biosynthetic trafficking of GluRs can be as important as the local synaptic trafficking events are for adjusting synaptic strength.

Figure 1-1. Ionotropic glutamate receptor subunit membrane topology

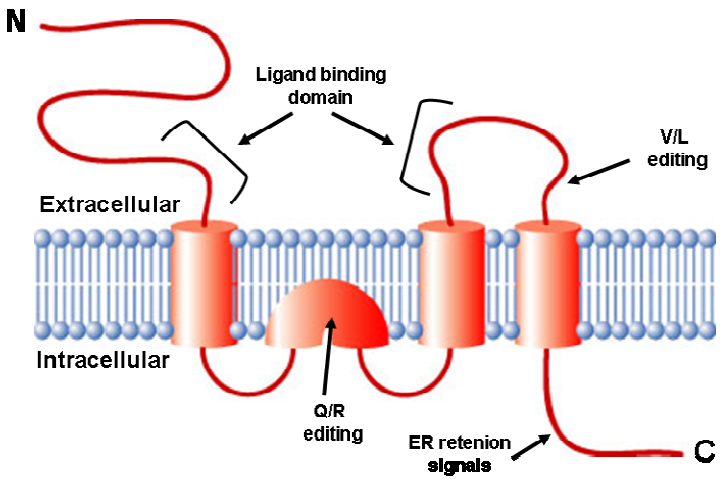

The *C. elegans* glutamate receptor *glr-1*

Despite significant progress made in understanding how GluR abundance at the synapse is regulated, the process is still largely unknown. We have only scratched the surface of identifying which genes are involved in this process. For this reason, unbiased gene discovery efforts are critical to the identification of novel regulators of synaptic GluR abundance. Ideally such work will be done *in vivo* because complete simulation of a brain or nervous system *in vitro* is impossible. Forward genetic screening in mammalian models is not practical because of the long time between generations and the cost of maintaining large numbers of animals. Simpler model organisms with shorter life cycles that are easier to maintain, like *C. elegans,* allow for screening the large numbers of animals over several generations that unbiased gene discovery efforts require. As such, *C. elegans* is an ideal system for identifying novel regulators of synaptic GluR abundance.

The *C. elegans* genome is predicted to contain 10 glutamate receptors, 2 NMDA-type and 8 non-NMDA-type (Brockie et al., 2001). The most well studied of these is *glr-1*, a non-NMDA receptor that is most similar to mammalian AMPA receptors (Hart et al., 1995; Maricq et al., 1995). *glr-1* is expressed in a subset of interneurons, including the 5 pairs of

command interneurons that control the locomotion pattern of the animal (Brockie et al., 2001; Hart et al., 1995; Maricq et al., 1995; Rongo et al., 1998). Animals with loss of function mutations in *glr-1* display defects in their response to light touch on the nose, in locomotion patterns and in learning and long-term memory (Hart et al., 1995; Maricq et al., 1995; Mellem et al., 2002; Morrison and van der Kooy, 2001; Rose et al., 2003; Zheng et al., 1999).

Cell bodies of the interneurons that express *glr-1* are located in either the head or tail of the animal. These neurons have a single axo-dendritic neuronal process that extends from the cell body into a structure called the ventral nerve cord (VNC) (White et al., 1976). The VNC is a bundle of neuronal processes that runs along the length of the ventral side of the animal. Synaptic connections between sensory neurons, interneurons and motor neurons are present along the length of the VNC (Rongo et al., 1998; White et al., 1976).

GLR-1 can be studied *in vivo* using a fusion protein that consists of a GFP molecule inserted into the C-terminal cytoplasmic tail of GLR-1 (Rongo et al., 1998). Expression of this GLR-1::GFP fusion protein under the control of the *glr-1* promoter results in fluorescent puncta along the length of the VNC (Rongo et al., 1998). The majority of these GLR-1::GFP puncta are immediately adjacent to fluorescently tagged presynaptic proteins, suggesting that GLR-1::GFP is postsynaptically localized (Burbea et al., 2002; Rongo et al., 1998). Additionally, GLR-1::GFP is a functional receptor because its expression rescues behavioral defects that are present in *glr-1* null animals (Rongo et al., 1998). Thus, GLR-1::GFP allows for direct visualization of a synaptically localized, functional glutamate receptor in a living animal. This valuable tool has allowed for the direct *in vivo* examination of synaptic localization and abundance of GLR-1 in animals of various genetic backgrounds, leading to the discovery of many genes that regulate the levels of glutamate receptors in the VNC of *C. elegans.*

GLR-1 regulation by ubiquitination, endocytosis and degradation

Several genes that regulate GLR-1 levels in the VNC are involved in endocytosis, ubiquitination and degradation of the receptor at the synapse. Collectively these processes are crucial for regulating synaptic levels of GluRs and synaptic function in *C. elegans* and mammals (Burbea et al., 2002; Dreier et al., 2005; Juo and Kaplan, 2004; Kowalski et al., 2011; Mabb and Ehlers, 2010; Park et al., 2009; Schaefer and Rongo, 2006). The first evidence that GluRs could be directly ubiquitinated to regulate synaptic receptor levels and synaptic activity was demonstrated with GLR-1 (Burbea et al., 2002). Interestingly, the ubiquitination motif identified in GLR-1 is conserved in the mammalian AMPAR, GluA2, and deletion of this sequence in GluA2 results in increased synaptic levels of the receptor (Lin et al., 2000). This suggested that the direct ubiquitination of GluRs as a mechanism for regulation of their synaptic levels could be conserved in mammals. Indeed, more recently it has been shown that mammalian AMPARs are ubiquitinated (Lin et al., 2011; Lussier et al., 2011; Schwarz et al., 2010).

Several ubiquitin ligases are known to play a role in regulating GLR-1 abundance. Mutations in subunits of the anaphase promoting complex (APC) caused increased abundance of GLR-1::GFP in the VNC of *C. elegans*. These mutant animals exhibited increased GLR-1 mediated behavior, suggesting that loss of function of APC results in increased synaptic GLR-1 levels. Genetic and biochemical evidence suggest that APC does not directly ubiquitinate GLR-1 and the relevant target protein for the APC ligase remains unknown (Juo and Kaplan, 2004).

The SCF (Skip1/Cullin/F-box$^{\beta TrCP}$) E3 ligase, *lin-23* also regulates GLR-1 levels in the VNC (Dreier et al., 2005). Animals with mutations in the F-box containing subunit of this E3 ligase, *lin-23,* display increased GLR-1 abundance in the VNC. One relevant target of LIN-23 is the WNT-signaling β-catenin protein BAR-1 (Dreier et al., 2005). Other components of

the WNT signaling pathway are involved in GLR-1 regulation in a manner that is consistent with the BAR-1 signaling pathway positively regulating GLR-1 abundance in the VNC. However genetic experiments suggest that the effects of the SCF ligase on WNT signaling can only partially account for the effects on GLR-1 levels in the VNC (Dreier et al., 2005). Biochemical and genetic experiments rule out the possibility that the SCF ligase might directly ubiquitinate GLR-1. Thus the other target or targets of this ligase that affect GLR-1 abundance remain undiscovered.

The E3 ligase CUL3 functions with the Kelch protein Kel-8 to regulate levels of GLR-1 in the VNC (Schaefer and Rongo, 2006). Animals with mutations in this complex have increased GLR-1 levels in the VNC and a corresponding increase in GLR-1-mediated behaviors. While it remains a possibility that the CUL3 ligase directly ubiquitinates GLR-1, this remains to be demonstrated through either biochemical or genetic methods (Schaefer and Rongo, 2006).

The PHR protein, RPM-1, an E3 ubiquitin ligase best known for its role in presynaptic organization (Collins et al., 2006; Nakata et al., 2005; Wan et al., 2000; Zhen et al., 2000), also affects synaptic GLR-1 levels. The MAPK/p38 signaling cascade promotes endocytosis of GLR-1 and RPM-1 negatively regulates this process, thereby having the effect of reducing endocytosis and stabilizing GLR-1 at synapses (Park et al., 2009). Despite the identification of several E3 ubiquitin ligases that affect GLR-1 levels, the ligase that directly ubiquitinates GLR-1 has not been discovered. This will be an important step toward understanding the regulation of the receptor. Indeed, the ubiquitin ligase Nedd4 has recently been identified as the ligase that targets mammalian AMPARs for ubiquitination (Schwarz et al., 2010). Interestingly, the *C. elegans* genome encodes for a homolog of Nedd4, suggesting that this could be a possible candidate for a ligase that ubiquitinates GLR-1.

Ubiquitination is dynamic and proteins that are ubiquitinated can be deubiquitinated by enzymes called deubiquitinases or DUBs. Recently, a novel DUB called USP-46 that acts directly on GLR-1 to remove ubiquitin moieties was identified (Kowalski et al., 2011). Animals with loss of function mutations in *usp-46* exhibit reduced GLR-1 levels in the VNC and a corresponding decrease in GLR-1-dependent behaviors. In the VNC of animals with loss of function mutations in *usp-46,* GLR-1 levels are reduced, as are GLR-1 dependent behaviors. Biochemical evidence demonstrates that USP-46 acts directly on GLR-1. Thus, deubiquitination of endocytosed GLR-1 by USP-46 is an important regulator of the fate of synaptic GLR-1 and may determine whether the receptor is targeted to the lysosome for degradation or for reinsertion into the plasma membrane (Kowalski et al., 2011).

While the ubiquitination of GLR-1 affects its protein levels posttranslationally, pretranslational regulation is another way in which GLR-1 in the VNC can be regulated. The RNA-binding protein GRLD-1 regulates GLR-1 levels throughout the cell. Animals with loss of function mutations in *grld-1* have decreased GLR-1-dependent mechanosensation behaviors as well as decreased GLR-1-mediated electrophysiological responses (Wang et al., 2010). Interestingly, GRLD-1 seems to have cell-specific effects on GLR-1 levels as its effects are not observed in all GLR-1 expressing cells (Wang et al., 2010).

Interestingly, synaptic activity can also affect GLR-1 levels in the VNC (Grunwald et al., 2004). In animals with a loss of function mutation in the presynaptic vesicular glutamate pump *eat-4*/VGlut, which causes chronically decreased presynaptic glutamate release, there is an increase in postsynaptic GLR-1 abundance in the VNC as measured by GLR-1::GFP levels and a corresponding increase in the magnitude of postsynaptic glutamate-evoked currents (Grunwald et al., 2004). This response appears to result from altered trafficking and localization of GLR-1 as the total level of GLR-1 is unchanged in these animals, although it is not clear whether the trafficking changes occur locally at the synapse or if

anterograde trafficking may also contribute to increased GLR-1 abundance (Grunwald et al., 2004). The increase in postsynaptic GluR abundance and activity is a form of synaptic plasticity called homeostatic synaptic scaling in which chronic changes in presynaptic activity trigger a compensatory postsynaptic change (Turrigiano, 2008).

Regulation of GLR-1 function

In addition to genes that regulate total GLR-1 levels, several auxiliary proteins that are required for proper GLR-1 function, but not for its overall expression level or localization to the VNC, have been identified (Walker et al., 2006; Zheng et al., 2004; Zheng et al., 2006). The type 1 transmembrane protein SOL-1 was identified in a screen for animals with decreased GLR-1 dependent locomotion behavior ((Walker et al., 2006; Zheng et al., 2004; Zheng et al., 2006). SOL-1 forms a complex with GLR-1 *in vitro* and regulates the gating properties of the channel by modulating its desensitization to glutamate (Zheng et al., 2006; Walker et al., 2006). The stargazin-like proteins STG-1 and STG-2 have also been shown to regulate GLR-1 receptor desensitization, as shown for members of the stargazin family in mammalian neurons. However, unlike their mammalian homolog, which regulates AMPAR trafficking and desensitization, STG-1 and STG-2 only regulate desensitization and deactivation (Chen et al., 2000; Vandenberghe et al., 2005; Wang et al., 2008).

GLR-1 anterograde trafficking

In addition to genes that regulate GLR-1 protein level, channel function and synaptic cycling, some components of the anterograde trafficking pathway of GLR-1 from the cell body to the VNC have been identified. Defects in anterograde trafficking are seen in animals with a loss of function mutation in *unc-43*, the calcium/calmodulin- dependent protein kinase 2 (CaMKII) (Rongo and Kaplan, 1999). In these animals, the amount of GLR-

1 in the VNC is reduced. There is a concomitant increase of GLR-1 levels in neuronal cell bodies of these animals, suggesting that loss of function of CaMKII results in a defect in the trafficking of GLR-1 from the cell body into the VNC (Rongo and Kaplan, 1999) . Similar GLR-1 trafficking defects are observed in animals with loss of function mutations in subunits of voltage gated calcium channels implicating calcium and possibly neuronal activity in this regulatory step (Rongo and Kaplan, 1999).

As mentioned above, components of the quality control process in the ER are required for the anterograde trafficking of GLR-1 (Grunwald and Kaplan, 2003). This quality control ensures proper folding and subunit assembly of multimeric complexes. ER quality control also monitors potential changes in receptor function as point mutations that change channel conductance or ligand-binding result in retention of the receptor in the ER and decreased GLR-1 abundance at synapses in the VNC (Grunwald and Kaplan, 2003).

Possible candidates for resident ER proteins that contribute to the quality control process required for GLR-1 anterograde trafficking are the unfolded protein response genes *ire-1* and *xbp-1* (Shim et al., 2004). Animals with loss of function in either of these two genes show decreased GLR-1 in the VNC and a correlated decrease in GLR-1-mediated behavior. Additionally, in these mutants GLR-1 co-localizes to a greater extent with ER markers in the cell body than in WT animals, suggesting that GLR-1 is retained in the ER. GLR-1 trafficking appears normal in animals with loss of function in other ER stress response genes, suggesting that the defects observed in *ire-1* and *xbp-1* mutants are not secondary to a general ER stress response (Shim et al., 2004).

Although several components of the GLR-1 anterograde trafficking pathway have been described, the molecular motor(s) involved in the trafficking of GLR-1 have not been identified. Multiple microtubule motors are involved in transporting GluRs in mammals (Kapitein et al., 2010; Kim and Lisman, 2001; Setou et al., 2000; Setou et al., 2002; Shin et

al., 2003; Wyszynski et al., 2002) and it is well established that these motors are important for regulating GluR function and synaptic activity (Guillaud et al., 2003; Kim et al., 2003; Kondo et al., 2012; Wong et al., 2002; Yin et al., 2011). Therefore, identification of the motors involved in GLR-1 transport would represent a significant step in understanding the mechanisms involved in regulating GLR-1 trafficking and function.

Microtubule-based molecular motor proteins

Synaptic cycling of receptors and early trafficking steps in the biosynthetic pathway are clearly very important and well-studied phenomena that contribute to regulating receptor abundance at the synapse and synaptic strength. Less well understood is the trafficking of receptors from the cell body to synapse. Work from the Hirokawa lab and others has identified some of the neuronal trafficking machinery necessary for various synaptic proteins. Chief among these are the microtubule-based motors cytoplasmic dynein and the kinesin superfamily (Hirokawa et al., 2010; Kardon and Vale, 2009). Recent studies of these molecular motors have shown that they play a crucial role in regulating the abundance of pre- and postsynaptic machinery at the synapse and the communication between neurons. Further research on the role of these motors in this process will lead to a greater understanding of the basic function of neurons and the brain.

Microtubule-based motors perform an essential function in neurons

The precise execution of cellular processes requires tight regulation of protein activity. Changes in protein expression and posttranslational modifications are two important ways in which this can be achieved. In large compartmentalized cells such as neurons, proteins must be specifically sorted to functionally and spatially distinct regions within the cell. In these cells spatial regulation of proteins is an equally important method of

regulation. Therefore in neurons, the machinery involved in protein transport plays an important role in regulating cellular function.

One main mechanism by which proteins and vesicular cargo are moved long distances to their proper locations in cells is active transport by molecular motors such as kinesins and cytoplasmic dynein (Hirokawa et al., 2010; Kardon and Vale, 2009). These are intracellular ATP-dependent motors that carry vesicular or soluble cargo along microtubules. All kinesins contain a motor domain, which consists of about 350 amino acids, usually positioned at the N-terminal end of the protein. These motor domains share about 40 % identity and contain binding sites for ATP and microtubules (see Figure 3-1A). The kinesin superfamily consists of 14 sub-families, most of which contain members that move towards the fast-growing plus-ends of microtubules. The majority of movement towards the minus-ends of microtubules is performed by the ATP-dependent motor dynein, although a small number of kinesins also move towards microtubule minus ends. Together, kinesins and cytoplasmic dynein account for long distance microtubule-dependent trafficking of all intracellular cargo (Hirokawa et al., 2009; Vale, 2003).

Neurons contain both axons and dendrites, which are spatially and functionally distinct and which extend processes out long distances from the cell body. These characteristics confer a unique importance on the ability of kinesins to transport cargo in a directed and processive fashion to neurons. There are forty-five kinesins in the mammalian genome and the vast majority are expressed in the brain (Hirokawa and Takemura, 2004; Hirokawa et al., 2010). Accordingly, the effects of genetically knocking out kinesins tend to be particularly dramatic in the brain (Hirokawa et al., 2010). In humans, several neurological diseases including the neurodegenerative diseases Charcot–Marie–Tooth disease type 2A, Alzheimer's Disease and Huntington's Disease are associated with defects in intracellular transport and mutations in either kinesins or genes that affect kinesin function (Chevalier-

Larsen and Holzbaur, 2006; Duncan and Goldstein, 2006; Hafezparast et al., 2003; Hirokawa and Takemura, 2004; Kanaan et al., 2011; Mandal et al., 2011; Salinas et al., 2008; Tien et al., 2011; Twelvetrees et al., 2010). Therefore, identifying the components and mechanisms involved in intracellular transport is a crucial part of understanding the health and function of the neuron. In particular, determining which kinesins traffic specific cargoes will be essential for understanding the basic cellular processes of the neuron.

Multiple motors traffic GluRs

Glutamate signaling requires the precise regulation and proper function of kinesins. The importance of microtubule motors to the regulation of synaptic GluR levels was first demonstrated with the application of function-blocking antibodies to either kinesin heavy chain (KHC) or dynein in hippocampal slice cultures (Kim and Lisman, 2001). Inhibition of either one of these motors decreased AMPAR-mediated currents. This implicated both the plus-end directed kinesin and the minus-end directed dynein in contributing to AMPAR-dependent synaptic activity (Kim and Lisman, 2001). One mechanism for the seemingly paradoxical effect of two directionally opposed microtubule motors contributing similarly to AMPAR-mediated activity is based on the microtubule orientation in hippocampal neurons (Kapitein et al., 2010). The orientation of microtubules in the proximal dendrite of these neurons is mixed, (i.e. both plus-end out and minus-end out are present). This is in contrast to the uniform microtubule orientation of axons, in which all plus ends are directed out (Baas et al., 1988; Conde and Caceres, 2009; Stepanova et al., 2003). The mixed microtubule layout of proximal dendrites allows dynein to play a role in trafficking dendritic cargo such as AMPARs into dendrites. In more distal segments of these dendrites, microtubule polarity is predominantly plus-end out, which allows plus-end directed kinesins to traffic dendritic cargo along the length of the distal dendrite (Kapitein et al., 2010). Thus, both dynein and kinesins

are required for proper trafficking of dendritic cargos including glutamate receptors in these neurons.

Exactly which kinesins are required to traffic glutamate receptors to synapses is somewhat of an open question. So far, several kinesins have been implicated in this process. In mammalian neurons, kinesin-1/Kif5 interacts directly with the adaptor protein GRIP1 (GluR2-Interacting Protein) (Dong et al., 1997; Wyszynski et al., 1999). These two proteins form a trafficking complex with the AMPAR subunit GluA2 (Setou et al., 2002). Interestingly, the interaction between kinesin-1/Kif5 and GRIP1 changes the inherent steering of Kif5 from axon-directed to dendrite-directed (Setou et al., 2002). This steering function of GRIP1 is what allows kinesin-1/Kif5 to traffic GluRs to dendrites.

A second kinesin implicated in the trafficking of GLuRs is the kinesin-3 family motor, UNC-104/Kif1A. UNC-104/Kif1A forms a complex with AMPARs via its interaction with the synaptic scaffolding protein SYD-2/liprin-α in neuronal cultures (Shin et al., 2003; Wyszynski et al., 2002). SYD-2 binds directly to GluR binding protein GRIP1, and forms a complex with AMPARs and GRIP1 in cultured neurons. Disruption of the interaction between GRIP1 and SYD-2 results in decreased surface levels of AMPARs (Wyszynski et al., 2002), suggesting that the GRIP1/SYD-2/Kif1A complex is required for normal AMPAR levels at the synaptic surface.

Finally the kinesin-2 family motor Kif17 was demonstrated to traffic the NMDAR subunit NR2B to synapses in mammalian neurons (Setou et al., 2002). Kif17 connects to NR2B indirectly through a complex containing the scaffolding proteins LIN-2/CASK, LIN-7/MALS and LIN-10/Mint (Setou et al., 2002). This particular trafficking complex has been the subject of interesting work, which demonstrates the complex relationship between kinesin motors and their cargos discussed below.

Co-regulation of motor / cargo expression levels

Several recent studies have revealed an interesting regulatory mechanism in which expression of a kinesin and its cargo is co-regulated. For example, expression level of kinesin-2/Kif17 appears to affect expression of its cargo, the NMDA type glutamate receptor subunit NR2B (Setou et al., 2000; Dhar and Wong-Riley, 2011; Guillaud et al., 2003; Wong et al., 2002; Yin et al., 2011). In mammalian hippocampal neurons, antisense oligonucleotide-mediated knockdown of Kif17 decreased the trafficking of NR2B in dendrites. Surprisingly, it also resulted in decreased NR2B protein levels (Guillaud et al., 2003). Inhibiting Kif17 activity by over-expressing a dominant-negative form of Kif17 also reduced trafficking of NR2B, however, unlike in cells treated with Kif17 antisense oligonucleotides, the expression level of NR2B in cells expressing dominant-negative Kif17 remained unchanged. This suggests that changes in the expression level of the kinesin, and not the synaptic level of NR2B, were responsible for triggering the change in expression of NR2B. Interestingly, treatment of neurons that increased expression levels of NR2B also resulted in increased levels of Kif17 demonstrating that this co-regulation is bi-directional (Guillaud et al., 2003).

The mechanism by which this regulation takes place was explored in a subsequent study (Yin et al., 2011). In neuronal slices and cultures from kif17$^{-/-}$ knockout mice, reduced NR2B receptor subunit expression was shown to result from decreased transcription. Interestingly, protein levels of a different NMDA receptor subunit, NR2A, were also reduced in these cultures. However rather than decreased transcription, NR2A protein levels were reduced due to increased proteasome-mediated degradation (Yin et al., 2011).

The positive correlation between expression of Kif17 and NR2B demonstrated in these studies raised the possibility that these genes may share common transcriptional machinery. In fact, it was subsequently shown that the transcription factor NRF-1 positively

regulates the expression of both the Kif17 and NR2B genes (Dhar and Wong-Riley, 2011). Together, these studies demonstrate a distinct relationship between the expression levels of this motor/cargo combination, and they suggest that in addition to their canonical role of spatial regulation of cargo, kinesin motors can also influence cargo expression levels.

Degradation of cargo proteins as a result of defects in trafficking has also been suggested for AMPA type glutamate receptors. The gene coding for the β subunit of the clathrin adaptor complex AP4 is a necessary component for the anterograde trafficking of AMPARs (Matsuda et al., 2008). In mice in which this subunit was disrupted, polarized trafficking of the receptors was disrupted. Interestingly, AMPARs did not simply accumulate in the cell body but rather were observed in large autophagosomes in axons (Matsuda et al., 2008). This result suggested that these AMPARs were targeted for degradation, potentially in the lysosome, and it supports the model in which decreased expression of GluR trafficking machinery can result in receptor degradation instead of or in addition to aberrant localization of the receptor.

In addition to GluRs, other neuronal cargo proteins may also be degraded in the absence of their kinesins. In *C. elegans,* the gene *apl-1* is the single ortholog of the mammalian amyloid precursor protein (APP). In animals with mutations in either the kinesin-3 *unc-104/*Kif1A or kinesin-1 *unc-116/*Kif5 total protein levels of APP-1 were reduced (Wiese et al., 2010). No change in *app-1* transcription was seen, implying that the decrease in APP-1 levels took place post-translationally (Wiese et al., 2010). These results further suggest that the expression level of cargo proteins can be affected by expression levels of the kinesins that are necessary for their trafficking.

Together, these studies suggest that the accumulation of mislocalized cargoes in neurons may be sufficiently harmful to have necessitated the evolution of a degradation mechanism to degrade the cargoes. This may further implicate kinesins in certain

neurological diseases, especially those diseases for which aberrant accumulation of proteins is thought to be a pathologically relevant occurrence, such as in Huntington's Disease and Alzheimer's Disease (De Vos et al., 2008; Duncan and Goldstein, 2006; Hafezparast et al., 2003; Koushika et al., 2004).

Orthologs of the C. elegans kinesin-3 family motor klp-4

The C. elegans genome contains three kinesin-3 family members, *unc-104, klp-4 and klp-6* (See Figure 3-S1 for alignment). *unc-104* is the founding member of the kinesin-3 family. It was originally identified in *C. elegans* as the motor that traffics synaptic vesicles from the cell body to synapses (Hall and Hedgecock, 1991). Its mammalian ortholog, Kif1A was subsequently showed to perform the same function in mammals (Okada et al., 1995). UNC-104, Kif1A and the closely related Kif1B perform a number of important functions in neurons including processive trafficking of mitochondria, RNA and synaptic proteins (Hirokawa et al., 2010; Vale, 2003). *klp-6* expression is restricted to a subset of ciliated sensory neurons where it localizes to cilia. It has been shown to regulate intraflagellar transport in sensory neurons and has been implicated in mitochondrial trafficking (Morsci and Barr, 2011; Peden and Barr, 2005; Tanaka et al., 2011). The functions of its homologous proteins in vertebrates have not been characterized.

klp-4 is the least well characterized of the kinesin-3 motors in *C. elegans.* Comparative sequence analysis predicts that it is a plus end-directed kinesin but its specific functions are unknown. Like *unc-104*, *klp-4* contains a fork-head associated (FHA) domain located C-terminally to the N-terminal motor domain (Figure 3-1A). However unlike *unc-104,* it does not contain a pleckstrin homology (PH) domain at the end of the C-terminal cargo binding domain. KLP-4 is homologous to *Drosophila* Kinesin-73 (KHC-73) and mammalian KIF13A and KIF13B/GAKIN. Of the two mammalian homologs, KLP-4 appears to be more

closely related to KIF13A based on sequence identity and the lack of a microtubule plus-end binding CAP-Gly domain, which is found at the C-terminus of KLP13B (Figure 3-1A). These *klp-4* orthologs are discussed in more detail in the following section.

Drosophila KHC-73

The *Drosophila* kinesin-3 family member KHC-73 is important for neuronal development and synaptic function. In *Drosophila* neuroblasts, KHC-73 forms a complex with the PDZ domain-containing scaffolding protein Discs large (Dlg). This complex is required for cell differentiation as it functions in the establishment of cortical polarity, which is necessary for asymmetric cell division (Siegrist and Doe, 2005).

KHC-73 has also been shown to be required for normal synaptic activity at the glutamatergic neuromuscular junction (NMJ) in *Drosophila*. Tsurudome *et al*., found that deletion of the microRNA (miRNA) family, miR310-313 resulted in increased synaptic levels of the presynaptic organizing protein Bruchpilot (Brp) and synaptic release defects. Both of these phenotypes were dependent on the ability of miR310-313 to negatively regulate KHC-73 translation (Tsurudome et al., 2010).

Finally, in a detailed description of the motor properties of KHC-73, the motor was shown to co-localize with Rab5-containing endosomes in *Drosophila* neurons *in vitro* (Huckaba et al., 2011a). This co-localization required the C-terminal cargo-binding tail of KHC-73 suggesting that KHC-73 may complex with and transport early endosomes in neurons

Kif13A

The first described role of the mammalian kinesin-3 family member Kif13A was in trafficking of the mannose-6-phosphate receptor (M6PR) from the golgi to the plasma

membrane in polarized epithelial cells. The AP-1 protein complex was identified as the linker between the Kif13A kinesin and the M6PR cargo (Nakagawa et al., 2000). This function established a role for the *klp-4* ortholog Kif13A in trafficking membrane proteins from intracellular locations to the cell surface. Interestingly, in melanocytes the Kif13A/AP-1 complex was subsequently shown to function in trafficking of enzymes required for melanin synthesis from recycling endosomes to melanocytes (Delevoye et al., 2009). Together, these two studies demonstrate that a given kinesin is able to bind to and traffic different cargos even when bound to the same adaptor protein.

Kif13A also plays a role in cell division. During cytokinesis, Kif13A transports the signaling/scaffolding protein FYVE-Cent to the mid body to act as a scaffolding protein for other necessary components of cell division. Loss of function of Kif13A in these cells results in inefficient cell division and aneuploidy of daughter cells (Sagona et al., 2010).

Kif13B

Kif13B or GAKIN (Guanylate kinase-associated Inverted) was first described as a kinesin-3 family member when it was cloned from T-lymphocytes and shown to bind to the mammalian ortholog of *Drosophila* Discs large, hDlg (Hanada et al., 2000). This interaction has subsequently been shown to be important for motor-cargo complex formation as well as direct regulation of motor activity (Hanada et al., 2000; Yamada et al., 2007). Similar to the Kif13A/FYVE Cent complex described above, both Kif13B and hDlg are important for cytokinesis because loss of function of either protein in mammalian cell culture resulted in delayed cell division and multi-nucleated daughter cells (Unno et al., 2008).

Kif13B can also bind to the neuronal scaffolding protein centaurin-α1/ADAP1 (Horiguchi et al., 2006). Through its association with this adaptor protein, Kif13B transports Phosphatidylinositol-(3,4,5)-trisphosphate (PIP3)–containing vesicles into the maturing

axon of hippocampal neurons in culture during the process of axon specification. Inhibition of Kif13B function in this system results in the failure to establish neuronal polarity (Horiguchi et al., 2006).

The previous sections demonstrate that incremental progress is being made on pairing specific kinesins with their physiologically relevant cargo. It is clear that kinesins play a large role in the transport of neuronal proteins to locations where they can perform their function and the previous studies demonstrate the importance of kinesins in regulating many cellular processes. Identification of the kinesins that traffic a particular cargo is therefore a necessary component of learning about the cellular process to which that cargo contributes. While we continue to gain a better understanding of cellular processes with each new motor/cargo complex discovery, the question of how the trafficking of such complexes is regulated remains an open question.

Regulation of kinesin-dependent transport

Much progress has been made in understanding the biophysical mechanisms by which kinesins move along microtubules (Hirokawa et al., 2009; Verhey et al., 2011). However intracellular regulation of kinesin movement, a very important issue in cell biology, is largely mysterious. Given the number of kinesins, and potential adaptor proteins and cargo molecules, along with the various steps at which activity can be regulated, it is perhaps not surprising that progress on answering this question has been relatively slow.

The single task of moving cargo along microtubules consists of several steps: 1) attachment to cargo / intitiation of movement, 2) termination of movement / release from microtubules and 3) release of cargo. Each of these steps contributes to the accurate transport of cargo from one location within a cell to another and each one has been shown to be a point at which kinesin function can be actively regulated.

One seemingly common mechanism for initiation of movement for various kinesins is release from auto-inhibition (Hammond et al., 2010; Verhey et al., 2011). Inactive kinesins are folded over on themselves, allowing for physical interaction between the C-terminal tail and the N-terminal motor domain. This results in inhibition of motor activity (Coy et al., 1999; Hackney et al., 1991; Hackney et al., 1992). Separation of the motor domain from the cargo binding tail results in release from autoinhibition and subsequent motor activity (Hammond et al., 2009; Hammond et al., 2010). In some cases, binding of cargo proteins to the C-terminal tail is the trigger for release of autoinhibition of the kinesin motor domain (Blasius et al., 2007; Sun et al., 2011; Yamada et al., 2007). While this is an interesting mechanical method of regulating movement it leads to more questions. What might trigger the binding of such activating cargo? What other control mechanisms regulate kinesin activity? These issues are of great interest to the fields of intracellular trafficking and cell biology.

Phosphorylation of motor

One way in which the activity of kinesins can be regulated is by phosphorylation. This was first demonstrated in experiments examining the effects of the cAMP-dependent protein kinase (PKA) on kinesin-1. PKA phosphorylates kinesin-1 *in vitro* resulting in decreased binding to vesicular cargo and to microtubules (Sato-Yoshitake et al., 1992). Interestingly, in addition to its effects on binding to cargo and microtubulues, PKA phosphorylation of the light chain of kinesin-1 was shown to increase the ATPase function of the kinesin-1 motor domain *in vitro* (Matthies et al., 1993).

Phosphorylation of a kinesin can contribute to its specificity for a particular cargo as well. For example, phosphorylation of Ser460 of kinesin light chain (KLC) reduces the binding of the adaptor protein calsyntenin-1, which is important for glutamate receptor-

dependent learning and memory in *C. elegans* (Hoerndli et al., 2009; Ikeda et al., 2008; Vagnoni et al., 2011). Interestingly, phosphorylation of this residue had no effect on the binding of other cargo proteins to KLC (Vagnoni et al., 2011). Additionally, phosphorylation of KLC by Glycogen synthase kinase 3 (GSK3) reduces it binding to a particular membrane bound cargo in squid axoplasm (Morfini et al., 2002).

In an interesting example of how the phosphorylation of a motor can affect the proper delivery of cargo to specific intracellular locations, phosphorylation of Kif17 at Ser1029 by the Ca2+/calmodulin-dependent protein kinase (CaMKII) causes release of the cargo NMDA receptor from the motor (Guillaud et al., 2008). It has been proposed that this could be a mechanism by which NMDA receptors are delivered to areas of high neuronal activity in neurons (Guillaud et al., 2008; Yin et al., 2012).

In some cases, the molecular effect of kinesin phosphorylation is not known but it is clear that the phosphorylation event is functionally relevant. An *in vivo* study shows the *Drosophila* microtubule polymerizing kinase KLP10A is phosphorylated at Ser573 in the motor domain and this phosphorylation appears to inhibit the kinesin's role in microtubule movement (Mennella et al., 2009). The *klp-4* ortholog Kif13B/GAKIN is phosphorylated at 2 C-terminal residues, S-1381 and S-1410 by the Ser/Thr kinase Par1B. This phosphorylation inhibits the role of Kif13B in axon specification, which was discussed earlier (Yoshimura et al., 2010).

Phosphorylation of non-motor substrates affecting motor transport

In addition to direct phosphorylation of kinesins, phosphorylation of adaptor proteins or cargo proteins can regulate how cargos are transported by kinesins. The c-Jun N-terminal Kinase (JNK)-Interacting Proteins (JIPs) are scaffolding molecules that bind to kinesin and target kinases in the JNK signaling cascade to their effector proteins (Byrd et al.,

2001; Horiuchi et al., 2007; Sakamoto et al., 2005; Verhey et al., 2001). In *C. elegans* and *Drosophila* neurons, JIPs act as adaptor proteins that facilitate binding between kinesin-1 and various neuronal cargos (Byrd et al., 2001; Horiuchi et al., 2007; Sakamoto et al., 2005). Loss of function of JIP-3 in *C. elegans* and JIP-1 in *Drosophila* result in an axonal phenotype similar to that of kinesin-1 loss of function, including mislocalization of neuronal cargo proteins, a result consistent with the role of JIPs as kinesin adaptor proteins. Interestingly, in *Drosophila,* activation of kinases in the JNK pathway causes release of JIP-1 from kinesin-1, demonstrating a role for JNK signaling in negatively regulating axonal transport (Horiuchi et al., 2005). However in *C. elegans*, JNK signaling appears to positively regulate JIP-3-mediated transport because the loss of function of JNK signaling members causes a similar phenotype to the loss of function of JIP-3 (Byrd et al., 2001; Sakamoto et al., 2005).

JNK signaling has been shown to negatively regulate the trafficking of axonal cargo in squid axoplasm and cultured mammalian neurons through a different mechanism, namely decreasing the association of kinesin-1 with microtubules (Stagi et al., 2006). This is interesting because it suggests that kinases can differentially regulate kinesin-driven trafficking depending on the cellular environment. Together, these studies demonstrate the complexity of trafficking regulation even by a single signaling cascade.

Interestingly, the cyclin-dependent kinase, Cdk-5, which has been shown to regulate trafficking of neuronal cargo in *C. elegans* (Goodwin et al., 2012; Juo et al., 2007; Ou et al., 2010; Park et al., 2011) also affects trafficking of axonal and synaptic cargos in other systems, including in mammals (Ratner et al., 1998; Morfini et al., 2004; Vacher et al., 2011). In rats, a subunit of the voltage-gated potassium channel Kv1, Kvβ2 is phosphorylated at 2 sites by Cdk-2 and/or Cdk-5 *in vivo.* This phosphorylation negatively regulates the interaction between Kvβ2 and the microtubule plus end binding protein EB1, potentially freeing Kvβ2 to move. Inhibition of kinase activity results in accumulation of

Kvβ2, Cdk2 and Cdk5, and EB1 at the axon hillock in neurons and decreased Kvβ2 surface expression in heterologous cells. Thus, Cdk2 and Cdk5 promote trafficking of this voltage-gated potassium channel from the axon hillock into the axon (Vacher et al., 2011).

In squid axoplasm, glycogen synthase kinase-3 (GSK3) phosphorylates the kinesin light chain (KLC) resulting in reduced binding to organelle cargo (Morfini et al., 2002). In addition to this direct phosphorylation by GSK3, axonal transport is also dependent on the activity of Cdk-5, which indirectly antagonizes the effects of GSK-3 and promotes axonal trafficking of the organelle cargo (Morfini et al., 2004; Ratner et al., 1998). This is an example of how multiple kinases can regulate the axonal trafficking of a single neuronal cargo, one acting through direct phosphorylation of the motor and the other acting indirectly (Morfini et al., 2004; Ratner et al., 1998). These studies indicate that kinases play an important role in intracellular transport by phosphorylating cargoes or adaptors and regulating their associations with kinesins.

Cyclin-dependent kinase-5 (CDK-5)

Cyclin-dependent kinase-5 (CDK-5) is a Ser/Thr kinase that was originally identified based on its sequence similarity to Cdk-2 and other cell cycle related kinases. Unlike these kinases however, CDK-5 activity is restricted to the nervous system because of the neuronal expression pattern of its activator protein p35 (Dhavan and Tsai, 2001). Numerous *in vitro* and *in vivo* studies have identified many essential functions of CDK-5 in the developing and mature brain (Dhavan and Tsai, 2001). *cdk-5* knockout mice die perinatally and their brains show signs of aberrant development including defects in axon guidance, neuronal migration and layering and cytoskeleton organization (Ohshima et al., 1996; Ohshima et al., 1999; Tanaka et al., 2001). While loss of CDK-5 activity is lethal, excess CDK-5 activity is also harmful to the brain. Hyperactive CDK-5 is implicated in a number of neurodegenerative

conditions including Alzheimer's disease and amyotrophic lateral sclerosis (Cruz and Tsai, 2004; Dhavan and Tsai, 2001; Patzke and Tsai, 2002)

Many targets of CDK-5 have been identified including several synaptic proteins, signaling molecules and regulators of cytoskeletal structure and CDK-5 can affect synaptic transmission in the central nervous system and at the neuro-muscular junction (Dhavan and Tsai, 2001; Lai and Ip, 2009). Due in large part to the multiple essential processes in which CDK-5 seems to be involved, the mammalian brain is a particularly difficult system in which to study individual mechanisms of CDK-5. Invertebrate models such as *C. elegans* and giant squid have offered the opportunity to study the effects of loss of function of CDK-5 on the mature nervous system. These model systems have demonstrated novel ways in which CDK-5 can affect synaptic transmission, namely through regulation of the trafficking of neuronal proteins.

CDK-5 regulates trafficking of neuronal cargo

A series of interesting studies demonstrated one way in which CDK-5 can regulate the actions of kinesins that are involved in neuronal anterograde trafficking (Morfini et al., 2002; Morfini et al., 2004; Ratner et al., 1998). In squid axoplasm the kinesin light chain (KLC) is an effector of glycogen synthase kinase-3 (GSK3) (2002). Direct phosphorylation of KLC by GSK3 negatively regulates axonal transport by causing separation of membrane bound organelles from KLC (2002). This GSK3 activity is in turn, negatively regulated by CDK-5. CDK-5 phosphorylates protein phosphatase-1 (PP1), increasing its phosphatase activity and its ability to dephosphorylate the site on KLC that is phosphorylated by GSK-3 (Morfini et al., 2004). In this model, CDK-5 activity indirectly decreases the activity of GSK3, the negative regulator of kinesin-mediated anterograde transport. This interesting work provides an exact mechanism by which CDK-5 can regulate

the ability of a kinesin to transport neuronal cargo from the cell body into neuronal processes.

CDK-5 can control neuronal trafficking in *C. elegans* as well. One way it does this is by regulating the activity of the microtubule minus-end directed motor dynein (Goodwin et al., 2012; Ou et al., 2010). In *C. elegans*, synaptic vesicles and dense core vesicles (DCV) are both trafficked into axons of motor neurons on the kinesin-3 motor UNC-104 (Hall and Hedgecock, 1991; Jacob and Kaplan, 2003; Lo et al., 2011; Sieburth et al., 2005). Recently CDK-5 was shown to play an important role in promoting this process (Goodwin et al., 2012; Ou et al., 2010). It does so in part, by inhibiting inappropriate dynein-mediated trafficking of vesicles into dendrites (Goodwin et al., 2012; Ou et al., 2010). Together these studies make clear that CDK-5 can have varied effects on the trafficking of neuronal motor/cargo complexes.

CDK-5 regulates GLR-1 trafficking in C.elegans

In *C. elegans* CDK-5 promotes the anterograde trafficking of the glutamate receptor GLR-1 (Juo et al., 2007). In animals with loss of function mutations in *cdk-5*, GLR-1 levels decrease in the VNC and increase in the cell bodies. These results are consistent with a role for CDK-5 in the trafficking of the receptor from the cell body into the VNC. Overexpression of wild type CDK-5, but not kinase-dead mutant versions of CDK-5 results in increased levels of GLR-1 in the VNC when compared to those in wild type animals. The scaffolding protein LIN-10/MINT was identified as one substrate of CDK-5 that regulates GLR-1, however genetic experiments suggest that there are other mechanisms by which CDK-5 promotes GLR-1 levels in the VNC.

In this thesis I used a forward genetic screen to identify novel genes that mediate the effects of *cdk-5* on GLR-1. We found that the kinesin-3 family motor, *klp-4* regulates the anterograde trafficking of GLR-1 in the VNC and that KLP-4 functions in the same cellular pathway as CDK-5. We also find that in the absence of functional KLP-4, its GLR-1 cargo undergoes lysosomal degradation. Finally, we investigate possible regulatory mechanisms for the KLP-4-mediated trafficking of GLR-1.

Chapter 2

A genetic screen to identify suppressors of increased GLR-1 abundance in the VNC of *C. elegans* that overexpress *cdk-5*

Attributes:

Experiments in the following chapter were performed by Michael Monteiro, Emily Malkin, Jennifer Kowalski and Steven Garafalo. Emily Malkin performed the screening of 2000 genomes and isolated *cdk-5(xs)* suppressor mutants *pz1-pz32.* Jennifer Kowalski performed the RNAi screen in which *klp-4* was identified as a regulator of GLR-1 in the VNC. Steven Garafalo performed sequencing of the *xbp-1* gene in *pz13* mutants and the non-complementation test between suppressor mutant *pz11* and *ire-1(v33).* All other experiments were performed by Michael Monteiro.

Introduction

Most excitatory activity in the mammalian brain is mediated by the neurotransmitter glutamate. Neuronal activity-induced changes in the strength of a glutamatergic synapse are thought to be important for the acquisition and retention of memories (Bredt and Nicoll, 2003; Shepherd and Huganir, 2007). Changes in glutamate signaling are also thought to play a role in several neurological diseases (Bowie, 2008; Kwak and Weiss, 2006). One mechanism by which the strength of glutamatergic synapses can change is through modulation in the number of glutamate receptors (GluRs) that are present in the postsynaptic membrane (Bredt and Nicoll, 2003; Shepherd and Huganir, 2007). Regulation of synaptic GluR levels has been the subject of a great deal of research. This has lead to a better understanding of synaptic trafficking of GluRs and the early biosynthetic trafficking of GluRs in the cell body (Collingridge et al., 2004; Vandenberghe and Bredt, 2004). However, less is understood about GluR trafficking from the cell body to the synapse.

In *C. elegans* the abundance of GLR-1 glutamate receptors in the ventral nerve cord (VNC) is regulated by cyclin-dependent kinase-5 (CDK-5) (Juo et al., 2007). Animals with genetic null mutations of *cdk-5* exhibit large decreases in the abundance of synaptically localized, fluorescently-tagged GLR-1 (GLR-1::GFP) in the VNC. Conversely, animals with increased expression of wild type, but not kinase-dead, *cdk-5* exhibit increased GLR-1 levels in the VNC. In addition to decreased GLR-1 in the VNC of *cdk-5* mutants, GLR-1 abundance is increased in neuronal cell bodies of these animals (Juo et al., 2007). This suggests that loss of functional CDK-5 results in defects in the anterograde trafficking of the receptor from the cell body to the VNC, an aspect of GluR trafficking about which relatively little is known. The scaffolding protein LIN-10/Mint was identified as one target of CDK-5 kinase activity that could mediate its effects on GLR-1 but genetic experiments suggest that there are other as yet unknown CDK-5 substrates that regulate GLR-1 trafficking (Juo et al.,

2007; Rongo et al., 1998)).

CDK-5 is a Ser/Thr kinase that functions primarily in the nervous system. CDK-5 activity is required during neuronal development as *cdk-5-/-* knockout mice die perinatally and exhibit wide spread and dramatic neuronal defects (Dhavan and Tsai, 2001; Ohshima et al., 1996). *In vivo* and *in vitro* experiments have identified numerous substrate proteins for CDK-5 and have implicated the kinase in multiple cellular functions including neuronal migration, axon outgrowth, polarized trafficking of neuronal cargo, learning and memory and neurotransmitter receptor activity (Cheung et al., 2006; Dhariwala and Rajadhyaksha, 2008; Goodwin et al., 2012; Hawasli et al., 2007; Ou et al., 2010; Su and Tsai, 2011).

Regulation of GLR-1 trafficking is a novel way in which CDK-5 could modulate neuronal function, and deciphering the mechanism by which CDK-5 exerts its effects on GLR-1 could lead to significant advances in our understanding of GluR trafficking. One strategy to uncover how CDK-5 regulates GluR trafficking is to identify genes that function in the same cellular pathway, which could include CDK-5 substrates and regulators. Given the large number of proteins already shown to be phosphorylated by CDK-5 and the expected large number of potential new effectors, a candidate approach is not a feasible strategy for identification of genes that CDK-5 might phosphorylate (Dhariwala and Rajadhyaksha, 2008; Su and Tsai, 2011). Here we take advantage of the genetic tools available in *C. elegans* to perform an unbiased forward genetic suppressor screen to identify novel genes and mechanisms that regulate the effects of *cdk-5* over expression [*cdk-5(xs)*] on the trafficking of the glutamate receptor GLR-1.

The advantage of using *cdk-5* suppression as a basis for the screen is two-fold. First, this strategy facilitates the identification of genes that affect the *cdk-5(xs)*-induced increase of GLR-1 in the VNC. Therefore, we expect to identify genes encoding proteins that may work in the same pathway as CDK-5 to regulate GLR-1 abundance (Jin et al., 1995;

Lee et al., 2001; Therrien et al., 2000). Such gene products could interact directly or indirectly with CDK-5, for example, a CDK-5 substrate or a downstream regulator of its activity, respectively. Importantly, in addition to genes that may function in the same pathway as CDK-5, this screen also allows for the identification of genes involved in GluR trafficking in general, which may function in a CDK-5-independent manner.

The second major advantage of the *cdk-5* suppressor strategy is a practical one. When visually screening animals for potential mutants, it is easier to detect a decrease from the elevated GLR-1::GFP abundance in animals that overexpress *cdk-5* than from the relatively dimmer levels in wild type animals. Thus the potential for false negatives is reduced by employing the suppressor strategy. The identification of *cdk-5* suppressors should facilitate the identification of novel genes and mechanisms involved in the anterograde trafficking of GluRs.

Results

Forward genetic screen to find suppressors of *cdk-5* overexpression

CDK-5 positively regulates the abundance of GLR-1 in the VNC. Over expression of *cdk-5* results in increased intensity and width of GLR-1::GFP puncta in the anterior VNC (Juo et al., 2007). To identify suppressors of these effects on GLR-1::GFP we are conducting an F1 clonal chemical mutagenesis screen on animals over expressing *cdk-5,* [*cdk-5(xs)*]. Mutagenesis was performed by exposure to the DNA alkylating agent ethyl methanesulfonate (EMS) (Brenner, 1974; Jorgensen and Mango, 2002). We have completed 17 rounds of EMS mutagenesis (rounds A-Q) followed by visual screening on a compound fluorescent microscope. In total 2500 genomes have been screened, nine rounds of 100 genomes and eight rounds of 200 genomes. To date we have isolated 43 suppressor mutants in which the abundance of GLR-1::GFP appears reduced compared to

cdk-5(xs) animals (Table 2-1). For 18 of these suppressor mutants the effect on GLR-1::GFP is categorized as strong (Table 2-1 and Figure 2-2). Images of the VNC from three of the strongest suppressor mutants, *pz13*, *pz17* and *pz19* are shown in Figure 2-1 A-D. Although quantitative imaging has not been performed on these mutants, visual examination of the VNCs indicates a highly penetrant decrease in GLR-1::GFP puncta intensity and density compared to *cdk-5(xs)* animals. In the VNC of suppressor mutants *pz37* and *pz35*, GLR-1::GFP abundance is decreased compared to *cdk-5(xs)* animals although the phenotype does not appear as strong as in the previous three mutants (Figure 2-2). *pz35* appears to affect primarily GLR-1::GFP puncta intensity, with little to no change in puncta density or width whereas *pz37* affects both GLR-1::GFP puncta intensity and density (Figure 2-2 E-G).

In addition to decreased GLR-1::GFP abundance in the VNC, the majority of mutants isolated in this screen also exhibit other phenotypes that are apparent upon inspection of a full plate of worms under a dissecting microscope. These “plate phenotypes” include low brood size, abnormal body shape, slow growth and/or abnormal movement. In all likelihood the majority of these plate phenotypes result from the many mutations throughout the genome induced by the non-specific mutagen EMS. Backcrossing suppressor mutants at least six times to the original, non-mutant screening strain to eliminate mutations that do not affect GLR-1 will be performed. To date this has been performed only for *pz19* mutants. However, some of these plate phenotypes might be linked to the mutation affecting GLR-1. For example, a null mutation in the gene *dpy-23* results in decreased GLR-1 abundance in the VNC and in a short, thick, or “dumpy” body shape (data not shown). The genetic linkage of a plate phenotype with the *cdk-5(xs)* suppression phenotype would aide in identification of the suppressor mutation. Once the suppressor mutation was mapped to a chromosome, we could focus our efforts in identifying that mutation on genes on the same chromosome

known to cause that particular plate phenotype when mutated.

Genetic mapping of *cdk-5(xs)* suppressor mutants

The *C. elegans* genome consists of 5 autosomal chromosomes (I-V) and one sex chromosome (X). We have begun mapping six of the strongest suppressor mutations to chromosomes using standard mapping techniques based on the principle that genes on different chromosomes should segregate independently of one another. Each suppressor mutant was crossed with mapping strains containing one recessive genetic mutation per chromosome that causes a unique plate phenotype when homozygosed. Details of these mapping mutations are listed in Table 2-2 A. F1 progeny of the cross between suppressor mutant and plate mutant are phenotypically wild type if both mutations are recessive. In the F2 generation, the *cdk-5(xs)* suppression phenotype and the plate phenotype will each be present in 25% of animals. To determine whether the suppressor mutation is on the same chromosome as the plate phenotype mutation, phenotypic plate mutants were selected for GLR-1 imaging on a fluorescent microscope. If the suppressor mutation and the plate phenotype mutation are on different chromosomes, then these two mutations should segregate independently of one another during meiosis resulting in 25% of plate phenotype mutants also displaying the *cdk-5(xs)* suppression phenotype. If, however the two mutations are on the same chromosome, their genetic linkage will prevent independent segregation resulting in fewer than 25% of plate phenotype mutants displaying the *cdk-5(xs)* suppression phenotype. While the exact predicted percentage of F2 double homozygosity for mutations on the same chromosome varies, depending on the recombination frequency between the two mutations, a frequency significantly below 25%, indicates the two mutations are on the same chromosome. Current chromosome mapping results are shown in Table 2-2 B. To date chromosome mapping for mutants *pz12, pz13* and *pz18* is

preliminary and a larger *n* of F2 progeny from mapping crosses will be required to obtain definitive results. However, for mutants *pz19* (chromosome X)*, pz17* (chromosome X), and *pz11* (chromosome II), mapping results appear definitive (Table 2-2 B).

Non-complementation testing identifies *cdk-5(xs)* suppressor mutations

Two strong suppressor mutants, *pz11* and *pz13,* display altered distribution of GLR-1 in neuronal cell bodies in addition to reduced GLR-1 abundance in the VNC (Figure 2-3). Normally GLR-1::GFP is diffuse and distributed throughout the cell body (Figure 2-3 A). However, in *pz11* and *pz13* mutants, GLR-1::GFP is highly concentrated in a ring-shaped structure, in a manner similar to that previously observed in animals with loss of function mutations in the unfolded protein response (UPR) genes, *ire-1* and *xbp-1* (Shim et al., 2004)(Figure 2-3 B-C).

The distinctive GLR-1 phenotype in the cell body and the similarity of phenotype in the VNC raises the possibility that the *pz11* and *pz13* suppressor mutants may harbor mutations in either *ire-1* or *xbp-1.* Because both *pz11* and *ire-1* are on the X chromosome (Table 2-2 B), a non-complementation test was performed to determine whether *pz11* could be a mutation in *ire-1*. Animals that are heterozygous for *pz11* do not display a reduction in GLR-1 levels in the VNC suggesting that *pz11* is a recessive mutation, as is *ire-1(v33)* (data not shown). Two recessive mutations are said to complement each other if an animal that is heterozygous for both mutations appears phenotypically normal. This indicates that the two mutations are in different genes because a wild type copy of each gene is present in the animals. Non-complementation occurs when a double heterozygote is phenotypically mutant. This result indicates the two mutations are alleles of the same gene (Brenner, 1974). If animals that are heterozygous for both *pz11* and *ire-1(v33)* display the low levels of GLR-1 in the VNC typical of either one of the homozygous mutants, then *pz11* would

have failed to complement *ire-1*, suggesting that both strains have a mutation in the same gene that causes the GLR-1 phenotype. We observed decreased GLR-1 abundance in the VNC of *pz11* + / + *ire-1* trans-heterozygous animals (data not shown). This suggests that *pz11* is a mutation in *ire-1*.

In a parallel genetic screen performed in the lab, candidate genes were targeted for RNAi-mediated knockdown. The kinesin-3 family motor *klp-4* was identified as a possible regulator of GLR-1 levels in the VNC. RNAi knockdown of *klp-4* in an RNAi sensitive strain, *eri-1(mg336); lin-35(n745)* resulted in decreased GLR-1::GFP abundance in the VNC (Figure 2-4). Because *klp-4* is located on the X chromosome and the strong *cdk-5(xs)* suppressor mutant *pz19* was mapped to the X chromosome (Figure 2-2 and Table 2-2 B), we tested whether pz19 could be an allele of *klp-4*. To determine if the *pz19* mutation could be a mutation in *klp-4* we performed a non-complementation test between the *pz19* mutant and a genetic null mutant *klp-4(tm2114)*. *pz19* failed to complement *klp-4(tm2114)*, as demonstrated by the strong effect on GLR-1::GFP of the *pz19/ klp-4(tm2114)* double heterozygote (Figure 2-5). This result suggests that *pz19* is a mutation in the *klp-4* gene. Subsequent sequencing of the *klp-4* open reading frame and all intron/exon boundaries in *pz19* mutants identified a C to T point mutation (C3076T) in the cargo binding tail of *klp-4* resulting in a premature stop codon (R1026Stop). This mutation is consistent with the predicted effects of EMS.

Discussion

Regulation of glutamate receptor trafficking is an important process for the health and function of the brain, and one which is not well understood. The identification of genes and mechanisms that control this process is important for our basic understanding of neuronal function and has important implications for the treatment of neurological diseases.

The identification of a kinase (CDK-5) as a regulator of GLR-1 levels in the VNC is an intriguing and challenging development as it is difficult to predict where it acts in the trafficking pathway. Transcription factors, ER resident proteins, or synaptic vesicle release proteins, for example, suggest mechanisms of action by which they could regulate targets. In contrast, a kinase, in principle can regulate many steps of the GluR trafficking pathway or ion channel function. We used a forward genetic suppressor screen to isolate several mutants that block the effects of *cdk-5* overexpression on GLR::GFP levels in the VNC to identify novel regulators of GLR-1 that might act in the same pathway as CDK-5.

Many novel genes involved in diverse aspects of cell biology including development, cell death, intracellular trafficking and synaptic transmission were discovered in forward genetic screens using *C. elegans* (Gengyo-Ando and Mitani, 2000; Nurrish, 2002). In particular, screens specifically designed to identify suppression of a mutant phenotype offer several advantages (Hodgkin, 2005). Suppressor screens can be used to elucidate the mechanism of action of a novel protein in a particularly complex cellular process like synapse development (Van Epps et al., 2010). Interestingly, a suppressor screen in *C. elegans* identified a novel gene that is essential for the function of GLR-1, *sol-1/* suppressor of lurcher-1, which was identified based on its ability to suppress the activity of a constitutively active GLR-1 mutant (Zheng et al., 2004). Suppressor screens of mutant kinase phenotypes have been used to find targets for that kinase as well as genes that interact indirectly to modify a pathway (Jin et al., 1995; Lee et al., 2001; Therrien et al., 2000).

Screen progress and potential

To date the potential value of our screen outweighs the realized value. All but two of the mutants isolated in this screen remain unidentified and sixteen of these are considered

to have strong effects on GLR-1 levels. There is potential that many of these are interesting novel regulators of GLR-1 levels in the VNC. Because this screen identifies mutants that suppress the effects of *cdk-5* overexpression, we reason that it could identify genes that function in the same pathway as CDK-5 to regulate GLR-1 trafficking. The identification of a CDK-5 substrate is an example of a gene that would interact directly with CDK-5. Such a discovery would likely provide great insight into where in the trafficking pathway CDK-5 acts. This screen should also identify CDK-5- dependent regulators of GLR-1 that are not direct effectors of CDK-5. These regulators should also shed light on the cellular process that CDK-5 regulates and for a process as complex as GluR trafficking it is likely that there are many such genes which are yet to be discovered.

In *cdk-5* null mutants, GLR-1 abundance in the VNC is significantly reduced but there is still GLR-1 present at the synapse (Juo et al., 2007). This demonstrates that CDK-5 independent trafficking can contribute significantly to GLR-1 abundance in the VNC. Our suppressor screen could also identify genes that are important for GluR trafficking in general and that function independently of CDK-5. The identification of novel regulators of GLR-1 abundance in the VNC should provide new insight into several cellular processes that include all aspects of GLR-1 synthesis and trafficking, anterograde and synaptic. Below are examples of genes that regulate GLR-1 abundance in various ways.

One possible cause of reduced GLR-1 abundance in the VNC is an overall reduction in GLR-1 protein levels. This could result from decreased GLR-1 translation as demonstrated by the loss of function of the splicing factor GRLD-1 (Wang et al., 2010). Decreased GLR-1 transcription might also cause a reduction in overall GLR-1 protein levels. Therefore, we expect that genes that promote *glr-1* transcription or translation may be found in this screen. It is worth noting that because both the GLR-1::GFP and CDK-5*(xs)* transgenes are under the control of the *glr-1* promoter, a loss of function mutation in a *glr-1*

transcription factor should affect the expression of both transgenes. This would result in decreased GLR-1::GFP expression as well as reduced CDK-5 expression and activity, likely resulting in a dramatic effect on GLR-1::GFP puncta in the VNC.

GLR-1 abundance in the VNC is also affected by post-translational regulation of GLR-1 protein levels. GLR-1 at the synapse is subject to ubquitin-mediated endocytosis from the plasma membrane into intracellular pools (Burbea et al., 2002). From these pools GluRs can be targeted for reinsertion into the plasma membrane or for lysosomal degradation (Chun et al., 2008; Kowalski et al., 2011; Park et al., 2009). Both ubiquitin-mediated endocytosis and subsequent targeting of internalized receptors are important regulators of the abundance of GLR-1::GFP in the VNC (Burbea et al., 2002; Chun et al., 2008; Dreier et al., 2005; Juo and Kaplan, 2004; Kowalski et al., 2011; Park et al., 2009; Schaefer and Rongo, 2006; Zhang et al., 2012). For example, the deubiquitinating enzyme *usp-46* deubiquitinates GLR-1, thereby reducing its trafficking to the lysosome and increasing GLR-1 abundance in the VNC (Kowalski et al., 2011). We expect that loss of function mutations in genes functioning in this or a parallel pathway would result in decreased GLR-1::GFP abundance in the VNC and we therefore expect that we could find such genes in this screen.

Genes promoting the anterograde trafficking of GLR-1 from cell body to VNC should also be identified in this screen. The calcium/calmodulin dependent protein kinase II (CaMKII) regulates GLR-1 trafficking. Loss of function of CaMKII results in decreased GLR-1::GFP puncta density in the VNC and increased GLR-1::GFP abundance in the cell body (Rongo and Kaplan, 1999). The role of CaMKII appears to be calcium dependent because loss of function mutations in voltage-gated calcium channels cause similar defects in GLR-1 trafficking (Rongo and Kaplan, 1999). We expect loss of function mutations in genes functioning in this calcium-dependent signaling pathway would result in decreased GLR-1

abundance in the VNC and could be identified in this screen.

Another class of genes we expect to find in this screen contains global regulators of synapse development. For example, a mutation that decreases the number or size of synapses would be predicted to exhibit decreased GLR-1::GFP density or intensity, respectively. These mutations could be interesting in their own right, if their effects on development are novel, but they would not be particularly relevant to the effort to understand GluR regulation. Identification of such a global regulator could be accomplished by examining the distribution of various synaptic proteins in the mutant. If most or all synaptic proteins appear to be mislocalized, it is likely that these animals have developmental synaptic defects, and therefore the mutated genes are unlikely to pertain specifically to GLR-1.

We are likely to find genes that are already known to regulate GLR-1 abundance, for example *ire-1(pz11)* (Shim et al., 2004). These genes serve as proof of principle for the screen, however, they clearly are not the intended targets. If a suppressor mutation has a similar phenotype to an already known GLR-1 regulator and chromosome mapping indicates that the two mutations are on the same chromosome, we would perform a non-complementation test as was the case with *pz11* and *ire-1*. Sequencing the candidate gene is another method that can be used to determine whether a suppressor mutation is in a gene already known to regulate GLR-1. Indeed, because of the similarity of VNC and cell body GLR-1 phenotypes in *xbp-1(zc12)* mutants and *pz13* suppressor mutants, (Shim et al., 2004) (Figures 2-2, 2-3 Table 2-1), sequencing of the *xbp-1* gene in suppressor mutant *pz13* was performed. Surprisingly, no mutation was identified in *xbp-1* of *pz13* mutants. This would seem to suggest that *pz13* is not a mutation in *xbp-1*. However, it sill remains a possibility that *pz13* is a mutation in the *xbp-1* promotor or 3' UTR that affects expression of *xbp-1*. Given the striking similarity between *pz13* and *xbp-1(zc12)* mutants, we believe this

is likely.

It is unlikely that this screen could be used to identify all genes that are involved in GLR-1 trafficking. It is possible that several GLR-1 regulators are mutated in a single animal given the random mutations throughout the genome caused by EMS exposure. If each of these mutations have a small effect on GLR-1 that can only be detected in combination with other mutations, we would be unlikely to be able to identify any of them. This is because back crossing these strains would separate these mutations from each other. In this case, the reduction of the *cdk-5(xs)* suppressor phenotype to the point at which it could no longer be visually distinguished from the original *cdk-5(xs)* animals. Thus, this screen is ideal for the identification of genes that have relatively large affects on their own on GLR-1 levels in the VNC.

It is interesting to note that, while we generated 43 suppressor mutants, only two, *ire-1(pz11)* and *klp-4*(*pz19)*, have been identified. While this is partly explained by the high priority given to fully characterizing the mechanism by which *klp-4* exerts its effects on GLR-1 levels (Chapter 3), it is also true that traditional methods of mapping genetic mutations can be labor-intensive and time-consuming. In fact until recently, the identification of mutations by mapping has been the rate-limiting step of forward genetic screens like this one. However, with the increasing speed and decreasing cost of whole genome sequencing, this is becoming less true (Hillier et al., 2008; Hobert, 2010). Widespread use of whole genome sequencing will make identifying lesions in isolated mutants quicker than the generation of animals with a desired phenotype (Hobert, 2010; Sarin et al., 2008). This is an exciting development for the effort to delineate genetic pathways of interest in model organisms. It will be interesting to see how these new technologies transform the practice of gene discovery and the extent to which that will translate to a better understanding of important cellular processes.

Methods

Strains

The following strains were used in this study: *nuIs24* (P*glr-1*::GLR-1::GFP), *klp-4(tm2114), pzIs2* (P*glr-1::cdk-5*), *bli-4(e937), rol-6(e187), vab-7(e1562), dpy-11(e224), lon-2(e678).* All strains were maintained at 20°C as described previously (Brenner, 1974)

EMS mutagenesis screen

An F1 clonal screen was performed by mutagenizing *cdk-5(xs)* animals (*nuIs24;pzIs2)* with ethyl methane sulfonate (EMS) and screening F2 progeny (Brenner, 1974).

To synchronize worms for mutagenesis, three L4 *nuIs24; pzIs2* animals were picked to plates with food and allowed to grow until plates were starved with lots of eggs. Larvae and adult worms were washed off of plates, leaving only eggs. The following day, starved L2/L3 animals were washed off plates and spotted onto fresh plates with food to grow overnight. The following day synchronized L4 animals were washed off of plates and incubated in 4 ml of 50 mM EMS (Sigma M-0880) in PBST with 10x concentrated OP50 food to keep animals from starving at room temperature for 4 hours. After removal of EMS, mutagenized animals were washed twice in PBS and transferred to fresh nematode growth medium (NGM) plates with food to recover until movement resumed. Healthy-looking mutagenized L4/young adult PO generation animals were then transferred to fresh NGM plates and grown overnight at 20° C. The following day, adult animals with eggs were transferred to new plates with food and allowed to lay eggs at 20° C for three days (5 plates of 5 animals each). Three days later, when F1 generation had grown to young adult age, 50 (for 100 genome screening rounds) or 100 (for 200 genome screening rounds) young adult F1 animals were picked onto 50 fresh NGM plates with food and incubated at 20° C for three days. At least 20 (for 100 genome screening rounds) or 40 (for 200 genome screening rounds) F2 animals were

screened on a compound microscope for mutants with decreased abundance of GLR-1::GFP in the VNC compared to *cdk-5(xs)* non-mutagenized animals. Putative suppressors were picked from the microscope slide and singled so that progeny could be checked for 100% penetrance of the suppressor mutations, as validation of a true suppressor mutant.

Chromosome mapping

Standard genetic mapping was used to map mutations to chromosomes. Suppressor mutant animals were crossed with animals carrying a known mutation causing a recessive visible plate phenotype. F1 progeny of this cross are phenotypically wild type for both *cdk-5* suppression and the plate phenotype mutation. In the F2 generation, both the plate mutation phenotype and the *cdk-5* suppressor phenotype should be present in 25% of animals. Several animals displaying the plate phenotype are picked for GLR-1 imaging on a fluorescence microscope. If the two mutations are on different chromosomes, they are expected to segregate independently during meiosis in F1 generation animals. Independent segregation is indicated by 25% of the plate phenotype mutants also displaying the GLR-1 suppressor phenotype, (i.e., 1/16 of F2 animals are double homozygous mutants). If the two mutations are on the same chromosome, then they will not segregate independently of one another. This will result in significantly fewer than 25% of animals that display both the plate phenotype and the GLR-1 suppressor phenotype. The percentage of double homozygous mutants in the F2 generation for 2 mutations on the same chromosome is expected to vary between 0% and 25%, depending on the frequency of recombination during meiosis.

Non-complementation test

Recessive *pz* mutants were crossed with recessive independent mutants of the candidate

gene. The presence of the common phenotype phenotype, (i.e. decreased GLR-1 abundance in the VNC) in the F2 generation indicated failure of *pz* mutation to complement the independent mutation and suggests the mutations are on a common gene. Positive identification of *pz19* lesion by sequencing is detailed in Chapter 2 methods.

Scoring of *cdk-5(xs)* suppressor mutants

Qualitative scoring of *pz* suppressor mutants was performed by assessing the magnitude of the decrease in GLR-1::GFP abundance in the VNC. Mutants were assigned qualitative scores to describe their effects (e.g., Good/Strong, Medium, etc.).

Figure 2-1.

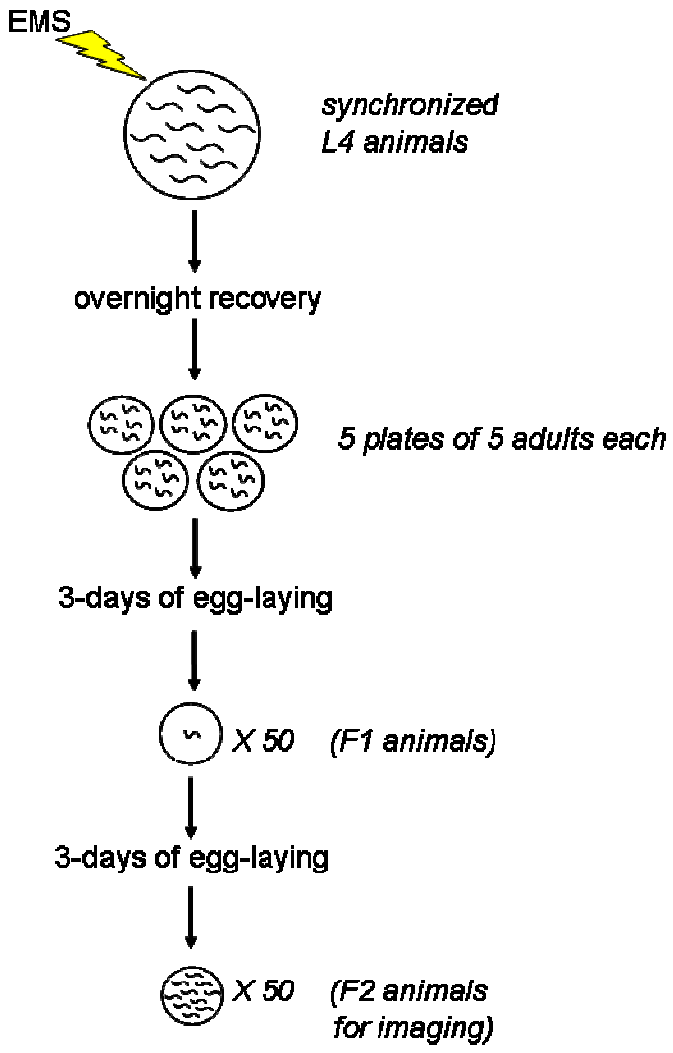

Figure 2-1. F1 clonal screen. Synchronized L4 stage *cdk-5(xs)* animals expressing GLR-1::GFP were exposed to EMS for 4 hours followed by overnight recovery. The following day, adult PO generation animals were transferred to new plates and allowed to lay eggs for three days. 50 young adult F1 animals were singled and incubated for three days. F2 animals were screened on a compound microscope for mutants with decreased abundance of GLR-1::GFP in the VNC compared to *cdk-5(xs)* non-mutagenized animals.

Figure 2-2.

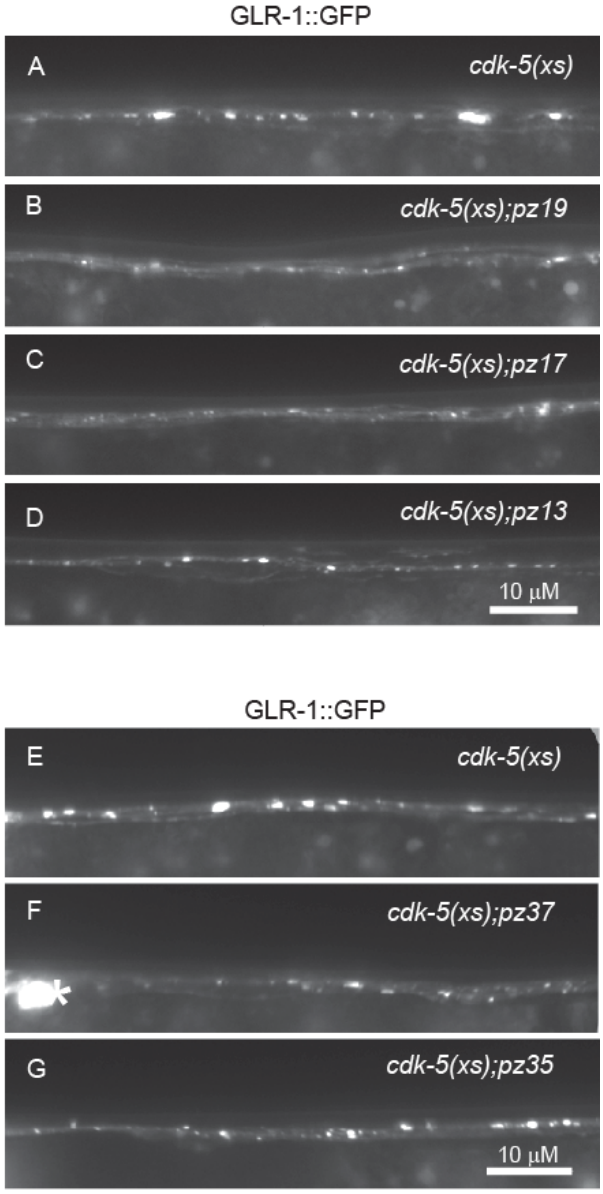

Figure 2-2. Isolation of five *cdk-5(xs)* suppressor mutants with decreased GLR-1::GFP in the VNC (A-G) Representative VNC images of animals over expressing *cdk-5 (cdk-5(xs))* (A, E), and five independent mutant lines from EMS mutagenesis, *cdk-5(xs);pz19* (B), *cdk-5(xs);pz17* (C), *cdk-5(xs);pz13* (D), *cdk-5(xs);pz37* (F) and *cdk-5(xs);pz35* (G), expressing GLR-1::GFP.

Figure 2-3.

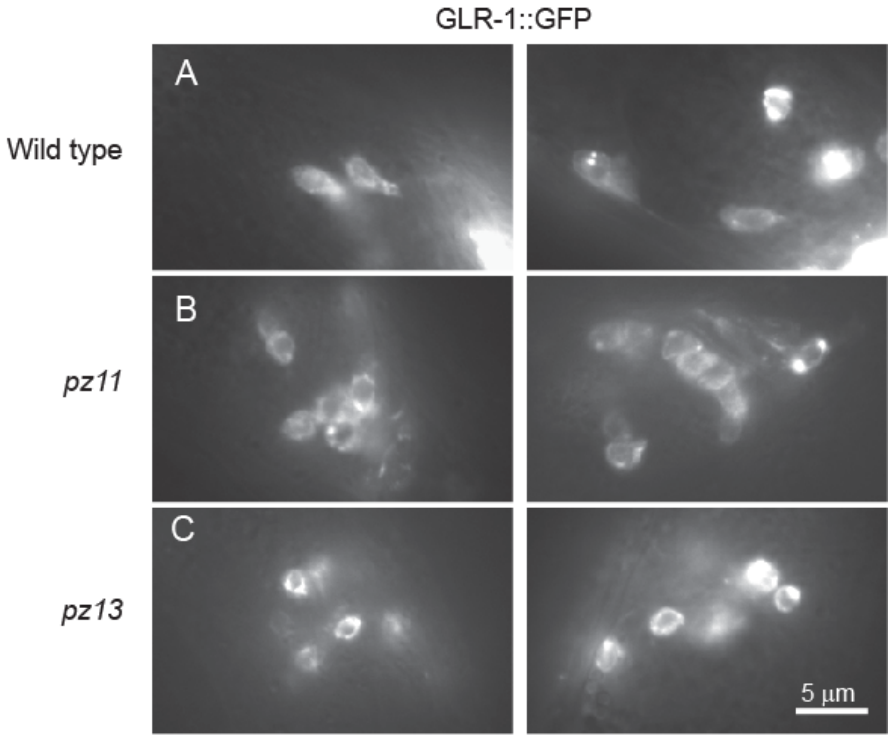

Figure 2-3. Two suppressor mutants alter GLR-1 distribution in the cell body

(A-C) Representative images of neuronal cell bodies in animals overexpressing *cdk-5 (cdk-5(xs))* (A), and two independent mutant lines from EMS mutagenesis, *cdk-5(xs); pz11* (B) and *cdk-5(xs); pz13* (C), expressing GLR-1::GFP.

Figure 2-4.

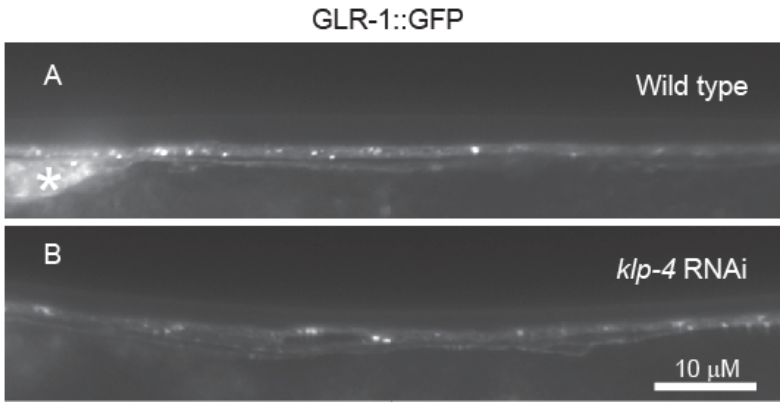

Figure 2-4. RNAi-mediated knockdown of *klp-4* decreased GLR-1 abundance in the VNC (A-B) Representative VNC images of RNAi-sensitized animals (*eri-1; lin-35*) animals (A), and *klp-4* knockdown *eri-1; lin-35* animals (B) expressing GLR-1::GFP. This reduction in GLR-1::GFP is seen in 60-70% of *klp-4* knockdown animals.

Figure 2-5.

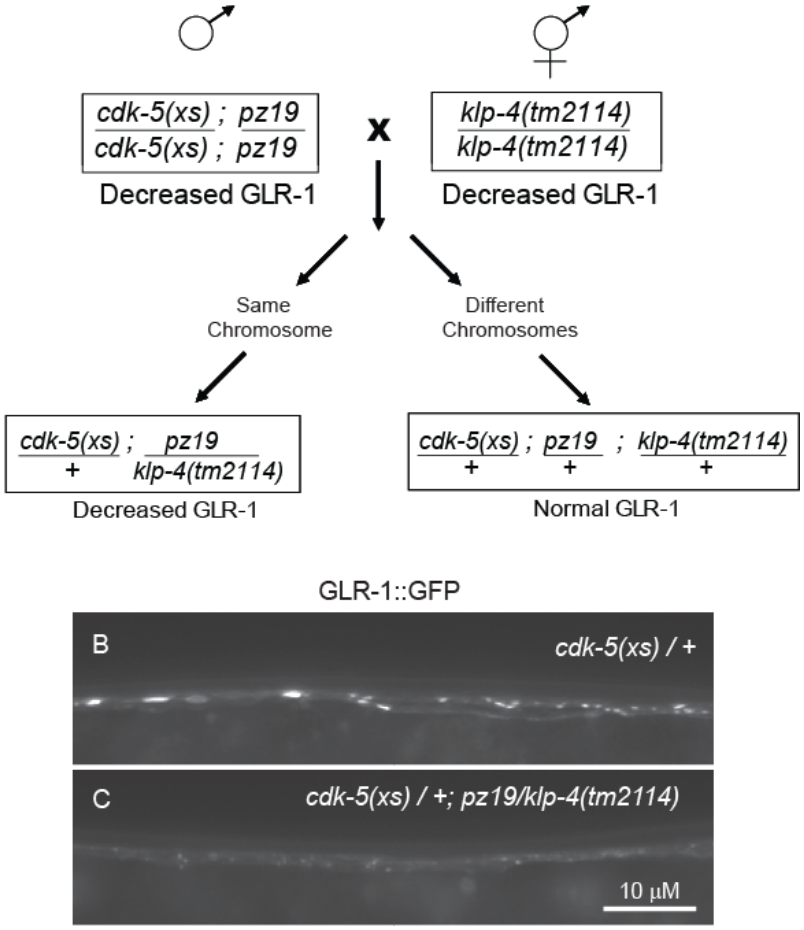

Figure 2-5. The *pz19* suppressor mutation does not complement *klp-4(tm2114)* (A) Diagram of non-complementation test. (B-C) Representative VNC images of *cdk-5(xs)/+* heterozygotes (B) and *cdk-5(xs)/+; pz19/klp-4(tm2114)* trans-heterozygous animals (C).

Table 2-1.

Allele	Strength of suppression	Plate # phenotpe	Additional notes
pz1	Good		
pz2	Strong		Most animals on F1 plate seemed suppressed
pz3	Good		
pz4	Good	4	
pz5			
pz6	Good	11	
pz7	Strong		
pz8	Strong	3	relaxed sinusoid at rest
pz9	Good		
pz10	Good		
pz11	Very Strong		some donut CB accumulation
pz12	Good	1, 5	GLR-1 appears stuck in CB (spots/golgi?)
pz13	Strong	1	Donut CB accumulation, looks like *ire-1 mutant*
pz14	Good	10	
pz15	Good	12	
pz16	Good		
pz17	Strong	2, 7	extra processes, some CB accumulation
pz18	Strong	2, 6	
pz19	Very Strong	3, 9	Curled on plate
pz20	Strong		
pz21	Strong		
pz22	Very Strong		few have ttx3::dsRED
pz23	Good	2, 3	
pz24	Strong	1	CB accumulation
pz25	Good		WT CB, some defasiculation
pz26	Good	1	CB accumulation (not like *ire-1* mutant)
pz27	Good	1, 2, 4	CB in NR very bright

Table 2-1. (contd.)

Allele	Strength of suppression	Plate phenotpe #	Additional notes
pz28	Medium		
pz29	Good	8	
pz30			
pz31			
pz32			
pz33	Good / Strong		
pz34	Good	8	
pz35	Medium		
pz36	Medium		
pz37	Strong	2	many don't express ttx-3::red
pz38	Medium		
pz39	Good / Strong	2	some males
pz40	Strong	4	
pz41	Strong		
pz42	Medium		
pz43	Strong		

Plate phenotype descriptions

1 = short / fat body	5 = irregular tail morphology	9 = curled body shape
2 = egg laying defect	6 = irregular vulval morphology	10 = pronounced sinusoid movement
3 = uncoordinated	7 = SLO	11 = twitches
4 = sterile	8 = bends body into coil	12 = slow growth / sick

Table 2-1*. cdk-5(xs)* suppressor mutants. Table of mutants isolated in *cdk-5(xs)* suppressor screen listed by *pz* allele number. For each mutant, the strength of suppression, plates phenotypes and any additional notes are listed.

CB = cell body, NR = nerve ring, *ttx3::dsRED* = *cdk-5(xs)* co-injection marker

Table 2-2 A.

Chromosome	Gene (mutation)	Plate phenotype
I	*bli-4(e937)*	blister growth along length of body
II	*rol-6(e187)*	rolling movement
III	*vab-7(e1562)*	abnormal tail morphology
IV	*unc-31(e928)*	uncoordinated movement
V	*dpy-11(e224)*	short / fat body shape
X	*lon-2(e678)*	long body

Table 2-2 B.

	I	II	III	IV	V	X	Mapped to
pz19		28% (18)	50% (8)			2% (50)	X
pz11		0% (22)	21% (19)			17% (30)	II
pz17						0% (55) *	X
pz18						11% (18)	n/a
pz13						0% (7)	n/a
pz12						24% (21)	n/a

*12 of 55 F2 animals singled as possible suppressors but 0 gave rise to suppressors in subsequent generation

Table 2-2. Mapping progress on *cdk-5(xs)* suppressor mutants (A) Names, chromosomal locations and description of plate phenotypes of mapping mutations. (B) Current mapping progress of *cdk-5(xs)* suppressor mutants. Data are presented as: % (*n*) , where % values indicate the percent of F2 animals in which the *cdk-5(xs)* suppressor phenotype was present in the respective homozygous plate mutant and (*n*) indicates number of homozygous plate mutants images for GLR-1::GFP.

Chapter 3

The kinesin-3 family motor KLP-4 regulates anterograde trafficking of GLR-1 glutamate receptors in the ventral nerve cord of *C. elegans*

Published in Molecular Biology of the Cell. *2012 Sep;23(18):3647-62. Epub 2012 Aug 1.*

Monteiro MI[1,2], Ahlawat S[3], Kowalski JR[1], Malkin E[1], Koushika SP[3], Juo P[1].

1. Department of Molecular Physiology and Pharmacology, Tufts University School of Medicine, Boston, MA 02111
2. Graduate Program in Cell and Molecular Physiology, Sackler School of Graduate Biomedical Sciences, Tufts University School of Medicine, Boston, MA 02111
3. Department of Biological Sciences, Tata Institute of Fundamental Research, Mumbai 400 005, India

Acknowledgments

Shikha Ahlawat and Sandhya Koushika contributed Figures 4, 5 and S6. Peter Juo drew Figure 8, performed co-migration experiment (Appendix 1), and contributed to Figure S1. All other experiments were performed by Michael Monteiro.

We would like to thank Josh Kaplan for strains and reagents, Ho-Yi Mak for Dendra2, Jeremy Dittman for custom written software, and Gian Garriga, Shohei Mitani (National Bioresource Project) and the *Caenorhabditis* Genetics Center for strains. We thank Victor Hatini for use of the Zeiss LSM510 confocal microscope and Stephen Straub for help with the Perkin Elmer Ultraview confocal microscope. We would like to thank Annette McGehee and Steven Garafalo for help in generating plasmids and strains, and the Juo lab for useful discussions and critical reading of this manuscript. This research was supported by National Institutes of Health (NIH) Grant NS059953 (P.J.), a Basil O'Connor March of Dimes Scholar Award (P.J.) and the Tufts Center for Neuroscience Research (NIH Grant P30 NS 047243). M.I.M. was supported in part by the Genetics and Development Training Grant (NIH Grant T32 HD 049341). J.R.K. was supported by the Training in Education and Critical Research Skills postdoctoral program (NIH Grant 5K12GM074869). S.A. was supported by a grant from DST (Government of India) and CSIR (Government of India) to S.P.K. Research in the laboratory of S.P.K. is supported by DBT (Government of India) and CSIR (Government of India).

Introduction

The neurotransmitter glutamate is responsible for the majority of fast excitatory synaptic transmission in the mammalian central nervous system. Activity-induced changes in synaptic strength are thought to be the cellular mechanism underlying learning and memory (Bredt and Nicoll, 2003; Shepherd and Huganir, 2007; Kessels and Malinow, 2009). One mechanism by which neurons regulate synaptic strength is through altering the number of glutamate receptors (GluRs) in the postsynaptic membrane. Many studies have focused on how activity-dependent exo- and endocytosis of AMPA-type GluRs regulate synaptic GluR abundance, however, much less is known about the mechanisms involved in the anterograde trafficking of GluRs from the cell body to synapses (Bredt and Nicoll, 2003; Shepherd and Huganir, 2007; Kessels and Malinow, 2009; van der Sluijs and Hoogenraad, 2011).

Kinesin and dynein superfamily proteins are ATP-dependent molecular motors that transport diverse cellular cargos along microtubules to various destinations in the cell (Vale, 2003 ; Goldstein *et al*., 2008; Hirokawa *et al*., 2010). Microtubule-dependent motors are essential for synapse development and synaptic transmission. Loss of motor function in *C. elegans*, *Drosophila* and mammalian neurons can result in the accumulation of cargo early in the secretory pathway and the mistrafficking of cargo to inappropriate subcellular compartments. For example, loss of function of kinesin UNC-104/KIF1A or kinesin UNC-116/KIF5 results in the accumulation of presynaptic cargos in neuronal cell bodies and axons, and in some cases, in the inappropriate trafficking of cargo into dendrites (Hall and Hedgecock, 1991; Ferreira *et al*., 1992; Okada *et al*., 1995; Yonekawa *et al*., 1998; Byrd *et al*., 2001; Sakamoto *et al*., 2005; Sieburth *et al*., 2005; Pack-Chung *et al*., 2007; Ou *et al*., 2010; Goodwin *et al.* 2012). Aberrant accumulation of cargo in neuronal processes is observed in several neurological diseases and can result in synaptic transmission defects,

paralysis and neurodegeneration (Yonekawa *et al.*, 1998; Martin *et al.*, 1999; Hafezparast *et al.*, 2003; Koushika *et al.*, 2004; Duncan and Goldstein, 2006; De Vos *et al.*, 2008). These studies illustrate the important role motor proteins play in the function and viability of neurons and suggest a link between inappropriate motor activity and neurodegenerative disorders.

Several microtubule-based motors are implicated in transporting AMPA receptors to synapses in mammalian cultured neurons. The microtubule minus-end directed motor cytoplasmic dynein transports AMPA receptors into proximal dendrites, which contain microtubules of mixed polarity (Kim and Lisman, 2001; Kapitein *et al.*, 2010). The scaffolding protein GRIP1 recruits AMPA receptors to the microtubule plus-end directed motor kinesin-1/KIF5 and steers the complex into dendrites (Kim and Lisman, 2001; Setou *et al.*, 2002). Finally, the kinesin-3 family motor UNC-104/KIF1A, which transports presynaptic cargo to synapses (Hall and Hedgecock, 1991; Okada *et al.*, 1995), has been implicated in trafficking AMPA receptors into dendrites via the scaffolding protein SYD-2/liprin-α (Wyszynski *et al.*, 2002; Shin *et al.*, 2003). These results illustrate a common theme in motor-dependent transport where one cargo utilizes multiple motors to reach its ultimate destination in the cell (Vale, 2003 ; Guzik and Goldstein, 2004; Hirokawa *et al.*, 2010).

The genetic model organism *C. elegans* has been used to identify many genes that are involved in GluR trafficking, however, the molecular motors involved in transporting GluRs from the cell body to synapses in *C. elegans* are not known. The *C. elegans* genome contains ten glutamate receptor subunits, two NMDA type and 8 non-NMDA type (Brockie *et al.*, 2001). GLR-1 is a non-NMDA receptor that is most homologous to AMPA-type glutamate receptors (Maricq *et al.*, 1995; Hart *et al.*, 1999; Brockie *et al.*, 2001). GLR-1 is expressed in a population of ventral cord interneurons where it is localized to sensory-

interneuron and interneuron-interneuron synapses (Hart *et al.*, 1995; Maricq *et al.*, 1995; Rongo *et al.*, 1998; Brockie *et al.*, 2001; Burbea *et al.*, 2002), and is required for several glutamate-dependent behaviors (Hart *et al.*, 1995; Maricq *et al.*, 1995; Zheng *et al.*, 1999; Mellem *et al.*, 2002; Chao *et al.*, 2004). In this study, we identify the kinesin KLP-4 as a novel regulator of glutamate receptor trafficking in *C. elegans.*

KLP-4 is a kinesin-3 family member that is distinct from UNC-104/KIF1A and most homologous to *Drosophila* kinesin Khc-73 and mammalian kinesins KIF13A and KIF13B. In *Drosophila*, Khc-73 regulates neuroblast polarity and mitotic spindle orientation, and has recently been shown to localize to endosomes (Siegrist and Doe, 2005; Huckaba *et al.*, 2011). In mammals, KIF13A transports the mannose-6-phosphate receptor from the *trans*-Golgi network to the plasma membrane (Nakagawa *et al.*, 2000), mediates endosomal sorting of cargo during melanosome biogenesis (Delevoye *et al.*, 2009), and regulates cytokinesis by recruiting PI(3)P and scission machinery to the midbody (Sagona *et al.*, 2010). KIF13B (also known as GAKIN) (Hanada *et al.*, 2000), mediates axonal polarity in hippocampal neurons in culture through its ability to transport PIP3-containing vesicles into axons (Venkateswarlu *et al.*, 2005; Horiguchi *et al.*, 2006).

We show here that KLP-4 promotes the abundance of the glutamate receptor GLR-1 in the ventral nerve cord (VNC). Genetic analysis and time-lapse data suggest that KLP-4 regulates the anterograde trafficking of GLR-1. We previously showed that cyclin-dependent kinase-5 (CDK-5) positively regulates the abundance of GLR-1 in the VNC (Juo *et al.*, 2007). Our genetic analyses indicate that KLP-4 functions in the same pathway as CDK-5 to regulate GLR-1 trafficking. Furthermore, we find that in the absence of functional KLP-4 motors, GLR-1 does not accumulate in the cell body but is instead targeted for degradation in the MVB/lysosome pathway. Our results suggest that regulating the amount or availability of a motor can influence the cellular fate of its cargo.

Results

Identification of KLP-4

We study GLR-1 trafficking in *C. elegans* by analyzing the distribution of GLR-1 tagged with GFP at an internal site in its cytoplasmic tail (GLR-1::GFP) (Rongo *et al.*, 1998). GLR-1::GFP, expressed under the *glr-1* promoter, localizes to puncta in the VNC (Fig. 1B). Greater than 80% of these puncta are closely apposed to presynaptic markers, indicating that the majority of GLR-1::GFP puncta in the VNC represent postsynaptic sites (Rongo *et al.*, 1998; Burbea *et al.*, 2002). Expression of GLR-1::GFP under its own promoter rescues the behavioral defects of *glr-1* null mutant animals indicating that the GFP-tagged receptor is functional (Rongo *et al.*, 1998).

In order to identify novel genes involved in GLR-1 trafficking, we took advantage of a previously identified gene, *cyclin-dependent kinase-5* (*cdk-5*), which regulates the abundance of GLR-1 in the VNC of *C. elegans* (Juo *et al.*, 2007). *cdk-5* loss-of-function mutants have decreased GLR-1 in the VNC and a corresponding accumulation of GLR-1 in the cell body. In contrast, overexpression of *cdk-5* results in increased levels of GLR-1 in the VNC (Juo *et al.*, 2007). We performed a forward genetic suppressor screen to identify mutants that blocked the effects of *cdk-5* overexpression on GLR-1 in the VNC. From this screen we isolated *pz19* as a strong suppressor mutant. Genetic mapping and sequencing analysis indicate that the *pz19* allele contains a mutation in the kinesin-3 family motor *klp-4* (see Materials and Methods). The *pz19* mutation corresponds to a single C to T point mutation (C3076T) in the cargo binding tail of *klp-4* that results in a premature stop codon (R1026Stop) (Figure 1A). The *C. elegans* genome encodes three kinesin-3 family members, UNC-104/KIF1A, KLP-4/KIF13 and KLP-6/KIF28 (alignment shown in Figure S1A) (Peden and Barr, 2005). KLP-4 is homologous to *Drosophila* Kinesin-73 (Khc-73) (48% identity) and mammalian KIF13A (46% identity) and KIF13B/GAKIN (44% identity)

(Figure 1A and S1B). KLP-4 is likely a microtubule plus-end-directed motor because its N-terminal motor domain is over 60% identical to the motor domains of plus-end-directed kinesins Khc-73, KIF13A and KIF13B (Figure 1A and S1B). In addition, KLP-4 contains the signature amino acids found in plus-end motors (Case *et al.*, 1997) (Figure S1). Of the two mammalian homologs, KLP-4 appears to be more closely related to KIF13A based on sequence identity and the lack of a microtubule plus-end binding CAP-Gly domain, which is found at the C-terminus of KLP13B (Figure 1A).

In order to investigate the expression pattern of *klp-4*, we generated a transcriptional reporter strain consisting of the *klp-4* promoter driving expression of GFP (*Pklp-4::GFP*). We found that *Pklp-4::GFP* is expressed in the pharynx, the intestine and throughout the nervous system including the nerve ring, and the lateral, dorsal and ventral nerve cords (Figure S2A-F and data not shown). This *klp-4* expression pattern is consistent with previous expression studies (McKay *et al.*, 2003; Hunt-Newbury *et al.*, 2007). In addition, *Pklp-4::GFP* is expressed in many head, tail and ventral cord neurons, including *glr-1*-expressing neurons based on the overlapping expression pattern of *Pklp-4::GFP* and a *glr-1* transcriptional reporter (*Pglr-1::dsRED*) (Figure S2, G-I)

Kinesin KLP-4 functions in GLR-1-expressing interneurons to positively regulate GLR-1 abundance

We initially identified *klp-4* mutants by their ability to suppress the effects of *cdk-5* over-expression on GLR-1. To determine whether mutation of *klp-4* alone affects the abundance of GLR-1 in the VNC in the absence of *cdk-5* overexpression, we examined the distribution of GLR-1::GFP in the anterior region of the VNC of *klp-4(pz19)* mutant animals. We found that *klp-4(pz19)* mutant animals expressing an integrated GLR-1::GFP transgene (*nuIs25*) exhibit a 37% decrease in GLR-1::GFP puncta intensity ($p<0.001$) and a 21%

decrease in puncta density ($p<0.001$) compared to wild type controls (Figure 1 B-C, G-H) (See Materials and Methods for quantification). We confirmed this effect by analyzing the distribution of GLR-1::GFP in a second, independent *klp-4* mutant, *klp-4(tm2114)*. The *tm2114* mutant allele corresponds to a 747 base pair deletion in *klp-4* resulting in the deletion of most of the motor domain followed by a frame shift and a premature stop codon near the end of the motor domain (Figures 1A and S1). Thus, *tm2114* likely represents a functional null mutant of *klp-4*. We found that *klp-4(tm2114)* mutants exhibit a 39% decrease in GLR-1::GFP puncta intensity ($p<0.001$) and a 27% decrease in puncta density ($p<0.001$) compared to wild type controls (Figure 1 B,E,G,H). Expression of wild type *klp-4* cDNA under the control of the *glr-1* promoter corrects the defects in GLR-1::GFP puncta intensities and densities in both *klp-4(pz19)* and *klp-4(tm2114)* mutants (Figure 1 D,F,G,H). In addition, GLR-1::GFP abundance decreases in *klp-4* mutants in the posterior VNC and in the nerve ring, suggesting that KLP-4 promotes GLR-1 levels at synapses throughout the neurons (Figure S3). Conversely, we found that increasing KLP-4 activity in wild type animals by overexpressing *klp-4* under control of the *glr-1* promoter results in increased levels of GLR-1 in the VNC (Figure S4). Taken together, these data indicate that KLP-4 functions in *glr-1*-expressing interneurons to positively regulate GLR-1 abundance in the VNC.

KLP-4 regulates GLR-1-dependent locomotion behavior

If KLP-4 regulates the synaptic levels of GLR-1, we might expect *klp-4* loss-of-function mutants and animals overexpressing *klp-4* to affect GLR-1 signaling and consequently glutamate-dependent behaviors, such as locomotion. *C. elegans* locomotion is characterized by periods of forward movement interrupted by brief periods of backward movement. The frequency of these spontaneous reversals is regulated by the level of

glutamatergic signaling (Zheng *et al.*, 1999). For example, animals with decreased glutamatergic signaling, such as mutants lacking *glr-1* or the vesicular glutamate transporter *eat-4*/VGLUT, exhibit decreased reversal frequencies (Zheng *et al.*, 1999; Burbea *et al.*, 2002), and conversely, animals with increased glutamatergic signaling have increased reversal frequencies (Zheng *et al.*, 1999; Burbea *et al.*, 2002; Juo and Kaplan, 2004; Schaefer and Rongo, 2006; Juo *et al.*, 2007). We found that *klp-4(tm2114)* mutants exhibit a small but significant ($p<0.05$) decrease in reversal frequency consistent with a decrease in glutamatergic signaling (Figure 1I). Conversely, we found that animals overexpressing *klp-4* (under control of the *glr-1* promoter) exhibit an increase in reversal frequency ($p<0.01$) consistent with increased glutamatergic signaling (Figure 1I). Importantly, this increase in reversal frequency was completely blocked by mutations in *glr-1* suggesting that the effect of KLP-4 on locomotion is dependent on endogenous GLR-1 (Figure 1I). Thus, loss- and gain-of-function of KLP-4 regulates GLR-1::GFP abundance in the VNC and has corresponding effects on GLR-1-dependent locomotion behavior.

KLP-4 does not affect the distribution of several other synaptic markers

The decrease in GLR-1::GFP in the VNC of *klp-4* mutants could be due to a decrease in synaptic connections. We tested this possibility by examining the distribution of the synaptic vesicle protein synaptobrevin tagged with GFP (SNB-1::GFP) in the VNC of wild type and *klp-4* mutant animals. We observed no difference in the intensity or density of SNB-1::GFP puncta in *klp-4* mutants compared to wild type controls (Figure 2A-D). We also analyzed the distribution of two other synaptic proteins that have been shown to colocalize with GLR-1 in the VNC, the PDZ protein LIN-10/Mint1 and the MAGUK protein, MAGI-1/S-SCAM (Rongo *et al.*, 1998; Emtage *et al.*, 2009). We found that the distribution of LIN-10::GFP (Figure 2E-H) and MAGI-1::YFP (Figure 2I-L) were unaltered in *klp-4* mutants when

compared to wild type controls. These results suggest that *klp-4* mutations do not result in a general defect in trafficking of synaptic proteins and *glr-1*-expressing interneurons likely have normal synaptic inputs in *klp-4* mutants. These data are consistent with a specific role for KLP-4 in regulating GLR-1 in the VNC.

KLP-4 is not required during early development to regulate GLR-1 in the VNC

To test more directly whether the decreased levels of GLR-1 observed in *klp-4* mutants could be due to defects in early development we expressed *klp-4* cDNA in *klp-4* mutants using a heat-shock inducible promoter (*hsp16.2*). We raised animals at 20^{o}C until the L4 stage of development, when all our static imaging is performed. We then induced expression of *klp-4* by shifting the animals to 30^{o}C and imaged GLR-1::GFP 16h later in adult animals. Similar to non-heat-shocked animals, we found that heat-shocked *klp-4(tm2114)* mutant animals exhibited a 27% decrease ($p<0.001$) in GLR-1::GFP puncta intensity in the VNC compared to heat-shocked wild type controls (Figure 2M-P). In contrast, heat-shocked *klp-4* mutants expressing *klp-4* cDNA under control of a heat-shock inducible promoter (*Phsp16.2::klp-4*), completely restored GLR-1::GFP puncta intensities to wild type levels (Figure 2M-P). These results suggest that KLP-4 is not required during early development to regulate GLR-1 levels in the VNC and that KLP-4 activity may be continuously required to maintain GLR-1 levels in the mature nervous system.

KLP-4 functions prior to endocytosis of GLR-1 at synapses in the VNC

One possible mechanism by which KLP-4 could regulate GLR-1::GFP abundance in the VNC is through regulation of *glr-1* transcription. If this were the case, we would expect decreased levels of *glr-1* transcript in *klp-4* mutants. We determined the relative amounts of *glr-1* to *act-1* (actin) mRNA in wild type, *klp-4(tm2114)* and *klp-4(pz19)* mutant animals using

real-time PCR. Rather than a decrease in transcription, we found that both *klp-4* mutants had an increase in *glr-1* transcript compared to wild type controls (Figure S5). This result indicates that the decrease in GLR-1::GFP in the VNC of *klp-4* mutants is not due to a decrease in *glr-1* transcription. The increased *glr-1* transcripts observed in *klp-4* mutants might be due to a compensatory feedback mechanism triggered by the decreased GLR-1 in the VNC.

We next tested whether KLP-4 was involved in one of several GLR-1 trafficking steps. GluRs are transported from the cell body to synapses, inserted into the postsynaptic membrane via exocytosis, internalized via endocytosis and subsequently either degraded in lysosomes or recycled back to the plasma membrane (Ehlers, 2000; Lin *et al.*, 2000; Shepherd and Huganir, 2007; van der Sluijs and Hoogenraad, 2011). Decreased GLR-1 levels observed in the VNC of *klp-4* mutants could be due to a function of KLP-4 in anterograde transport of GLR-1 from the cell body to the VNC or at one of the postendocytic trafficking steps (i.e. by inhibiting trafficking to the lysosome or by promoting reinsertion into the membrane). We tested whether *klp-4* functions prior to clathrin-mediated endocytosis at the plasma membrane by analyzing GLR-1 in the VNC of *klp-4;unc-11* double mutant animals. Mutations in the clathrin adaptin *unc-11*/AP180 result in defects in clathrin-mediated endocytosis (Zhang *et al.*, 1998; Nonet *et al.*, 1999), and the accumulation of GLR-1::GFP in the VNC (Burbea *et al.*, 2002). If KLP-4 acts at a step prior to GLR-1 endocytosis in the VNC (i.e. to promote the anterograde trafficking of GLR-1 from the cell body), we would expect *klp-4;unc-11* double mutants to have decreased GLR-1::GFP in the VNC as observed in *klp-4* single mutants. However, if KLP-4 functions at a postendocytic trafficking step, we would expect GLR-1::GFP to accumulate in the VNC of *klp-4;unc-11* double mutants as observed in *unc-11* single mutants. We found that *klp-4;unc-11* double mutants had decreased GLR-1::GFP fluorescence intensities in the VNC and this effect was

indistinguishable from *klp-4* single mutants (p=0.99) (Figure 3 A-E). Thus, mutations in *klp-4* prevent GLR-1::GFP accumulation in the VNC of *unc-11* mutants. This result suggests that KLP-4 acts prior to GLR-1 endocytosis at the synapse and is consistent with a role for this motor in the anterograde trafficking of GLR-1.

To investigate further whether KLP-4 acts prior to clathrin-mediated endocytosis and degradation of GLR-1 at the synapse, we tested whether *klp-4* mutations affect the abundance of a non-ubiquitinatable version of GLR-1::GFP. Clathrin-mediated endocytosis and degradation of GLR-1 in the lysosome is dependent on the ubiquitination of GLR-1 (Burbea *et al.*, 2002; Chun *et al.*, 2008; Kowalski *et al.*, 2011). Ubiquitination is a process in which the 76 amino acid protein ubiquitin is conjugated to lysine residues on target proteins. A mutant version of GLR-1::GFP that has all four intracellular lysine residues mutated to arginines (GLR-1(4KR)::GFP) cannot be ubiquitinated and therefore accumulates in the VNC (Burbea *et al.*, 2002). We analyzed the levels of GLR-1(4KR)::GFP in the VNC of *klp-4* mutants to test whether KLP-4 functions prior to degradation of GLR-1 at the synapse. We found that the fluorescence intensity of GLR-1(4KR)::GFP in the VNC decreased by 39% in the VNC of *klp-4* mutants compared to wild type controls, ($p<0.001$) (Figure 3 F-H). The magnitude of this decrease was similar to that observed with wild type GLR-1::GFP in *klp-4* mutants (Figure 1). These data suggest that KLP-4 functions prior to clathrin-mediated endocytosis and degradation of GLR-1 at synapses in the VNC, providing support for a role of KLP-4 in the anterograde trafficking of GLR-1.

KLP-4 promotes the anterograde transport of GLR-1

If KLP-4 functions as a motor to regulate the anterograde trafficking of GLR-1, we would expect KLP-4 to exhibit transport characteristics similar to other fast neuronal motors. We tagged KLP-4 with mCherry on its C-terminus and expressed the tagged motor in

interneurons using the *glr-1* promoter in order to investigate the subcellular localization and transport characteristics of KLP-4. We found that KLP-4::mCherry was localized to puncta in the cell body and throughout the VNC (Figure 4). Time-lapse microscopy and kymograph analysis revealed that KLP-4::mCherry puncta were mobile in cell bodies and the VNC and moved with an average velocity of 1.0 μm/s and an average run length of 9.2 μm (Figure 4 and Supplemental Videos 1 and 2). This velocity of KLP-4 is comparable to the average *in vitro* velocities observed for other kinesin-3 family motors such as Khc-73, KIF13A and KIF13B (Okada *et al.*, 1995; Horiguchi *et al.*, 2006; Huckaba *et al.*, 2011), and *in vivo* velocity of GFP-tagged UNC-104 (Zhou *et al.*, 2001), and indicates that KLP-4 is a fast neuronal motor that is mobile in interneuron cell bodies and VNC processes.

To test directly whether KLP-4 regulates GLR-1 transport, we first analyzed the movement of GLR-1::GFP puncta in the VNC of wild type and *klp-4* mutant animals using time-lapse microscopy and kymograph analysis (Figure S6) (see Materials and Methods). The vast majority of GLR-1::GFP expressing ventral cord neurons possess cell bodies in the head of the animal and send processes towards the tail, however two GLR-1::GFP expressing neurons that contribute processes to the VNC possess cell bodies in the tail (White *et al.*, 1976; Hart *et al.*, 1995; Maricq *et al.*, 1995; Brockie *et al.*, 2001). In wild type animals, we observed that GLR-1::GFP puncta moved with a maximum velocity of 2.2 μm/s from the head towards the tail and 2.7 μm/s from the tail towards the head. For GLR-1::GFP puncta moving from the head towards the tail, the average velocity was 1.0 μm/s and the average run length was 9.1 μm. Time-lapse analysis of *klp-4* mutants revealed several differences in the movement of GLR-1::GFP puncta from the head towards the tail in the VNC compared to wild type animals. First, there was a 31% decrease in the flux of GLR-1::GFP puncta in *klp-4* mutants compared to controls ($p<0.005$) (Figure S6). Second, the average run length of mobile GLR-1::GFP puncta was decreased by 45% ($p<0.005$) (Figure

S6) and the average pause frequency was increased by 56% in *klp-4* mutants compared to wild type ($p<0.005$) (average No. pauses/μm: Wild type: 0.09±0.008; *klp-4*: 0.14±0.007, $p<0.001$). This reduced run length combined with the increased pause frequency of GLR-1::GFP puncta in *klp-4* mutants is consistent with an overall reduction in the processivity of cargo motion. Third, the average velocity of GLR-1::GFP puncta was decreased by 32% in *klp-4* mutants compared to controls ($p<0.005$) (average head to tail velocity (μm/s): Wild type: 1.0±0.02 (n=158); *klp-4*: 0.67±0.05 (n=196), $p<0.001$). We found no significant differences in any of the parameters for GLR-1::GFP puncta moving in the VNC from the tail towards the head (Figure S6) (average tail to head velocity (μm/s): Wild type: 1.29±0.06 (n=79); *klp-4*: 1.29±0.06 (n=68); $p>0.05$). Taken together with our previous data, these results suggest that KLP-4 positively regulates trafficking of GLR-1::GFP from the head towards the tail in the VNC. Because the majority of *glr-1* expressing cell bodies are in the head, these data implicate a role for KLP-4 in the anterograde trafficking of GLR-1.

In order to measure anterograde trafficking of GLR-1 more accurately, we repeated our time-lapse analysis on transgenic animals (*pzIs18*) expressing GLR-1 tagged with the photoconvertible fluorescent protein Dendra2. Dendra2 fluorescence is irreversibly converted from green to red by ultra-violet light providing an optical method to photolabel and track a defined population of proteins within cells (Gurskaya *et al.*, 2006; Chudakov *et al.*, 2007). We used a confocal microscope to locally photoconvert GLR-1::Dendra2 from green to red in cell bodies of *glr-1*-expressing head neurons (Figure 5A) of wild type and *klp-4* mutants, and performed time-lapse microscopy of the red mobile GLR-1::Dendra2 puncta in the VNC about 20 minutes post-conversion (Figure 5D-H). Control experiments show that prior to photoconversion or immediately after local photoconversion of neuron cell bodies in the head, there is no red GLR-1::Dendra2 signal in the VNC (Figure 5B and data not shown), whereas 20 minutes postconversion, we observe red GLR-1::Dendra2 puncta in the

VNC (Figure 5C). Time-lapse analysis of red GLR-1::Dendra2 puncta moving in the anterograde direction revealed an average anterograde velocity of 1.0 μm/sec in wild type animals. Similar to our analysis of mobile GLR-1::GFP, we found that *klp-4* mutants had a 44% decrease in anterograde flux ($p<0.005$) (Figure 5D-E, G), a 32% decrease in anterograde run length ($p<0.005$) (Figure 5D-E, H), and a 26% decrease in anterograde velocity [average Anterograde velocity (μm/s): Wild type: 1.0±0.02 (n=165); *klp-4*: 0.73±0.01 (n=120), $p<0.001$)] of red GLR-1::Dendra2 puncta compared to wild type controls. The low number of retrogradely moving puncta at this time point precluded accurate quantitative analysis of retrograde movement. Taken together, these data suggest that KLP-4 promotes the anterograde trafficking of GLR-1 from neuronal cell bodies in the head to the VNC.

CDK-5 and KLP-4 act in the same genetic pathway to regulate GLR-1 in the VNC.

Because we initially identified *klp-4* in a *cdk-5* genetic suppressor screen and have previously implicated CDK-5 in regulating the anterograde trafficking of GLR-1 (Juo et al., 2007), we repeated our time-lapse analysis of mobile, red GLR-1::Dendra2 puncta in the VNC of *cdk-5* mutant animals. As described above, GLR-1::Dendra2 was locally photoconverted in head neuron cell bodies and red GLR-1::Dendra2 puncta movements in the VNC were measured in wild type and *cdk-5* mutant animals. Similar to our *klp-4* mutant data, we found that *cdk-5* mutants had a 42% decrease in anterograde GLR-1::Dendra2 flux ($p<0.005$) (Figure 5D, F, G) and a 32% decrease in anterograde run length ($p<0.005$) (Figure 5D, F, H). However, we observed no change in the anterograde velocity of GLR-1 in *cdk-5* mutant animals (average anterograde velocity (μm/s): Wild type 1.0±0.02 (n=165); *cdk-5*: 1.0±0.02 (n=151), $p>0.05$). Time-lapse analysis of GLR-1::GFP in the VNC of *cdk-5* mutants revealed similar decreases in GLR-1 transport (Figure S6). These data indicate that, similar to KLP-4, CDK-5 promotes the anterograde trafficking of GLR-1 in the VNC.

Because *cdk-5* and *klp-4* mutants have very similar defects in GLR-1 trafficking, we performed two complementary experiments to formally test whether *cdk-5* and *klp-4* function in the same genetic pathway. First, we analyzed the abundance of GLR-1::GFP in the VNC of animals with mutations in both *cdk-5(gm336)* and *klp-4(tm2114)* (Figure 6A-E). The *gm336* allele is a predicted molecular null (Juo *et al*., 2007). If *cdk-5* and *klp-4* act in separate genetic pathways, we would expect that the combination of the two mutations would cause an additive decrease in GLR-1::GFP levels in the VNC compared to either single mutant. Conversely, if *cdk-5* and *klp-4* act in the same genetic pathway, then *cdk-5;klp-4* double mutants would have non-additive effects on GLR-1::GFP levels compared to the single mutants. We found that the puncta intensity of GLR-1::GFP in the VNC of *cdk-5;klp-4* double mutants decreased by 44% compared to wild type controls ($p<0.001$) and was not significantly different from either single mutant ($p=0.1$ vs *klp-4*, $p=0.5$ vs *cdk-5*) (Figure 6A-E). Similarly, GLR-1::GFP puncta densities in *cdk-5;klp-4* double mutants were not significantly different from either single mutant (average puncta density (per 10μm)±SEM: Wild type: 2.88±0.08; *cdk-5*: 2.56±0.14; *klp-4*: 2.55±0.08; *cdk-5;klp-4*: 2.25±0.08, $p<0.001$ vs WT, $p=0.11$ vs *cdk-5*, $p=0.09$ vs *klp-4*), suggesting that *cdk-5* and *klp-4* function in a common pathway. Second, we tested whether *klp-4* mutations could prevent the ability of overexpressed *cdk-5* to increase GLR-1::GFP abundance in the VNC. We previously showed that overexpression of *cdk-5* in *glr-1* expressing neurons [*cdk-5(xs)*] causes an increase in GLR-1::GFP puncta intensities and widths in the VNC (Juo *et al*., 2007). If *klp-4* acts in the same genetic pathway as *cdk-5*, we would expect mutations in *klp-4* to completely occlude the effects of *cdk-5* overexpression on GLR-1::GFP abundance. We found that GLR-1::GFP puncta intensity and width in *cdk-5(xs);klp-4(tm2114)* animals are identical to *klp-4(tm2114)* single mutant animals (Figure 6F-J) (average puncta width (μm)±SEM: Wild type: 0.84±0.02; *cdk-5(xs)*: 1.1±0.03, $p<0.001$; *klp-4(tm2114)*: 0.83±0.03;

cdk-5(xs);klp-4: 0.74±0.02 p=0.2 vs *klp-4* and p<0.001 vs *cdk-5(xs)*). Similarly, the effects of overexpressed *cdk-5* on GLR-1::GFP puncta intensity and width were occluded by a second *klp-4(pz19)* loss-of-function mutant (Figure S7) (average puncta width (μm)±SEM: Wild type: 0.89±0.03; *cdk-5(xs)*: 1.3±0.06, p<0.001 vs WT; *klp-4(pz19)*: 0.87±0.03; *cdk-5(xs);klp-4*: 0.84±0.03, p=0.4 vs *klp-4* and p<0.001 vs *cdk-5(xs)*). These results suggest that *cdk-5* and *klp-4* act in the same genetic pathway to regulate the trafficking of GLR-1 in the VNC.

GLR-1 accumulates in *klp-4* mutant cell bodies under conditions of decreased degradation

We have previously shown that GLR-1::GFP decreases in the VNC and accumulates in cell bodies of *cdk-5* mutant animals (Juo *et al.*, 2007) (Figure 6). Because our analysis of *cdk-5* and *klp-4* double mutants suggest that these genes function in the same genetic pathway, we tested whether *klp-4* mutations also result in the accumulation of GLR-1::GFP in the cell body. Surprisingly, we observed no difference in the amount of GLR-1::GFP in *klp-4* mutant cell bodies compared to wild type controls (p=0.08) (Figure 7A and B). One possible explanation for the lack of GLR-1::GFP accumulation in *klp-4* mutant cell bodies is that in the absence of functional KLP-4 motors, GLR-1 is targeted for degradation in the cell body. We tested this hypothesis using two approaches to inhibit the degradation of GLR-1. GLR-1 is ubiquitinated and targeted for degradation in the MVB/lysosome pathway and this process likely occurs in both the VNC and cell body (Burbea *et al.*, 2002; Chun *et al.*, 2008; Kowalski *et al.*, 2011). As mentioned above, degradation of GLR-1 in this pathway can be prevented by using a non-ubiquitinatable version of GLR-1 (GLR-1(4KR)::GFP) (Burbea *et al.*, 2002). In the first approach, we measured the levels of non-ubiquitinatable GLR-1(4KR)::GFP in the cell bodies of wild type and *klp-4* mutants. We found that GLR-1(4KR)::GFP abundance in the cell body increases by 58% in *klp-4* mutants compared to

wild type controls (Figure 7C and D). Similarly, GLR-1(4KR)::GFP levels in the cell body also increases in *cdk-5* mutants compared to controls (Figure 7C and D). This result demonstrates that in contrast to wild type GLR-1::GFP, which does not accumulate in *klp-4* mutant cell bodies, GLR-1(4KR)::GFP does accumulate in *klp-4* mutant cell bodies. In the second approach, we inhibited the degradation of GLR-1 in the MVB/lysosome pathway by expressing a dominant-negative version of *vps-4 (vps-4(dn))*. VPS-4 is an AAA-ATPase required for the formation of MVBs and degradation of ubiquitinated proteins in the MVB/lysosome pathway (Babst et al., 2002; Katzmann et al., 2002). Expression of *vps-4(dn)* in interneurons results in increased GLR-1::GFP abundance in the cell body and VNC (Figure 7 and data not shown) (Chun *et al.*, 2008; Kowalski *et al.*, 2011). We measured the levels of GLR-1::GFP in cell bodies of wild type and *klp-4* mutants expressing *vps-4(dn)*. We found that GLR-1::GFP abundance increased by 34% in *klp-4* mutant cell bodies expressing *vps-4(dn)* compared to cell bodies expressing *vps-4(dn)* alone (Figure 7E-F). Thus, inhibiting the degradation of GLR-1 in the MVB/lysosome pathway by expressing *vps-4(dn)* results in the accumulation of GLR-1::GFP in wild type cell bodies and this cell body accumulation is enhanced in *klp-4* mutant animals. Taken together, these experiments suggest that in the absence of functional KLP-4 motors, GLR-1 is inefficiently trafficked to synapses in the VNC and, instead of accumulating in the cell body, is targeted for degradation in the MVB/lysosome pathway.

Discussion

The trafficking of GluRs to synapses is important during synapse formation in development and during synaptic plasticity in the mature nervous system (Shepherd and Huganir, 2007; Kessels and Malinow, 2009; van der Sluijs and Hoogenraad, 2011). Although much research has focused on the insertion and removal of glutamate receptors at synapses, less

is known about the mechanisms involved in transporting receptors from the cell body to synapses. Here we describe a function for the kinesin-3 family motor, KLP-4, for the first time and identify KLP-4 as a novel regulator of glutamate receptor trafficking in *C. elegans*.

KLP-4 regulates anterograde trafficking of GLR-1

Several pieces of evidence suggest that KLP-4 functions in interneurons to promote the anterograde trafficking of GLR-1. First, the abundance of GLR-1::GFP decreases in the VNC of two independent *klp-4* loss-of-function mutants and is rescued by expression of wild type *klp-4* under the control of the *glr-1* promoter (Figure 1). Second, KLP-4 functions prior to GLR-1 endocytosis and degradation at the synapse because *klp-4* mutations prevent the accumulation of GLR-1 at synapses in the VNC when endocytosis is blocked with *unc-11*/AP180 mutations or when receptor ubiquitination and degradation is prevented (Figure 3). Third, time-lapse imaging revealed that several aspects of the anterograde trafficking of GLR-1 including anterograde flux, velocity and run length are decreased in *klp-4* mutants (Figure 5 and S6). The role of KLP-4 in promoting the anterograde trafficking of GLR-1 receptors is consistent with the function of a mammalian homolog of KLP-4, KIF13A, which has been shown to transport Mannose-6-Phosphate receptors from the *trans*-golgi network (TGN) to the plasma membrane in non-neuronal cells (Nakagawa *et al.*, 2000).

Previous work in mammalian neurons has demonstrated that multiple motors are required for efficient GluR trafficking (Setou *et al.*, 2000; Setou *et al.*, 2002; Wyszynski *et al.*, 2002; Shin *et al.*, 2003; Kapitein *et al.*, 2010). Our data are consistent with the idea that KLP-4 functions together with other motors to transport GLR-1 from the TGN in the cell body to synapses in the VNC. In *klp-4* mutants, there is a 40% decrease in the abundance of GLR-1 (Figure 1) and a 38% decrease in the anterograde flux of GLR-1 (Figure 5 and S6) in the VNC. Thus, although GLR-1 trafficking is greatly reduced in *klp-4* mutants, it is not

eliminated, suggesting that other mechanisms exist to traffic GLR-1 to synapses in the VNC**.** We propose that KLP-4 functions together with other motors to regulate the anterograde trafficking of GLR-1 from the TGN to synapses in the VNC (see Model in Figure 8).

One possible model is that KLP-4 functions in the cell body and VNC together with other motors to transport GLR-1 to synapses (Figure 8). In support of this model, our data show that KLP-4 can move processively in the VNC at a velocity that is comparable to GLR-1::GFP (Figure 4 and Supplemental Video 1). Alternatively, KLP-4 could function in the cell body to transport GLR-1-containing endosomes to the cell periphery where GLR-1 is then loaded onto other motors for trafficking in the VNC (Figure 8). Consistent with this model, we were able to observe co-migration of KLP-4::mCherry and GLR-1::GFP in neuronal cell bodies (Supplemental Video 2). Interestingly, KLP-4 homologs in other organisms have been shown to associate with and traffic RAB-5 and PI(3)P-containing early endosomes to the cell periphery (Hoepfner *et al.*, 2005; Horiguchi *et al.*, 2006; Delevoye *et al.*, 2009; Huckaba *et al.*, 2011). Although our initial attempts to observe co-migration of KLP-4 and GLR-1::GFP in the VNC were unsuccessful, we cannot rule out a direct role of KLP-4 in transporting GLR-1 in the VNC because it remains possible that our imaging conditions are not sensitive enough to detect cargo being moved by one or a few motors. Regardless of whether KLP-4 functions with other motors in the cell body and/or the VNC, our data show that KLP-4 is required for the efficient trafficking and accumulation of GLR-1 at synapses. In the future, it will be interesting to identify other motors that function together with KLP-4 and to understand how multiple motors coordinate trafficking of GLR-1 cargo.

CDK-5 functions in the same pathway as KLP-4 to regulate GLR-1

Genetic analysis of the *unc-11*/AP180 clathrin adaptin mutant together with *cdk-5* (Juo *et al.*, 2007) or *klp-4* mutants (Figure 3) suggest that both CDK-5 and KLP-4 act prior to

endocytosis of GLR-1 in the VNC. In addition, genetic analysis of *cdk-5;klp-4* double mutants and *klp-4* mutants overexpressing *cdk-5* suggest that CDK-5 and KLP-4 function in the same pathway to regulate GLR-1 in the VNC (Figures 6). Furthermore, our time-lapse analyses revealed that anterograde trafficking of GLR-1 is reduced to a similar extent in both *cdk-5* and *klp-4* mutants (Figure 5 and S6), suggesting that CDK-5 may directly regulate KLP-4-dependent trafficking of GLR-1. However, *cdk-5* and *klp-4* have different effects on GLR-1 in the cell body. Our data show that GLR-1 accumulates in *cdk-5* but not *klp-4* mutant cell bodies (Figure 7), suggesting that CDK-5 may also function prior to KLP-4 to make receptors competent for KLP-4-dependent anterograde trafficking. Further studies will be necessary to investigate the precise mechanism by which CDK-5 regulates KLP-4-dependent GLR-1 trafficking. However, we anticipate that the effect of CDK-5 on trafficking will be specific to the particular cargo and neuronal cell type being investigated given the many different effects of CDK-5 on axonal and dendritic trafficking (Ratner *et al.*, 1998; Morfini *et al.*, 2004; Juo *et al.*, 2007; Ou *et al.*, 2010; Park *et al.*, 2011; Goodwin *et al.*, 2012). Intriguingly, although GLR-1 does not accumulate in *klp-4* mutant cell bodies, the receptor does accumulate if receptor degradation in the MVB/lysosome pathway is blocked by expression of *vps-4(dn)* or non-ubiquitinatable GLR-1(4KR) (Figure 7). These data suggest that in the absence of the kinesin *klp-4*, GLR-1 is targeted, likely in an ubiquitin-dependent manner, for degradation in the MVB/lysosome pathway (Figure 8). Interestingly, studies in yeast indicate that membrane proteins can be targeted for degradation early in the secretory pathway. For example, ubiquitination of the amino acid permease Gap1p in the Golgi can target the protein to a pre-multivesicular endosome where it can either be sent to the vacuole for degradation or recycled back to the Golgi for transport to the plasma membrane (Helliwell *et al.*, 2001; Risinger and Kaiser, 2008).

Recent studies suggest that vesicular cargo may be targeted for degradation in the

absence of motors or cargo adaptors. In mammalian neurons lacking the adaptor protein AP-4, AMPA receptors are not trafficked to dendrites but instead accumulate in autophagosomes, which often results in protein degradation when they fuse with lysosomes (Matsuda *et al.*, 2008). In *C. elegans*, amyloid precursor protein APL-1 is normally trafficked from the cell body to the plasma membrane of neuronal processes by kinesins UNC-104/KIF1A and UNC-116/KIF5 (Wiese *et al.*, 2010). Loss of function of either of these motors results in decreased levels of APL-1 in neuronal processes. However, instead of accumulating in neuronal cell bodies of these motor mutants, APL-1 protein levels decrease implying that APL-1 may be degraded in the absence of its normal motors (Wiese *et al.*, 2010). Interestingly, another study demonstrated that antisense oligonucleotide knockdown of kinesin KIF17 expression results in decreased protein levels of its cargo, the NMDA receptor NR2B subunit (Guillaud *et al.*, 2003). These studies are consistent with our data showing that GLR-1 is targeted for degradation in the MVB/lysosome pathway in the absence of KLP-4 motors. Together, these data suggest an interesting potential cellular regulatory mechanism that targets cargo for degradation in the absence of its appropriate anterograde motor or adaptor. Such a mechanism could prevent excess membrane proteins from accumulating early in the secretory pathway, which may be detrimental to the neuron. These results imply that the fate of GLR-1 receptors early in the secretory pathway, and consequently the abundance of GLR-1 at synapses, could be controlled by regulating the expression level or availability of KLP-4 motors.

Implications for synaptic plasticity

Regulation of the number of glutamate receptors in the postsynaptic membrane contributes to activity-dependent synaptic plasticity. In particular, many studies have focused on the activity-dependent regulation of exocytosis and endocytosis of AMPA

receptors at the synapse (Shepherd and Huganir, 2007; van der Sluijs and Hoogenraad, 2011). However, other studies suggest that activity-dependent regulation of GluRs can also occur earlier in the secretory pathway. For example, activity-blockade regulates alternative splicing of NMDA receptor subunit NR1 resulting in increased ER exit and synaptic levels of the receptor (Mu *et al*., 2003). In *C. elegans*, *glr-1* splicing and the abundance of GLR-1 at synapses can be regulated by the RNA binding protein GRLD-1 (Wang *et al*., 2010). Interestingly, several studies suggest that anterograde motors are limiting in neurons and that regulation of motor expression influences synaptic plasticity. For example, overexpression of KIF17 in the mouse forebrain increases expression and trafficking of its cargo NMDA receptors to synapses resulting in increased spatial and working memory (Wong *et al*., 2002). Activity can influence motor/cargo expression because activity-blockade of NMDA receptors results in the coordinated upregulation of the NMDA receptor and its KIF17 motor (Guillaud *et al*., 2003). In addition, raising mice in an enriched-environment results in BDNF-dependent upregulation of KIF1A and transport of its cargoes in the hippocampus (Kondo *et al*., 2012). Similarly, in *Aplysia*, neuronal activity results in increased expression of kinesin heavy chain motors and its cargoes, and upregulation of the motor is required and sufficient for long-term synaptic plasticity (Puthanveettil *et al*., 2008). These studies show that regulation of motor expression can impact synaptic plasticity and that activity-dependent expression of motors is coordinated with expression of their respective cargoes. Our work identifies KLP-4 as a novel motor that regulates anterograde trafficking of GluRs and reveals an interesting regulatory mechanism where expression or availability of the motor influences receptor degradation and ultimately the abundance of GLR-1 in the VNC. Future studies will be necessary to determine whether GLR-1 and KLP-4 expression are coordinated *in vivo* and whether this concerted regulation influences synaptic plasticity.

Materials and Methods

Strains

The following strains were used in this study: *nuIs25* (P*glr-1::glr-1::gfp*), *nuIs24* (P*glr-1*::*glr-1::gfp*), *nuIs108* (P*glr-1*::*glr-1(4kr)::gfp*), *nuIs125* (P*glr-1*::*snb-1::gfp*), *nuIs145* [P*glr-1*::*vps-4 (dn*)], *pzIs2* (P*glr-1::cdk-5*), *pzIs15 (*P*glr-1::dsRED), pzIs18 (*P*glr-1::Dendra2)*, *pzIs20* (P*glr-1*::*klp-4*), *nuEx993* (P*glr-1*::*lin-10::gfp*)*, nuEx1004* (P*glr-1::magi1::yfp*), *pzEx167 (*P*glr-1::klp-4), pzEx169 (Pglr-1::klp-4), pzEx188* (P*glr-1*::*klp-4::gfp), *pzEx234* (P*glr-1*::*klp-4::mCherry*), *pzEx237* (P*hsp-16.2*::*klp-4*), *pzEx244 (*P*klp4::NLS::GFP::LacZ), pzEx256* (P*klp-4*::*GFP), klp-4(tm2114), klp-4(pz19), unc-11(e47)*, *cdk-5(gm336),* and *glr-1(n2461).* All strains were maintained at 20°C as described previously (Brenner, 1974).

Transgenes and germline transformation

Standard techniques were used to isolate transgenic strains by microinjection of various plasmids. *nuIs24, nuIs25*, *nuIs125*, *nuEx993*, *nuEx1004*, *nuIs108, nuIs145* and *pzIs2* have been described previously (Rongo *et al.*, 1998; Burbea *et al.*, 2002; Juo and Kaplan, 2004; Juo *et al.*, 2007; Chun *et al.*, 2008; Kowalski *et al.*, 2011). The *klp-4* (F56E3.3) open reading frame (ORF) was obtained by reverse transcription-PCR from cDNA isolated from wild type animals. The *klp-4* cDNA was put under control of the *glr-1* promoter by subcloning *klp-4* into pV6 using NheI/KpnI restriction sites to create P*glr-1*::*klp-4*. *pzEx169* and *pzEx167* were created by injecting P*glr-1*::*klp-4* plasmid at 25ng/μL along with co-injection marker P*myo-2*::*NLS::mCherry* (10ng/μL). *pzIs20* (P*glr-1::klp-4*) was created by UV integrating *pzEx167*. *pzEx188* (P*glr-1*::*klp-4::gfp*) and *pzEx234* (P*glr-1*::*klp-4::mcherry*) were constructed by subcloning GFP or mCherry flanked by NotI restriction sites into a plasmid containing (P*glr-1::klp-4*) with a NotI restriction site engineered immediately before

the *klp-4* stop codon. These constructs were injected at 25ng/μL (*pzEx188*) or 100ng/μL (*pzEx234*) along with injection marker P*myo2*::*NLS-mCherry* (5ng/μL). *pzEx237* (P*hsp-16.2*::*klp-4::mCherry*) was made by subcloning the *klp-4::mCherry* coding sequence from (P*glr-1::klp-4::mCherry*) into the NheI/KpnI restriction sites of the heat shock promoter plasmid pPD49.78 (gift from Dr. Andrew Fire). P*hsp-16.2*::*klp-4::mCherry* was injected at 25ng/μL along with injection marker P*myo2*::*NLS-mCherry* (5ng/μL). *pzEx244 (*P*klp-4::NLS::GFP::LacZ)* was made by PCR amplifying the 3kb segment of genomic DNA immediately upstream of the *klp-4* coding region flanking it with PstI/BamHI restriction sites and subcloning it into the GFP expression plasmid pPD96.04 (gift from Dr. Andrew Fire). This construct was injected at 25ng/μL. *pzEx256* (P*klp-4*::*gfp*) was generated by subcloning the *klp-4* promoter from (P*klp-4*::*NLS::GFP::LacZ*) into the PstI/BamHI restriction sites of the GFP expression plasmid pPD95.75 (gift from Dr. Andrew Fire). This construct was injected at 25ng/μL along with injection marker P*myo2*::*NLS-mCherry* (5ng/μL). The plasmid KP#889 (P*glr-1*::*dsRED*) (gift from Dr. Lars Dreier) was injected at 25ng/μL to make *pzEx96* and UV integrated to generate *pzIs15 (*P*glr-1::dsRED*). Dendra2 (gift from Dr. HoYi Mak) was subcloned into HindIII sites flanking the *gfp* coding sequence in (P*glr-1*::*glr-1::gfp*) to make (P*glr-1*::*glr-1::dendra2*). This construct was injected at 25ng/μL along with co-injection marker P*ttx3*::*GFP* at 50ng/μL to make *pzEx160* and subsequently UV integrated to generate *pzIs18* (P*glr-1*::*glr-1::dendra2*). All constructs were confirmed by sequencing. Full details of plasmids and oligonucleotides are available upon request.

Fluorescence imaging

All static images of the ventral nerve cord (VNC) were taken of the anterior portion of the ventral nerve cord, posterior to the RIG and AVG neuronal cell bodies in larval stage 4 (L4) animals unless otherwise stated. Images of the posterior nerve cord in Figure S3 were taken

posterior to the vulva. Nerve ring images in Figure S3 were taken immediately anterior to the terminal bulb of the pharynx. Imaging of heat-shocked animals shown in Figure 2 was performed on young adult animals. For all images of the VNC, animals were immobilized in 30 mg/mL 2,3-butanedione monoxamine (Sigma-Aldrich) for 5–7 min before imaging. Imaging was performed using a Carl Zeiss Axioimager M1 microscope with a 100x Plan Apochromat (1.4 numerical aperture) objective with GFP filter and captured with an Orca-ER CCD camera (Hamamatsu) using MetaMorph (version 7.1) software (Molecular Devices). To quantitate VNC fluorescence, maximum intensity projections from Z-series stacks of 1 µm total depth were used. For nerve ring images Z-series stacks of 3 µm total depth were used. Exposure settings and gain were set to fill the 12 bit dynamic range and to avoid saturation. Settings were identical for each image acquired within an experiment for a given fluorescent marker. MetaMorph (version 6.0) software was used to generate line scans of maximum intensity projection images of the VNC. Linescans were analyzed with Igor Pro (version 5 or 6) (Wavemetrics) using custom-written software (gift from J. Dittman) as described previously (Burbea *et al.*, 2002). The fluorescence intensity of 0.5 µm FluoSphere beads (Invitrogen) was measured for each day of imaging and used to normalize daily arc lamp intensity. Puncta intensities were normalized to the average bead intensity for the corresponding day. Puncta intensities are shown normalized to wild type. Puncta widths were calculated by measuring the width of each punctum at half the maximal peak fluorescence intensity. Puncta densities represent the average number of puncta per 10 µm of the ventral nerve cord. For all imaging quantification in the VNC, average ± SEM values are reported, and statistical significance was determined using the Student's *t* test for experiments in which two genotypes were compared or the Tukey-Kramer test for experiments comparing more than 2 genotypes.

To quantify the amount of GLR-1::GFP in interneuron cell bodies, images were

taken of PVC cell bodies, and maximum intensity projections were generated from *Z*-series stacks (2 µm total depth) as described previously (Juo *et al*., 2007; Kowalski *et al*., 2011). Average pixel intensities of two to three separate regions of each cell body were measured using MetaMorph (version 7.1) software.

Heat shock was performed by shifting L4 stage animals from normal growth conditions at 20°C to 30°C for 16 hours. Following heat shock, animals were allowed to recover at 20°C for at least one hour prior to imaging.

Time-lapse imaging and data analysis

For all *in vivo* time-lapse imaging of the VNC, 1 day adult hermaphrodites were immobilized with 3mM levamisole in M9 and mounted on a 2% agarose pad. VNC Imaging was performed in an anterior region (70-80 µm) of the VNC just posterior to the RIG and AVG neuronal cell bodies.

VNC time-lapse image acquisition. GLR-1::GFP time-lapse images were obtained with an OLYMPUS IX81 microscope using a Plan Apochromat objective (100X, 1.4 NA) attached with a spinning disk confocal head (YOKOGAWA CSU22) and equipped with an EMCCD camera (ANDORiXon-897EMCCD). KLP-4::mCherry time-lapse images were obtained with an Andor Spinning Disk confocal microscope.

Photoconversion and time-lapse imaging of GLR-1::Dendra2. GLR-1::Dendra2 was locally photoconverted in neuronal cell bodies in the head in a 10x20µm ROI using a 405nm laser on a ZEISS LSM 510 meta-confocal with a 60X/1.45 NA oil objective (Carl Zeiss, Jena, Germany). Prior to photoconversion, interneuron cell bodies in the head were identified using a 488nm Argon laser (30mW) at low 2% power (60X objective, scan speed of 400Hz

and 100μm pinhole size) to avoid accidental photoconversion of Dendra2. Photoconversion was performed using a 405nm Diode laser (25mW) at 20% power for 4-5 mins (60x objective, scanspeed of 200 Hz, pinhole size 100μm). Twenty minutes after local photoconversion of the cell bodies in the head, time-lapse images of the VNC were obtained using an Andor Spinning Disk confocal microscope using a Plan Apochromat objective (100x, 1.4 NA) attached to a spinning disk confocal head (YOKOGAWA CSU22) and equipped with an EMCCD camera (ANDORiXon-897EMCCD). We focused on the VNC using the 488nm laser (25mW) at 10% power (100x objective, 150ms exposure). There was no accidental photoconversion of Dendra2 using these conditions. Time-lapse imaging of photoconverted red GLR-1::Dendra2 in the VNC was performed using a 561nm laser (25mW) at 60-80% power (100x objective, exposure of 300ms/image).

VNC time-lapse analysis. Moving particles were defined as puncta that were displaced by at least 3 pixels in successive time frames, while stationary particles were defined as puncta that were immobile for more than three consecutive frames. The flux of particles was calculated as the number of puncta moving in either direction in a 15-20 μm region (just posterior to the RIG and AVG cell bodies) divided by the total time. Run length was calculated as the length in microns of each distinct movement event in the x-coordinate plane. The start and end of each movement event was defined by pauses, reversals or length of movie. Images (512x512 pixels) were acquired at a constant framerate of 3-4 frames per second for a total of 300-400 frames. Image analysis was performed using Image J software (version 1.37, NIH) and statistical significance was determined using the Student's *t* test.

Co-migration time-lapse imaging. Co-migration time-lapse imaging of GLR-1::GFP and

KLP-4::mCherry were performed on animals expressing both GLR-1::GFP (*nuIs25*) and KLP-4::mCherry under control of the *glr-1* promoter (*pzEx234).* Time-lapse imaging was performed using a Perkin-Elmer Ultraview Spinning Disk confocal microscope and assembled into time-lapse movies using Velocity and Quick Time software.

Real-Time PCR

Total RNA was isolated from mixed-stage wild-type *(nuIs25)* and *klp-4* mutant [*nuIs25*;*klp-4(tm2114)* or *nuIs25; klp-4(pz19)]* animals using an RNeasy fibrous tissue kit (Qiagen) as previously described (Kowalski *et al*., 2011). First strand cDNA was synthesized using Superscript III Reverse Transcriptase (Invitrogen), and real-time PCR was performed using the Brilliant SYBR Green Master Mix and SureStart Taq (Stratagene) on the MX3000P real-time PCR machine (Tufts Center for Neuroscience Research). Standard curves were used to calculate the efficiency of primers for both *glr-1* and *act-1* and the relative amount of *glr-1* mRNA compared to *act-1* mRNA in each of 6 replicate samples was determined as previously described (Pfaffl, 2001). The ratio of *glr-1* : *act-1* mRNA in *klp-4(tm2114)* and *klp-4(pz19)* mutant animals was normalized to that in wild type animals. For all genotypes Mean ± SEM of n=3 replicates of two different starting cDNA concentrations was determined.

Locomotion Behavior Assay

The spontaneous reversal assay was performed as previously described (Kowalski *et al*., 2011). Fresh standard NGM agar plates were poured and allowed to dry at room temperature. Young adult hermaphrodites were transferred using halocarbon oil from a plate with food to the center of a fresh NGM standard plate without food and allowed to acclimate to the plate for two minutes. The number of spontaneous reversals was recorded over the

subsequent 5 minutes. The genotypes of the animals being studied in the behavioral assay were coded so that they were unknown to the experimenter during the observation period. The average number of reversals per minute ± SEM was determined for each genotype.

EMS mutagenesis and mutations

The *klp-4(pz19)* allele was isolated in a forward genetic suppressor screen for mutants that suppressed the effects of overexpressed *cdk-5* (*pzIs2*) on GLR-1::GFP (*nuIs24*). An F1 clonal screen was performed by mutagenizing *nuIs24;pzIs2* animals with Ethyl methane sulfonate (EMS) and screening F2 progeny on a compound microscope for mutants with decreased abundance of GLR-1::GFP in the VNC. Briefly, synchronized L4 animals were incubated with 5 mM EMS at room temperature for 4 hours as previously described (Brenner, 1974). After removal of EMS, the treated animals were allowed to recover on NGM plates with food until movement resumed. Mutagenized L4 animals were transferred to fresh NGM plates and incubated at 20^{o}C to allow for growth of the F1 generation. 100 young adult F1 animals were singled and incubated at 20^{o}C. F2 animals were screened for GLR-1::GFP abundance in the VNC as detailed above. *pz19* was one of the strong suppressor mutants isolated in this screen and was mapped to the X chromosome using standard genetic mapping techniques. A parallel, independent RNAi screen for genes that decrease GLR-1::GFP in the VNC also identified *klp-4* as a gene that regulates GLR-1 and aided our mapping of *pz19*. Sequencing of the exons and intron/exon junctions of *klp-4* revealed that the *pz19* allele contains a C to T point mutation at nucleotide 3076 resulting in a premature stop codon at amino acid 1026 (Arg1026Stop) in the ORF of KLP-4 (numbering based on F56E3.3a splice form). The *klp-4* deletion allele *tm2114* was isolated by Shohei Mitani (National Bioresource Project) and consists of a 747-base pair deletion. The

tm2114 allele deletes exons 4-6 of *klp-4*, eliminating over half of the motor domain including the microtubule binding sites, and thus likely represents a functional null mutant. The *tm2114* deletion also causes a frame shift resulting in a predicted premature stop codon after the first 167 amino acids of KLP-4 eliminating the entire cargo binding tail. *pz19* fails to complement *tm2114* in a non-complementation test.

FIGURE 3-1.

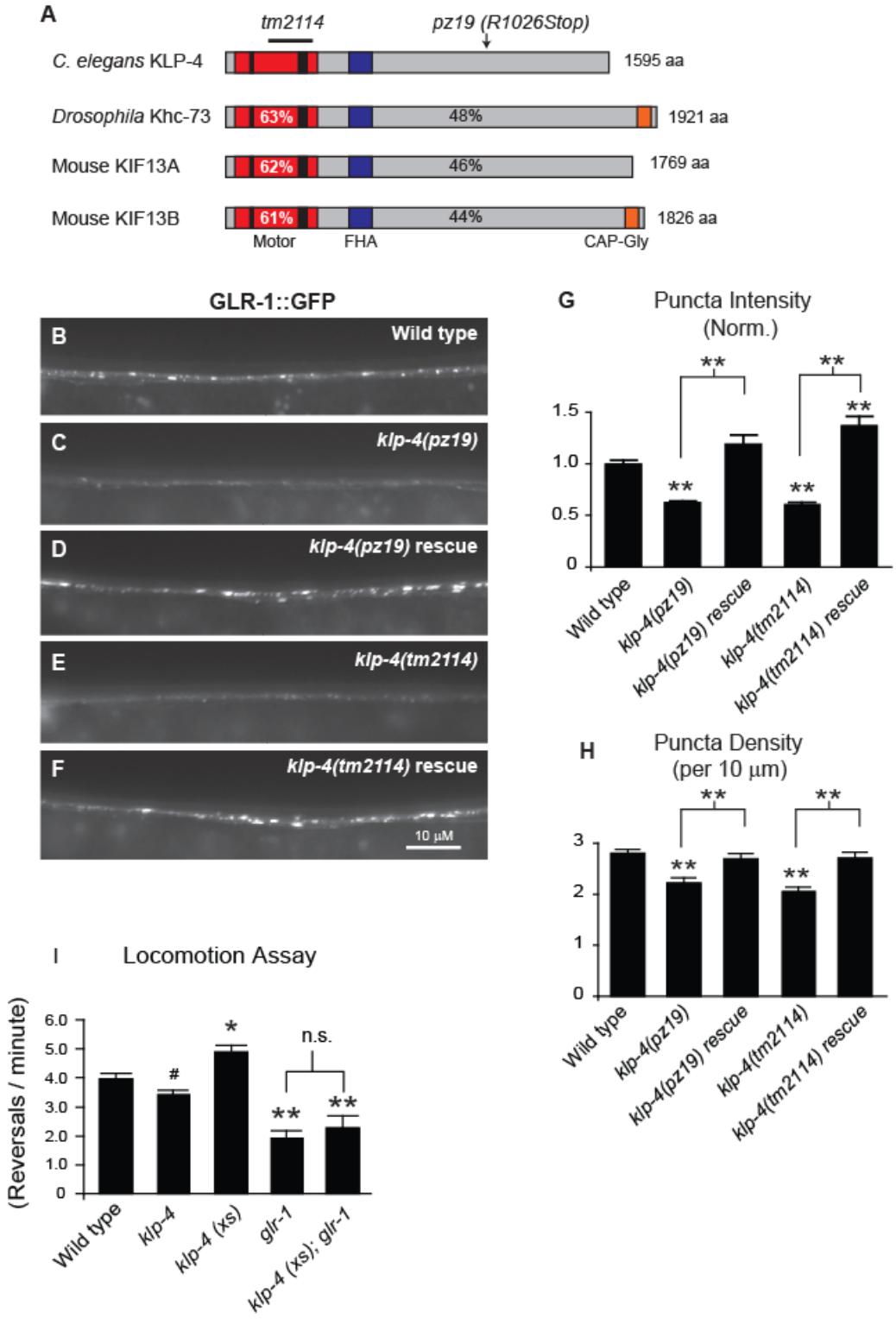
A
tm2114
pz19 (R1026Stop)
C. elegans KLP-4
1595 aa
Drosophila Khc-73
63%
48%
1921 aa
Mouse KIF13A
62%
46%
1769 aa
Mouse KIF13B
61%
44%
1826 aa
Motor
FHA
CAP-Gly
GLR-1::GFP
B Wild type
C klp-4(pz19)
D klp-4(pz19) rescue
E klp-4(tm2114)
F klp-4(tm2114) rescue
10 µM
G
Puncta Intensity (Norm.)
1.5
1.0
0.5
0
Wild type
klp-4(pz19)
klp-4(pz19) rescue
klp-4(tm2114)
klp-4(tm2114) rescue
H
Puncta Density (per 10 µm)
3
2
1
0
I
Locomotion Assay
(Reversals / minute)
6.0
5.0
4.0
3.0
2.0
1.0
0
n.s.
Wild type
klp-4
klp-4 (xs)
glr-1
klp-4 (xs); glr-1

FIGURE 3-1. The kinesin KLP-4 functions in the VNC to regulate the abundance of GLR-1 and GLR-1-dependent behavior. (A) Protein domain organization of *C. elegans* KLP-4, *Drosophila* Khc-73 and mouse KIF13A and KIF13B. The N-terminal motor domain (red box) containing the signature ATP binding motif (thin black bar) and MT binding regions (thick black bar), the cargo binding domain (gray box), the Fork-head associated domain (FHA) (purple box) and the microtubule plus-end binding domain (CAP-Gly) (orange box) are shown. The percent identity of the motor domain of *C. elegans* KLP-4 (white percentages) or full length KLP-4 (black percentages) versus *Drosophila* Khc73, mouse KIF13A and KIF13B are indicated. (B-F) Representative images of the anterior VNC of larval stage 4 (L4) wild-type (B), *klp-4(pz19)* (C), rescued *klp-4(pz19)* (D), *klp-4(tm2114)* (E), and rescued *klp-4(tm2114)* (F) animals expressing an integrated GLR-1::GFP transgene *(nuIs25)*. In these and all subsequent images anterior is to the left and ventral is up. (G-H) Quantification of GLR-1::GFP puncta intensities (normalized) (G) and densities (H) for the strains pictured in B-F. Means and SEM are shown for $n = 38$ wild type, $n = 23$ *klp-4*(*pz19)*, $n = 21$ rescued *klp-4(pz19)*, $n = 20$ *klp-4(tm2114),* and $n = 21$ rescued *klp-4(tm2114)* animals. (I) Quantification of number of spontaneous reversals per minute for $n = 20$ wild-type, $n = 20$ *klp-4(tm2114)*, $n = 23$ animals expressing an integrated *klp-4* transgene under the control of the *glr-1* promoter (*klp-4(xs)*) *(pzIs20)*, $n = 14$ *glr-1(n2461)*, and $n = 13$ *glr-1(n2461)* animals overexpressing *klp-4* (*klp-4(xs)*). Values that differ significantly from wild type are indicated by asterisks above each bar, whereas other comparisons are marked by brackets (**$p \leq 0.001$, *$p \leq 0.01$, #$p \leq 0.05$, Tukey-Kramer Test).

FIGURE 3-2.

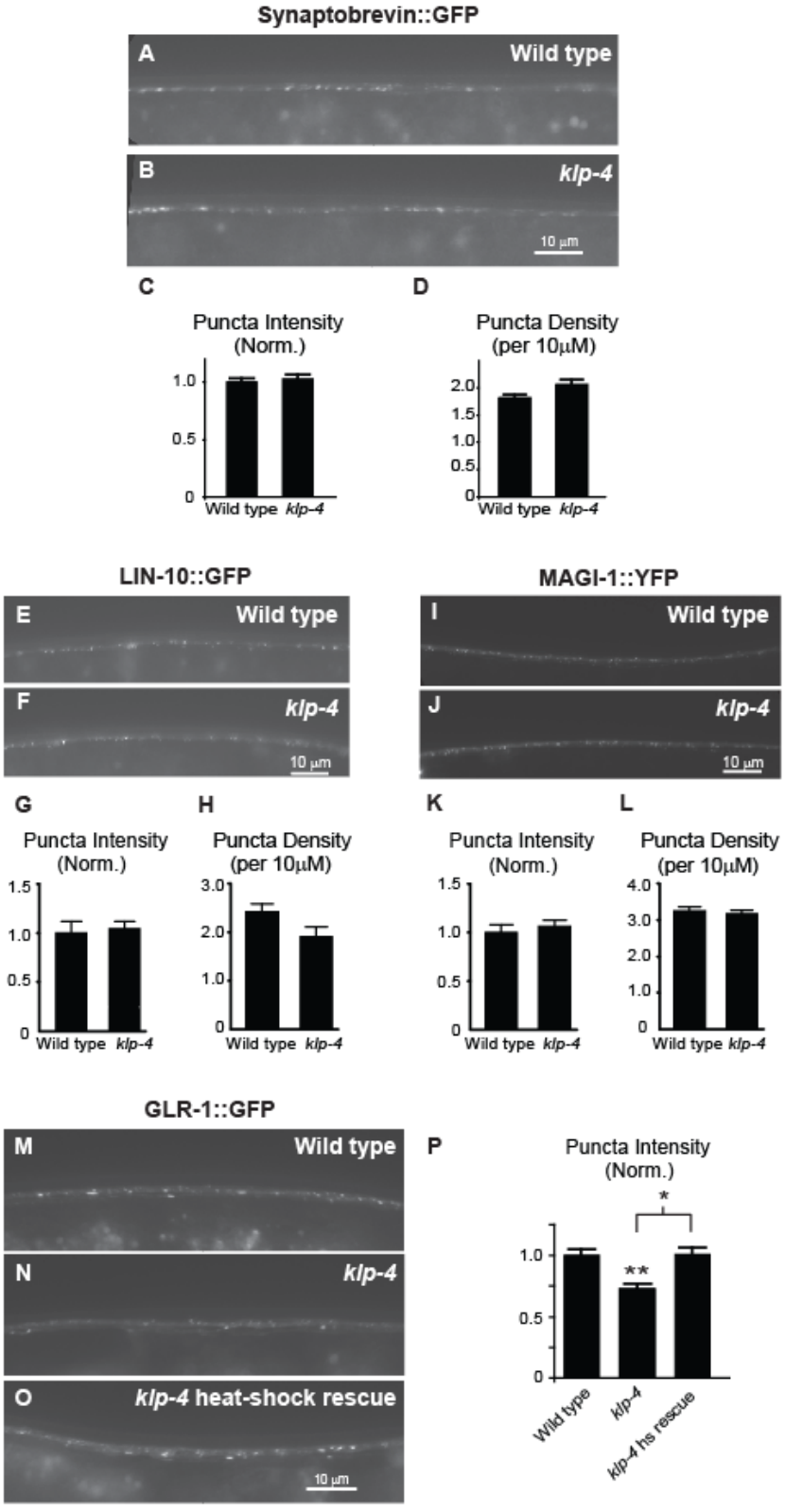
Synaptobrevin::GFP
A
Wild type
B
klp-4
10 µm
C
Puncta Intensity (Norm.)
1.0
0.5
0
Wild type
klp-4
D
Puncta Density (per 10µM)
2.0
1.5
1.0
0.5
0
Wild type
klp-4
LIN-10::GFP
E
Wild type
F
klp-4
10 µm
G
Puncta Intensity (Norm.)
1.5
1.0
0.5
0
Wild type
klp-4
H
Puncta Density (per 10µM)
3.0
2.0
1.0
0
Wild type
klp-4
MAGI-1::YFP
I
Wild type
J
klp-4
10 µm
K
Puncta Intensity (Norm.)
1.5
1.0
0.5
0
Wild type
klp-4
L
Puncta Density (per 10µM)
4.0
3.0
2.0
1.0
0
Wild type
klp-4
GLR-1::GFP
M
Wild type
N
klp-4
O
klp-4 heat-shock rescue
10 µm
P
Puncta Intensity (Norm.)
*
**
1.0
0.5
0
Wild type
klp-4
klp-4 hs rescue

FIGURE 3-2. KLP-4 does not affect the distribution of multiple synaptic markers and is not required during early development to regulate GLR-1. (A-B, E-F, I-J) Representative images of the anterior VNC of L4 wild-type (A, E, I) and *klp-4(tm2114)* (B, F, J) animals expressing either Synaptobrevin::GFP (*nuIs125)*(A-B), LIN-10::GFP (*nuEx993*) (E-F) or MAGI-1::YFP (*nuEx1004*)(I-J) under the control of the *glr-1* promoter. (C-D, G-H, K-L) Quantification of puncta intensities (normalized)(C, G, K) and densities (D, H, L) for the strains pictured. Mean and SEM are shown for at least $n = 20$ animals per genotype. No significant difference was found in puncta fluorescence intensities or densities between wild-type and *klp-4* mutant animals for any of the synaptic markers ($p>0.05$, Student's *t* test). (M-O) Representative images of the anterior VNC of adult wild-type (M), *klp-4(tm2114)*(N), and heat-shock rescued *klp-4(tm2114)* (O) animals expressing GLR-1::GFP *(nuIs25)* after 16h heat-shock. Heat-shock rescued *klp-4* mutant animals express wild type *klp-4::mCherry* under control of the heat-shock inducible promoter (*pzEx237*). (P) Quantification of GLR-1::GFP puncta intensities (normalized) for the strains pictured in M-O. Means and SEM are shown for $n = 18$ wild type, $n = 35$ *klp-4*(*tm2114)*, and $n = 23$ heat-shock rescued *klp-4(tm2114)* animals. Values that differ significantly from wild type are indicated by asterisks above each bar, whereas other comparisons are marked by brackets (**$p \leq 0.001$, *$p \leq 0.01$ Tukey-Kramer Test).

FIGURE 3-3

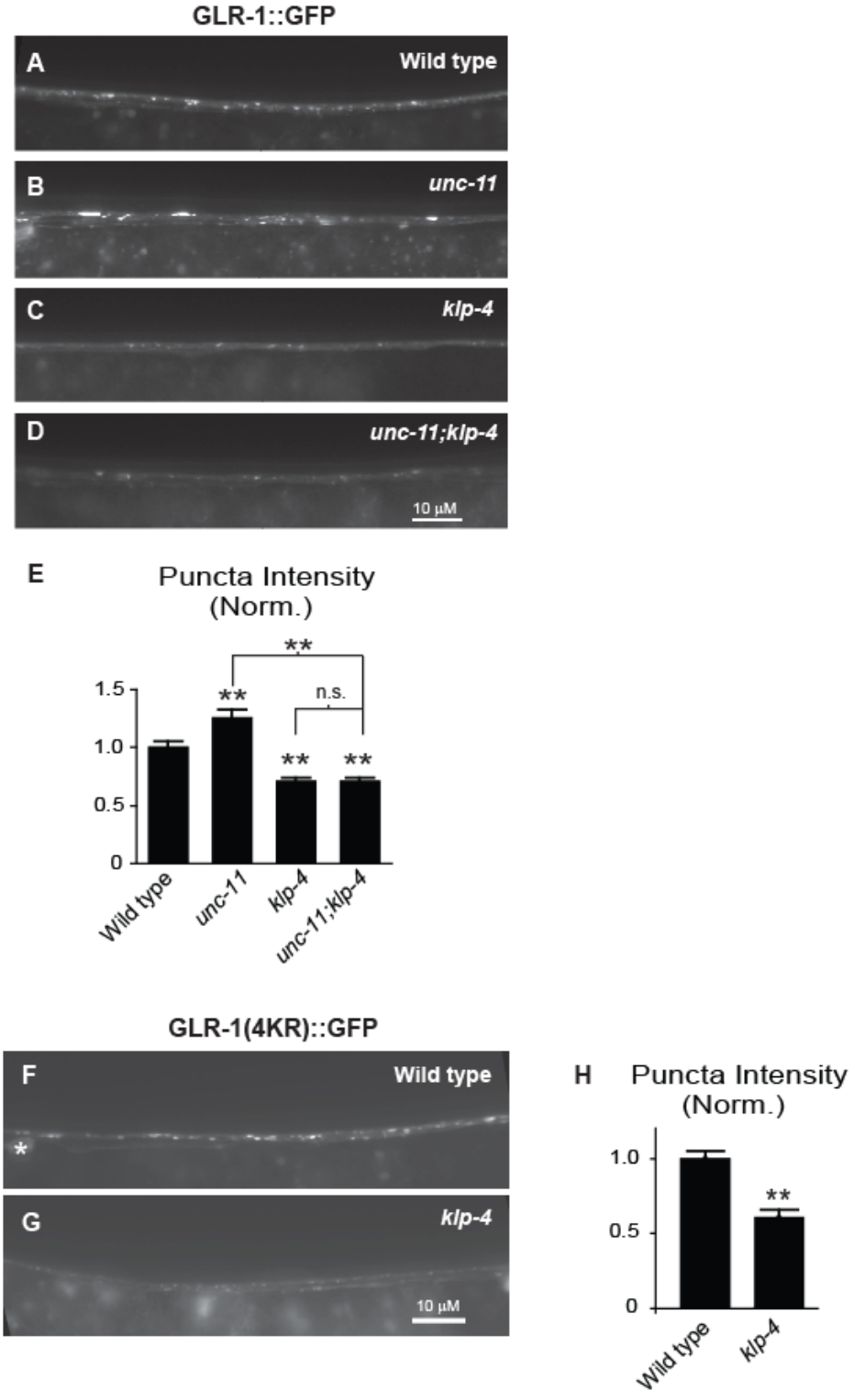
GLR-1::GFP
A
Wild type
B
unc-11
C
klp-4
D
unc-11;klp-4
10 µM
E
Puncta Intensity
(Norm.)
**
**
n.s.
**
**
1.5
1.0
0.5
0
Wild type
unc-11
klp-4
unc-11;klp-4
GLR-1(4KR)::GFP
F
Wild type
*
G
klp-4
10 µM
H
Puncta Intensity
(Norm.)
1.0
0.5
0
**
Wild type
klp-4

FIGURE 3-3. KLP-4 functions prior to GLR-1 endocytosis in the VNC. (A-D) Representative images of the anterior VNC of wild type (A), *unc-11(e47)* (B), *klp-4 (tm2114)* (C) and *unc-11(e47);klp-4(tm2114) (*D) L4 animals expressing GLR-1::GFP *(nuIs25)*. (E) Quantification of GLR-1::GFP puncta intensities (normalized) for the strains pictured in A-D. Mean and SEM are shown for $n = 24$ wild type, $n = 25$ *unc-11,* $n = 22$ *klp-4* and $n = 22$ *unc-11;klp-4* animals. (F-G) Representative images of the anterior VNC of wild type (F) and *klp-4(tm2114)* (G) L4 animals expressing GLR-1(4KR)::GFP under the control of the *glr-1* promoter (*nuIs108)*. The white asterisk marks a neuronal cell body. (H) Quantification of GLR-1(4KR)::GFP puncta intensities (normalized) for the strains pictured in F-G. Mean and SEM are shown for $n = 25$ wild type and $n = 19$ *klp-4* animals. (E, H) Values that differ significantly from wild type are indicated by asterisks above each bar, whereas other comparisons are marked by brackets (**$p \leq 0.001$, Tukey-Kramer test). n.s. represents no significant difference ($p>0.05$).

FIGURE 3-4

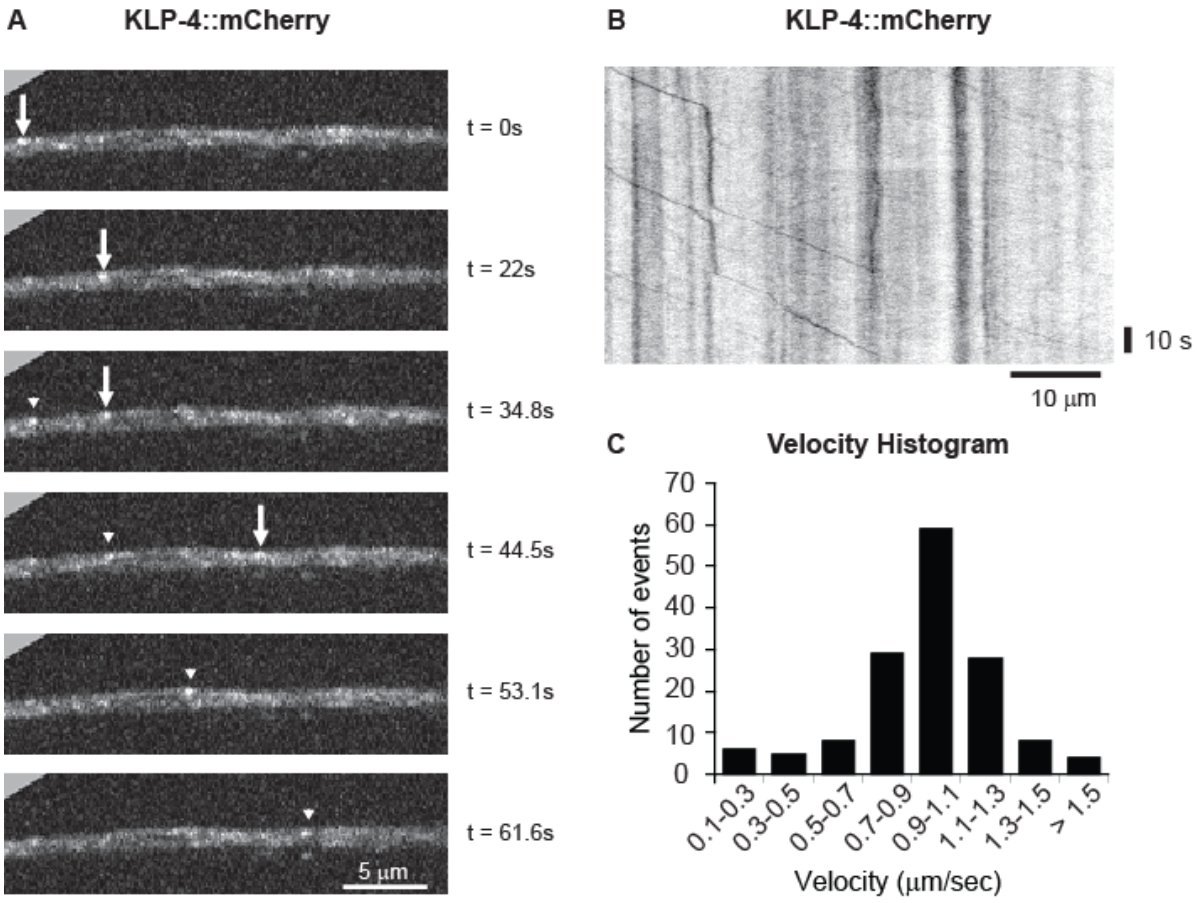
A
KLP-4::mCherry
t = 0s
t = 22s
t = 34.8s
t = 44.5s
t = 53.1s
t = 61.6s
5 µm
B
KLP-4::mCherry
10 s
10 µm
C
Velocity Histogram
Number of events
70
60
50
40
30
20
10
0
0.1-0.3
0.3-0.5
0.5-0.7
0.7-0.9
0.9-1.1
1.1-1.3
1.3-1.5
> 1.5
Velocity (µm/sec)

FIGURE 3-4. KLP-4 is a fast neuronal motor that moves in the VNC. (A) Individual frames from a time-lapse movie (Supplemental Video 1) show KLP-4::mCherry puncta in the anterior VNC of young adult wild type animals expressing KLP-4::mCherry under the control of the *glr-1* promoter (*pzEx234*). The arrow and arrowhead mark two different KLP-4::mCherry puncta moving from the head towards the tail in the interneuron processes of the VNC. Images are oriented with anterior to the left. Time in seconds is marked on the right. (B) A representative kymograph showing mobile and stationary KLP-4::mCherry puncta was generated from the same time-lapse movie (Supplemental Video 1) of KLP-4::mCherry in the anterior VNC. The kymograph is oriented with anterior to the left. (C) Velocity histogram of KLP-4::mCherry puncta moving in the VNC from the head towards the tail (n = 147 mobility events). The maximum KLP-4::mCherry velocity was 2.0 μm/s from the head towards the tail and 2.6 μm/s from the tail towards the head.

FIGURE 3-5

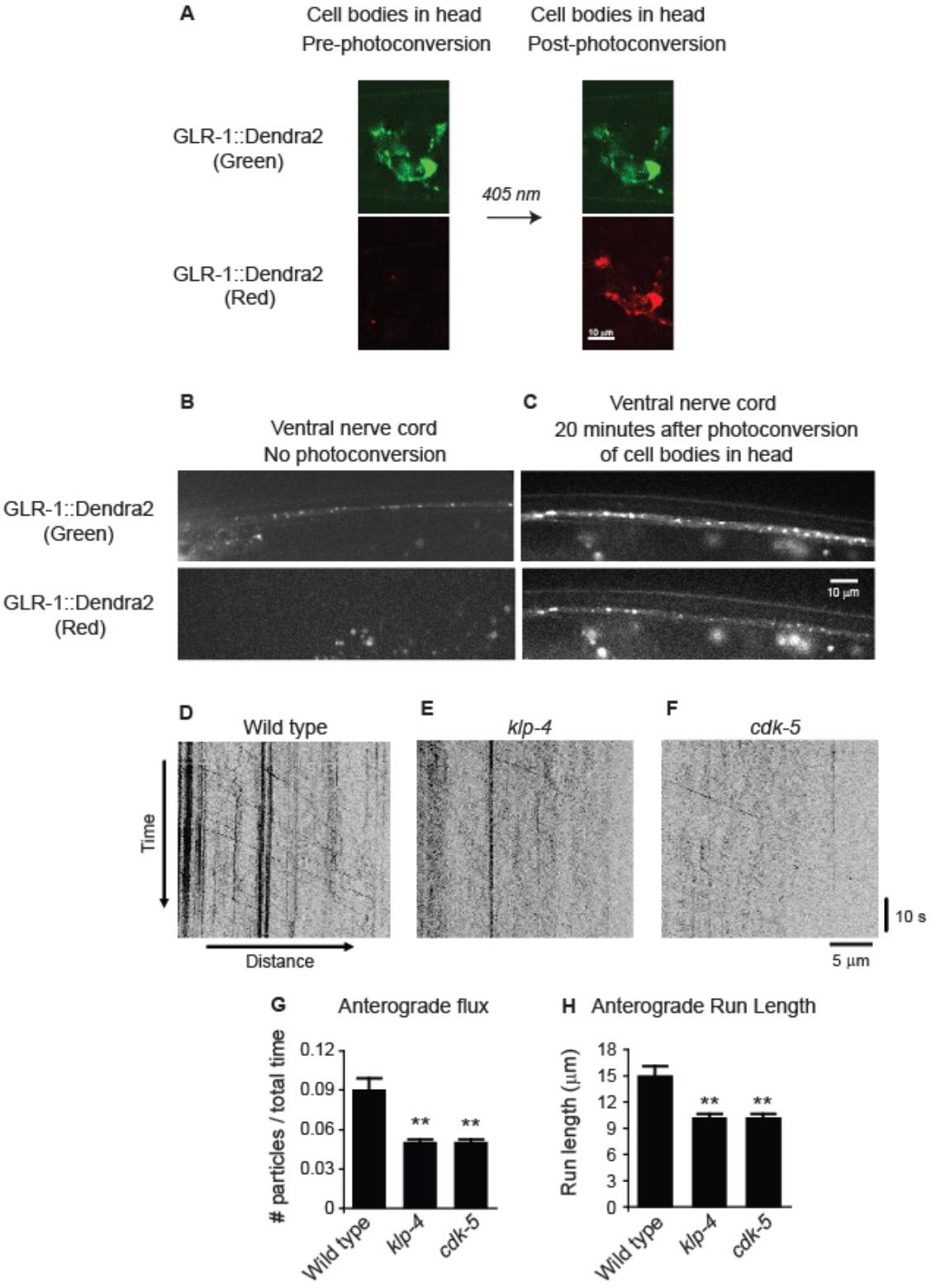
A
Cell bodies in head
Pre-photoconversion
Cell bodies in head
Post-photoconversion
GLR-1::Dendra2
(Green)
GLR-1::Dendra2
(Red)
405 nm
10 µm
B
Ventral nerve cord
No photoconversion
C
Ventral nerve cord
20 minutes after photoconversion
of cell bodies in head
GLR-1::Dendra2
(Green)
GLR-1::Dendra2
(Red)
10 µm
D
Wild type
E
klp-4
F
cdk-5
Time
Distance
10 s
5 µm
G
Anterograde flux
particles / total time
0.12
0.09
0.06
0.03
0
**
**
Wild type
klp-4
cdk-5
H
Anterograde Run Length
Run length (µm)
18
15
12
9
6
3
0
**
**
Wild type
klp-4
cdk-5

FIGURE 3-5. KLP-4 and CDK-5 promote the anterograde trafficking of GLR-1 in the VNC. (A) Green (488nm) and Red (543nm) images of cell bodies in the heads of young adult animals expressing integrated GLR-1::Dendra2 under the control of the *glr-1* promoter *(pzIs18)* before and immediately after photoconversion using 405nm light. (B-C) Images of the anterior VNC of young adult animals expressing GLR-1::Dendra2 without photoconversion (B) and 20 minutes after local photoconversion (C) of GLR-1::Dendra2 in cell bodies in the head. (D-F) Representative kymographs made from time-lapse imaging using a 543nm laser showing mobile and stationary red GLR-1::Dendra2 puncta in the anterior VNC of young adult wild type (D), *klp-4(tm2114)* (E) and *cdk-5(gm336)* (F) animals. For all kymographs, anterior is to the left (proximal) and posterior is to the right (distal). (G) Quantification of average anterograde flux for red GLR-1::Dendra2 puncta for wild type (n = 86 mobility events), *klp-4* (n = 42 mobility events) and *cdk-5* (n = 45 mobility events). (H) Quantification of average anterograde run length for red GLR-1::Dendra2 puncta for wild type (n = 101 mobility events), *klp-4* (n = 125 mobility events) and *cdk-5* (n = 104 mobility events). Mean and SEM are shown. Values that differ significantly from wild type are indicated by asterisks above each bar (**$p<0.001$, Student's t test).

FIGURE 3-6

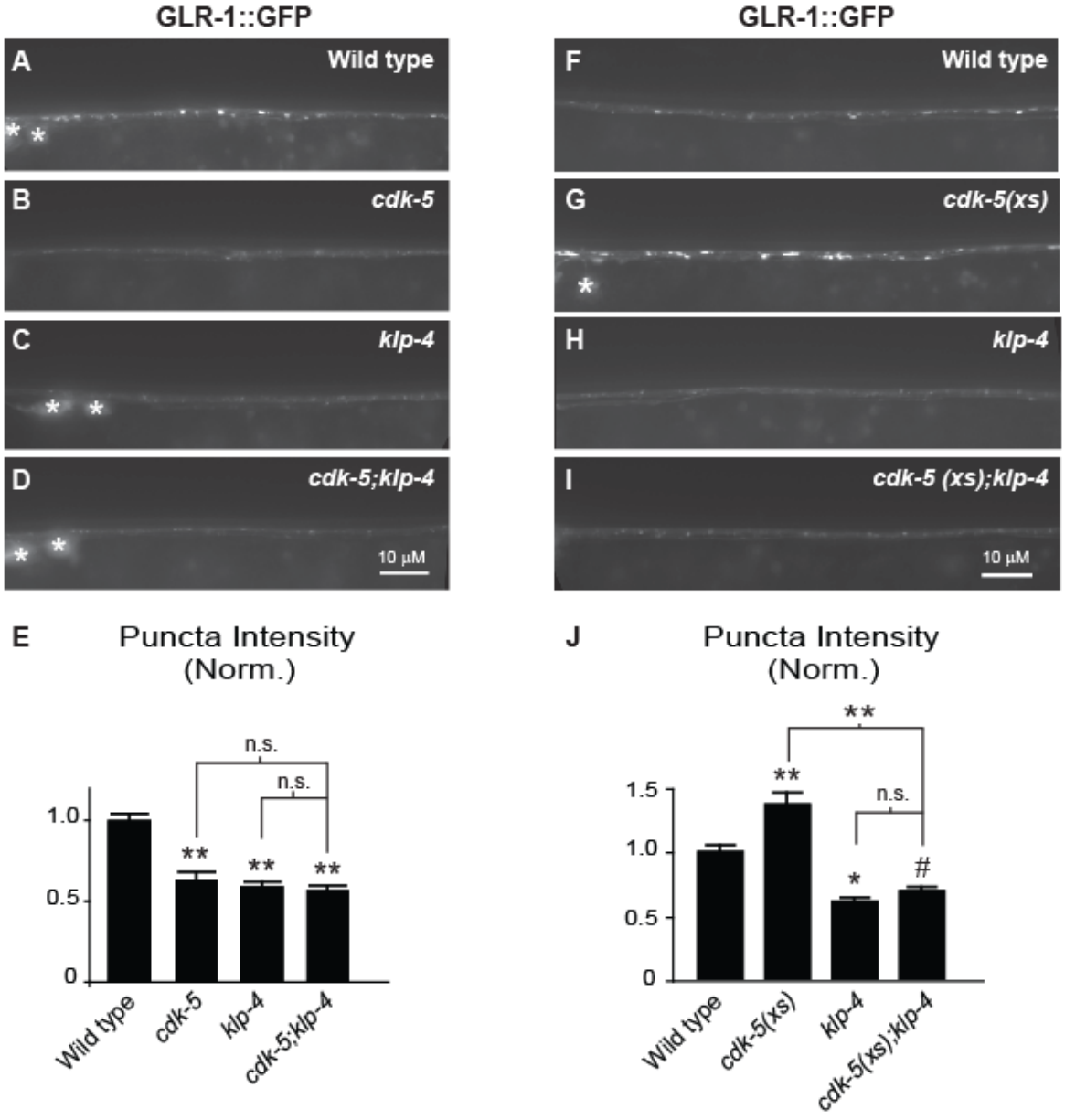
GLR-1::GFP
A
Wild type
B
cdk-5
C
klp-4
D
cdk-5;klp-4
10 µM
GLR-1::GFP
F
Wild type
G
cdk-5(xs)
H
klp-4
I
cdk-5 (xs);klp-4
10 µM
E
Puncta Intensity
(Norm.)
n.s.
n.s.
1.0
0.5
0
**
**
**
Wild type
cdk-5
klp-4
cdk-5;klp-4
J
Puncta Intensity
(Norm.)
**
**
n.s.
1.5
1.0
0.5
0
*
#
Wild type
cdk-5(xs)
klp-4
cdk-5(xs);klp-4

FIGURE 3-6. KLP-4 and CDK-5 act in the same genetic pathway to regulate GLR-1 levels in the VNC. (A-D) Representative images of the anterior VNC of wild type (A), *cdk-5(gm336)*(B), *klp-4(tm2114)*(C), and *cdk-5(gm336);klp-4(tm2114)* double mutant (D), L4 animals expressing GLR-1::GFP (*nuIs25*). White asterisks mark neuronal cell bodies.(E) Quantification of GLR-1::GFP puncta intensities (normalized) for the strains pictured in A-D. Mean and SEM are shown for $n = 35$ wild type, $n = 22$ *cdk-5,* $n = 29$ *klp-4* and $n = 32$ *cdk-5;klp-4* animals. (F-I) Representative images of the anterior VNC of L4 stage wild type animals (F), animals overexpressing *cdk-5* under the control of the *glr-1* promoter [*cdk-5(xs*)] (G), *klp-4(tm2114)* mutants (H), and *klp-4(tm2114)* mutants overexpressing *cdk-5* [*cdk-5(xs*)](*pzIs2*)(I). The white asterisk marks a neuronal cell body. (J) Quantification of GLR-1::GFP puncta intensities (normalized) for the strains pictured in F-I. Mean and SEM are shown for $n = 21$ wild type, $n = 24$ *cdk-5(xs)*, $n = 21$ *klp-4* and $n = 21$ *cdk-5(xs);klp-4* animals. Values that differ significantly from wild type are indicated by asterisks above each bar, whereas other comparisons are marked by brackets (#$p \leq 0.05$, *$p \leq 0.01$, **$p \leq 0.001$, Tukey-Kramer test). n.s. denotes no significant difference between the indicated strains ($p > 0.05$).

FIGURE 3-7

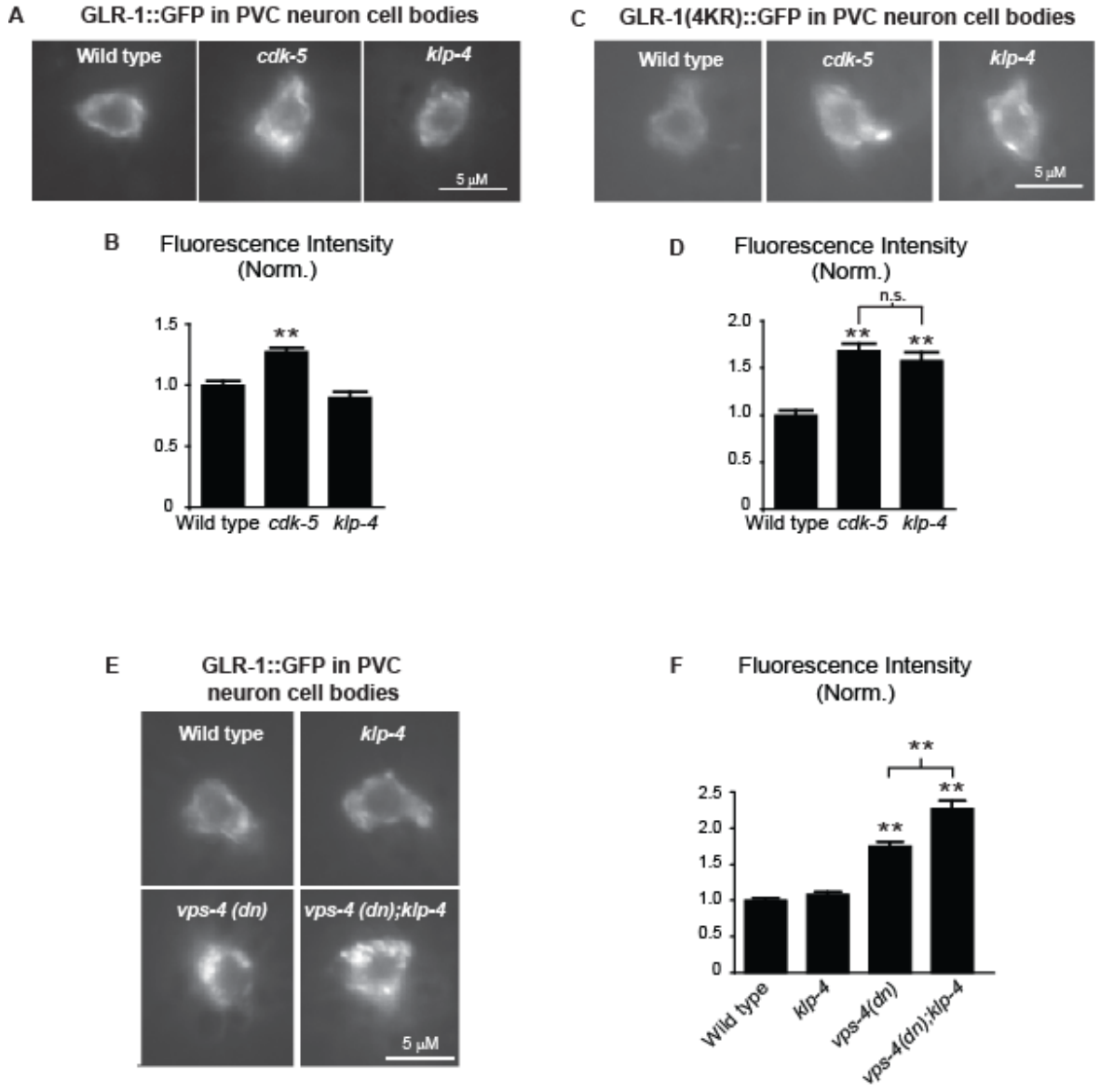
A
GLR-1::GFP in PVC neuron cell bodies
Wild type
cdk-5
klp-4
5 μM
C
GLR-1(4KR)::GFP in PVC neuron cell bodies
Wild type
cdk-5
klp-4
5 μM
B
Fluorescence Intensity (Norm.)
1.5
1.0
0.5
0
**
Wild type
cdk-5
klp-4
D
Fluorescence Intensity (Norm.)
n.s.
2.0
1.5
1.0
0.5
0
**
**
Wild type
cdk-5
klp-4
E
GLR-1::GFP in PVC neuron cell bodies
Wild type
klp-4
vps-4 (dn)
vps-4 (dn);klp-4
5 μM
F
Fluorescence Intensity (Norm.)
**
**
**
2.5
2.0
1.5
1.0
0.5
0
Wild type
klp-4
vps-4(dn)
vps-4(dn);klp-4

FIGURE 3-7. GLR-1 accumulates in cell bodies of *klp-4* mutants when receptor degradation is blocked. (A, C) Representative images of PVC neuron cell bodies of wild type, *cdk-5(gm336)* and *klp-4(tm2114)* L4 animals expressing GLR::GFP (*nuIs25)* (A) or GLR-1(4KR)::GFP *(nuIs108)* (C). (B) Quantification of GLR-1::GFP mean fluorescence intensity (normalized) for the strains pictured in A. Mean and SEM are shown for $n = 34$ wild type, $n = 32$ *cdk-5*, and $n = 20$ *klp-4*. (D) Quantification of GLR-1(4KR)::GFP mean fluorescence intensity (normalized) for the strains pictured in C. Mean and SEM are shown for $n = 24$ wild type, $n = 25$ *cdk-5*, and $n = 23$ *klp-4*. (E) Representative images of GLR::GFP (*nuIs24)* in PVC neuron cell bodies of L4 stage wild type animals, *klp-4(tm2114)* mutants, wild type animals expressing *vps-4(dn)*, and *klp-4(tm2114)* mutants expressing *vps-4(dn).* (F) Quantification of GLR-1::GFP mean fluorescence intensity (normalized) for the strains pictured in (A). Mean and SEM are shown for $n = 24$ wild type, $n = 20$ *klp-4*, $n = 22$ *vps-4(dn)* and $n = 22$ *vps-4(dn);klp-4*. Values that differ significantly from wild type are indicated by asterisks above each bar (**$p \leq 0.001$). n.s. denotes no significant difference between the indicated strains ($p > 0.05$).

FIGURE 3-8

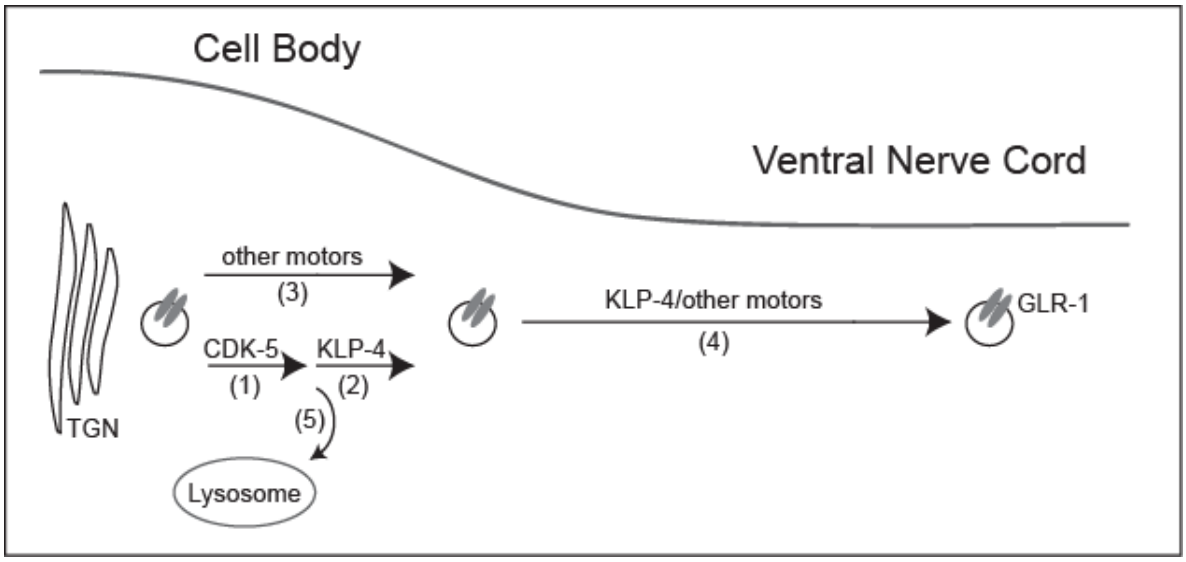

FIGURE 3-8. Model illustrating KLP-4 regulation of GLR-1 trafficking. (1, 2) In the cell body, CDK-5 and KLP-4 function in the same pathway to regulate the anterograde trafficking of GLR-1 receptors. (3) Other motors may function together with KLP-4 in the cell body to traffic GLR-1. (4) In the VNC processes, GLR-1 is transported to synapses by KLP-4 and/or other motors. (5) In the absence of KLP-4 motors, GLR-1 is targeted for degradation in the MVB/lysosome pathway.

FIGURE 3-S1.

A

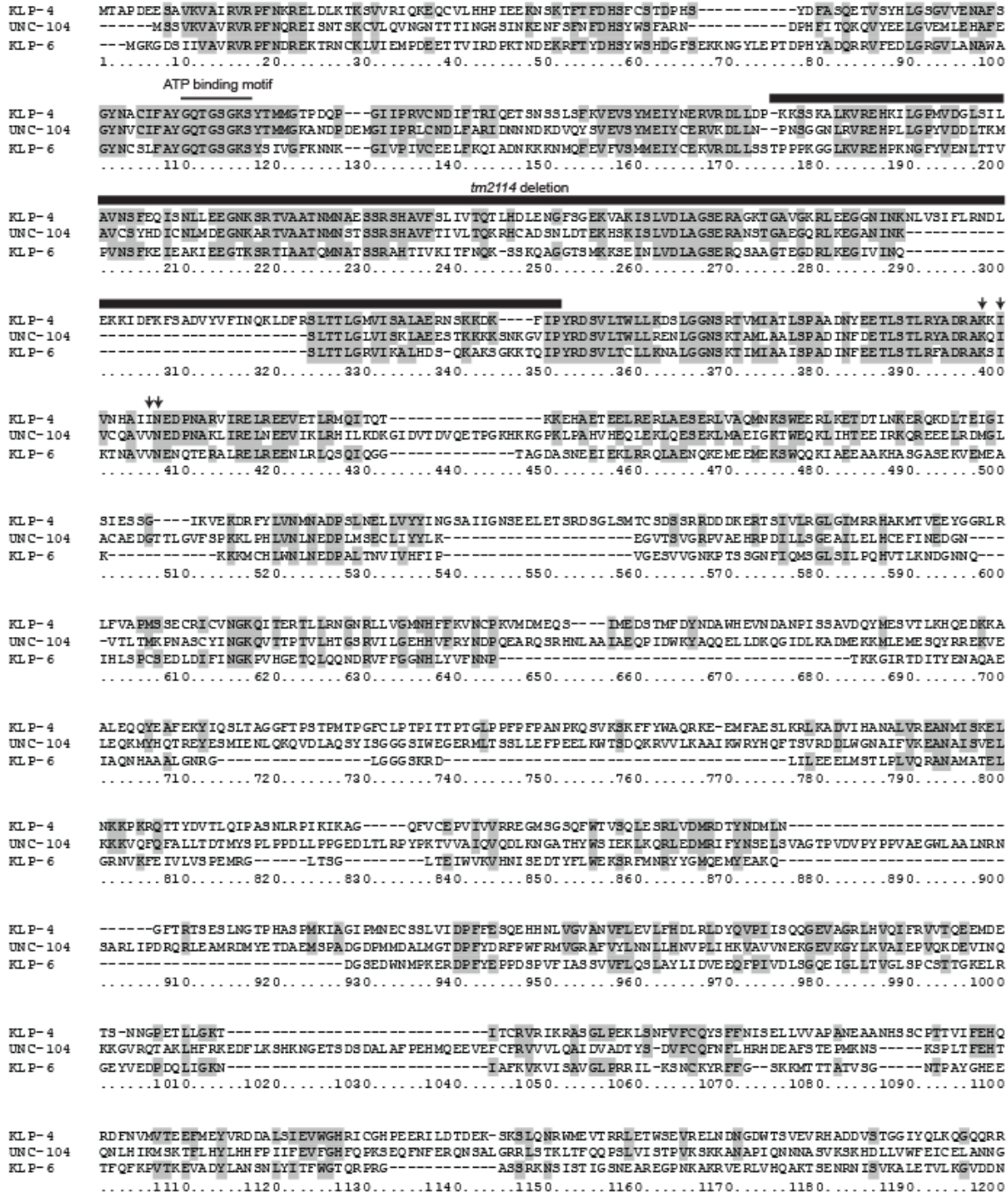

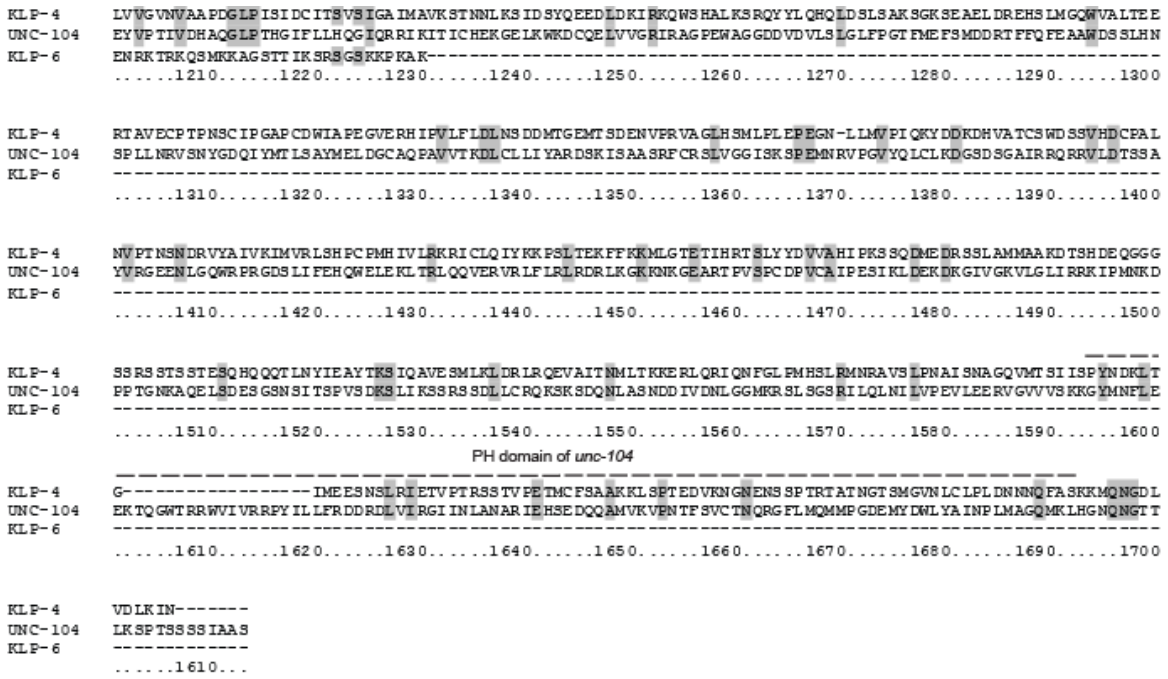
KLP-4
UNC-104
KLP-6
PH domain of unc-104

B

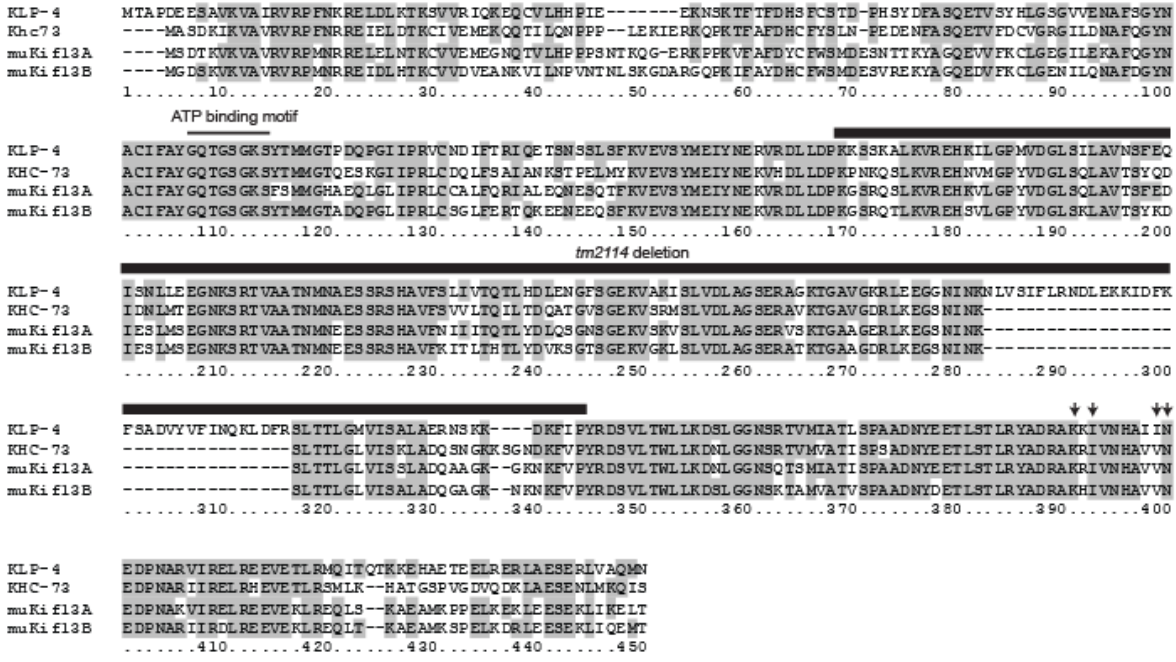
KLP-4
Khc73
muKif13A
muKif13B
ATP binding motif
tm2114 deletion

FIGURE 3-S1. Protein alignment of the motor domain of KLP-4 and its homologs. (A) ClustalW2 multiple sequence alignment of amino acids in *C. elegans* KLP-4, UNC-104 and KLP-6. Identical residues between KLP-4 and the other homologs are boxed and shaded in grey. The thin black line marks the ATP binding motif. Black arrows mark the conserved residues found in microtubule plus-end directed kinesins. The thick black line demarcates the *tm2114* deletion. The dotted line indicates the location of the PH domain in UNC-104. (B) ClustalW2 multiple sequence alignment of amino acids in the motor domains of *C. elegans* KLP-4, *Drosophila* Khc73, mouse KIF13A and mouse KIF13B. Identical residues between KLP-4 and the other three homologs are boxed and shaded in grey. The thin black line marks the ATP binding motif. Black arrows mark the conserved residues found in microtubule plus-end directed kinesins. The thick black line demarcates the *tm2114* deletion.

FIGURE 3-S2.

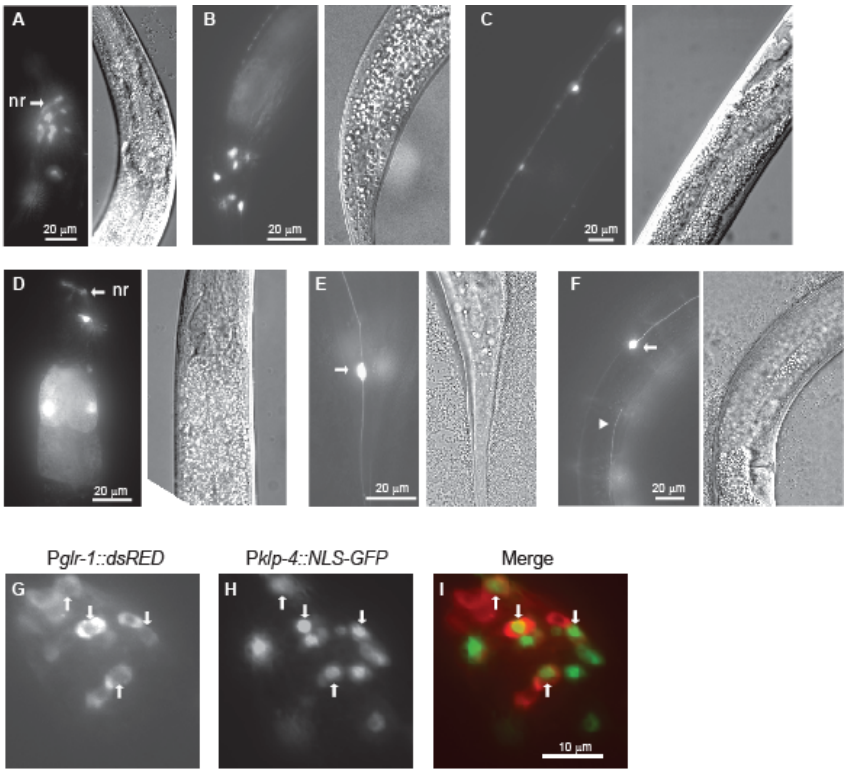

FIGURE 3-S2. KLP-4 is expressed throughout the nervous system and in other tissues. (A-F) Images of animals expressing a *klp-4* transcriptional reporter consisting of GFP under the control of the *klp-4* promoter *(pzEx256)*. GFP signal is shown in neuronal cell bodies of the head (A) and tail (B), and ventral nerve cord (C) as well as in the nerve ring (nr) (A, D) and the mechanosensory neurons PLM (E) and ALM (F) Arrows mark the cell body of PLM in (E) and ALM in (F), respectively. An arrowhead marks the anterior process of PLM in (F). In all images, anterior is oriented towards the top of the image. (G-I) Images of neuronal cell bodies in the head of an animal co-expressing a *glr-1* transcriptional reporter (P*glr-1::dsRED*) (G) and a *klp-4* transcriptional reporter (P*klp-4::NLS::GFP*) (H). (I) Merged image of (G) and (H). Neurons co-expressing *klp-4* and *glr-1* are indicated by the white arrows.

FIGURE 3-S3.

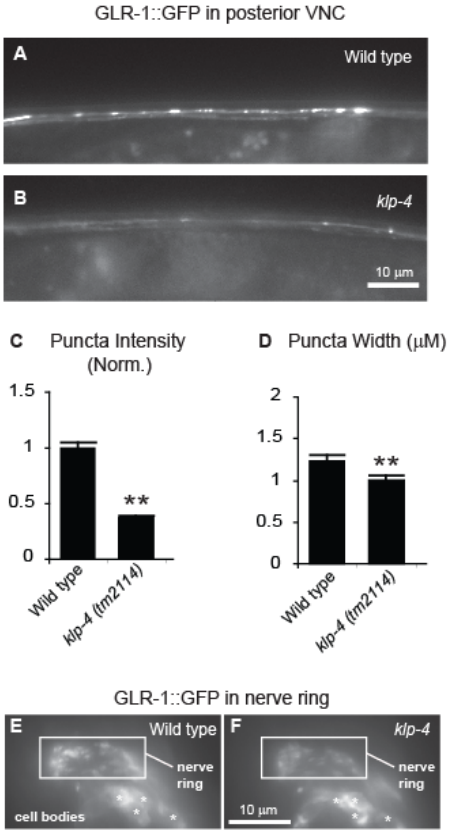

FIGURE 3-S3. KLP-4 promotes the abundance of GLR-1 in the posterior VNC and nerve ring of *C. elegans*. (A-B) Representative images of the posterior VNC (immediately posterior to the vulva) of L4 stage wild-type (A), and *klp-4(tm2114)* (B) animals expressing GLR-1::GFP *(nuIs25)*. (C-D) Quantification of GLR-1::GFP puncta intensities (normalized) (C) for the strains pictured in A-B. Means and SEM are shown for $n = 28$ wild type and $n = 21$ *klp-4*(*tm2114)* animals. Values that differ significantly from wild type are indicated by asterisks above each bar (**$p \leq 0.001$, Student's *t*-test). (E-F) Representative images of a section of the nerve ring and adjacent cell bodies of L4 stage wild-type (E) and *klp-4(tm2114)* (F) animals expressing GLR-1::GFP *(nuIs25)*. The nerve ring section is demarcated by a white box and cell bodies are marked with white asterisks. Images are oriented with anterior to the top.

FIGURE 3-S4

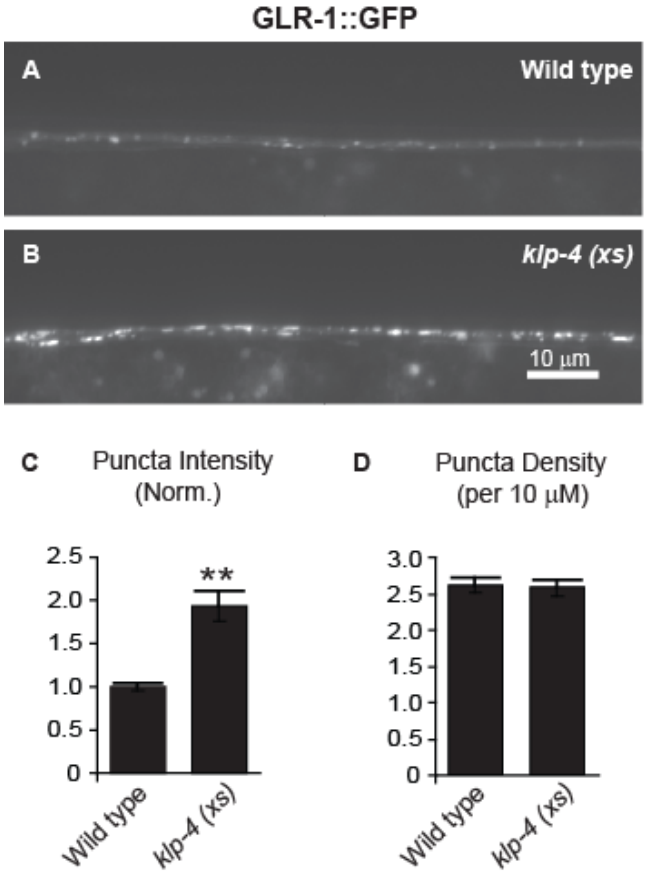

FIGURE 3-S4. KLP-4 overexpression increases GLR-1 abundance in the anterior VNC of *C. elegans*. (A-B) Representative images of GLR-1::GFP *(nuIs25)* in the anterior VNC of L4 stage wild-type (A), and wild-type animals that express *klp-4* cDNA under the control of the *glr-1* promoter [*klp-4(xs)*] (*pzIs20*) (B). (C-D) Quantification of GLR-1::GFP puncta intensities (normalized) (C) and densities (D) for the strains pictured in A-B. Means and SEM are shown for $n = 15$ wild type and $n = 18$ *klp-4(xs)* animals.

FIGURE 3-S5

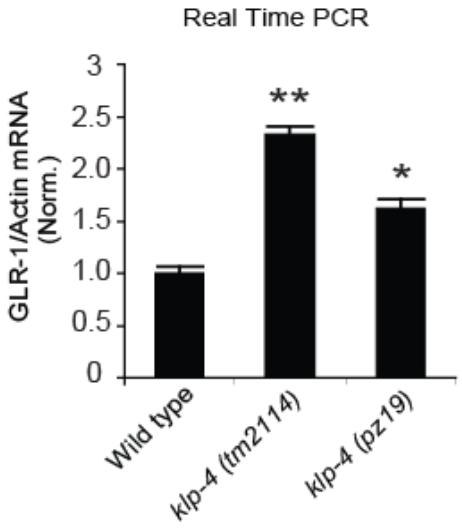

FIGURE 3-S5. Analysis of *glr-1* transcript levels in *klp-4* mutants. Results of real-time quantitative PCR are shown. *glr-1* to *act-1* (actin) mRNA ratios are shown for wild-type, *klp-4(tm2114)* and *klp-4(pz19)* animals expressing GLR-1::GFP *(nuIs25)* (normalized to wild-type). For each genotype, $n = 6$ replicate measurements of *glr-1* mRNA level were normalized to the average of $n = 6$ replicate measurements of actin mRNA level. Mean and SEM are shown. Values that differ significantly from wild type are indicated by asterisks above each bar (**$p \leq 0.001$, *$p \leq 0.01$ Student's *t*-test).

FIGURE 3-S6.

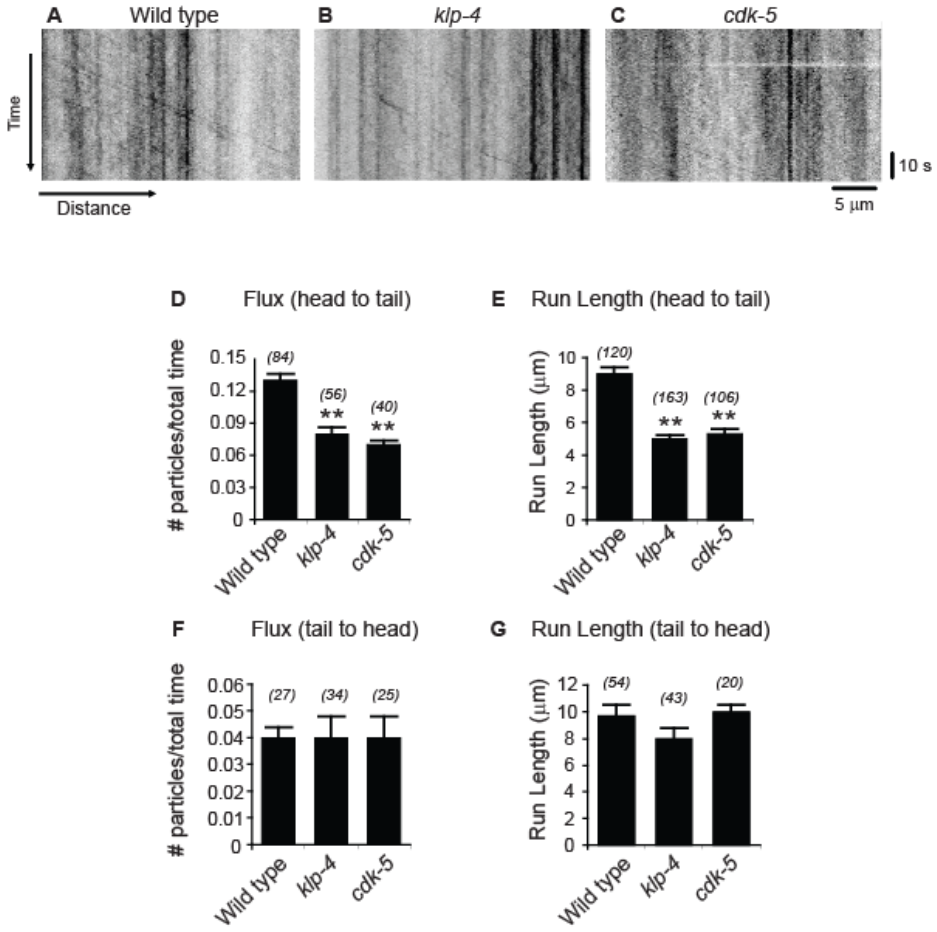

FIGURE 3-S6. KLP-4 and CDK-5 regulate the trafficking of GLR-1::GFP in the VNC. (A-C) Representative kymographs showing mobile and stationary GLR-1::GFP puncta in the anterior VNC of young adult wild type (A), *klp-4(tm2114)* (B) and *cdk-5(gm336)* (C) animals expressing GLR-1::GFP (*nuIs25*). For all kymographs, anterior is to the left. (D-G) Quantification of average flux (D, F), and run length (E, G) for GLR-1::GFP puncta moving towards the tail (D-E) or towards the head (F-G) for wild type, *klp-4* and *cdk-5*. Mean and SEM are shown. The number of events (*n*) analyzed for each parameter is indicated above the bars on the graphs. Values that differ significantly from wild type are indicated by asterisks above each bar (**p<0.001, Student's t test).

FIGURE 3-S7

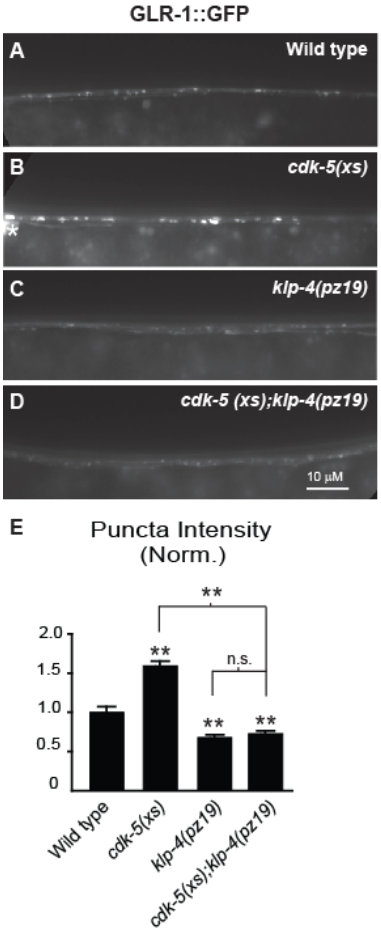

FIGURE 3-S7. *klp-4(pz19)* mutation blocks the effects of *cdk-5* overexpression on GLR-1 in the VNC. (A-D) Representative images of GLR-1::GFP (*nuIs24*) in the anterior VNC of L4 wild type (A), wild type animals overexpressing *cdk-5* under the control of the *glr-1* promoter [*cdk-5(xs)*] (*pzIs2*) (B), *klp-4(pz19*) mutants (C) and *klp-4(pz19)* mutants overexpressing *cdk-5* [*cdk-5(xs)*] (D). The white asterisk marks a neuronal cell body. (E) Quantification of GLR-1::GFP puncta intensities (normalized) for the strains pictured in A-D. Mean and SEM are shown for $n = 23$ wild type, $n = 23$ *cdk-5(xs)*, $n = 23$ *klp-4* and $n = 26$ *cdk-5(xs);klp-4* animals. Values that differ significantly from wild type are indicated by asterisks above each bar, whereas other comparisons are marked by brackets (**$p \leq 0.001$, Tukey-Kramer test). n.s. denotes no significant difference between the indicated strains ($p>0.05$).

Chapter 4

Potential mechanisms of KLP-4 regulation and identification of novel regulators of GLR-1 abundance in the VNC

Attributes:

All experiments in the following chapter were performed by Michael Monteiro.

Introduction

In the previous two chapters we identified the kinesin-3 family motor KLP-4 as a positive regulator of the anterograde trafficking of the AMPA-type glutamate receptor, GLR-1. *klp-4* was identified in a forward genetic screen for suppressors of the increased GLR-1 abundance in the VNC of animals over expressing the cyclin-dependent kinase *cdk-5*. Subsequent genetic analyses determined that KLP-4 acts in the same genetic pathway as CDK-5 to promote GLR-1 trafficking in the VNC of *C. elegans.* The mechanism by which CDK-5 regulates KLP-4 dependent trafficking of GLR-1 is unknown. This chapter focuses on: 1) Potential mechanisms to regulate KLP-4 activity and 2) Identification of novel regulators of GLR-1 abundance at synapses.

Vesicular trafficking along microtubules by molecular motors is an essential cellular process, particularly for large polarized cells such as neurons. The trafficking of intracellular cargos must be spatially and temporally precise and, as such, the activity of molecular motors must be carefully regulated. There are several points in the transport process at which the transport of cargo on motors is subject to regulation. These include formation of a motor/cargo complex, initiation of movement along microtubules, motor velocity and processivity, and at the appropriate intracellular location, release of cargo from motor or release of motor from microtubule (Akhmanova and Hammer, 2010; Hirokawa et al., 2010; Vale, 2003). Indeed, control of motor expression level, either through transcript level or protein level also contributes to the regulation of cargo transport by microtubule motors (Kumar et al., 2010; Tsurudome et al., 2010).

Phosphorylation plays a crucial regulatory role in most cellular processes and can affect intracellular transport in several ways (Akhmanova and Hammer, 2010; Hirokawa et al., 2010). Kinase activity can affect the specificity of a given kinesin for a particular cargo complex. For example the adaptor protein calsyntenin-1 (CASY-1) binds to kinesin light

chain (KLC) of kinesin-1 to facilitate trafficking of certain vesicular cargo (Vagnoni et al., 2011). Phosphorylation of KLC at a predicted MAPK target site reduces the binding of KLC to CASY-1 but has no effect on binding to two other adaptor proteins, huntingtin-associated protein 1 (HAP1) and JNK-interacting protein 1 (JIP1) (Vagnoni et al., 2011). Thus, MAPK phosphorylation of KLC selects for the binding of particular cargo.

In addition to regulating cargo-specificity, phosphorylation can regulate disassembly of a motor/cargo complex. The kinesin-2 motor Kif17 transports NMDA receptor subunits in mammalian neurons (Guillaud et al., 2008; Setou et al., 2000; Yin et al., 2011). Kif17 is directly phosphorylated by the calcium/calmodulin dependent protein kinase, CamKII resulting in release of the cargo NMDA receptor from the Kif17 trafficking complex (Guillaud et al., 2008).

Kinesin motor activity can also be regulated by phosphorylation. The cAMP-dependent protein kinase, PKA increases ATPase activity of the KHC motor domain *in vitro* by phosphorylating the KLC, which presumably causes a conformational change of the motor (Matthies et al., 1993). The cell cycle associated cyclin dependent kinases phosphorylate several cell-cycle associated kinesins, kinesins 5-7 and 13, to directly affect their motor activity, often by regulating binding to microtubules (Avunie-Masala et al., 2011; Cahu et al., 2008; Espeut et al., 2008; Jang et al., 2009; Mishima et al., 2004).

In some cases phosphorylation of a kinesin affects a particular cellular process but the molecular effect of the phosphorylation event is unknown. The kinesin-3 family member Kif13B/GAKIN, one of the mammalian orthologs of *C. elegans klp-4,* plays an important role in axon specification and establishment of neuronal polarity in neuronal cell culture (Yamada et al., 2007). Phosphorylation at two Ser residues in the C-terminal cargo binding domain by the Par1B kinase inhibits Kif13B from performing this role (Yoshimura et al., 2010).

Direct phosphorylation of a kinesin itself is not necessary for a signaling cascade to

affect the transport of intracellular cargo. Kinase activity can have indirect effects on the ability of a kinesin to perform a particular trafficking function. The c-jun N-terminal kinase (JNK) signaling cascade, ATG1 kinase, the ERK/MAPK cascade and the cyclin-dependent kinase CDK-5 have all been shown to affect kinesin-driven transport through effects on targets other than kinesins themselves. These signaling events can affect a variety of processes from motor/cargo complex formation to association of the trafficking complex with microtubules (Deacon et al., 2005; Horiuchi et al., 2007; Morfini et al., 2002; Morfini et al., 2006; Stagi et al., 2006; Toda et al., 2008).

In *C. elegans* CDK-5 has been shown to regulate trafficking of neuronal cargo mediated by multiple motors. CDK-5 promotes trafficking of synaptic vesicles and dense core vesicles into motor neuron axons by inhibiting inappropriate dynein-mediated transport of these cargos into dendrites (Goodwin et al., 2012; Ou et al., 2010). CDK-5 also contributes to UNC-104-dependent trafficking of synaptic proteins during a developmental remodeling process in motor neurons, although the mechanism of CDK-5 action in this process is not understood (Park et al., 2011). As we have shown, CDK-5 also promotes the KLP-4 dependent trafficking of GLR glutamate receptors in the VNC (Juo et al., 2007) (Chapter 3).

In neurons, kinesin-dependent transport can also be regulated by synaptic activity. Activity-induced synaptic plasticity often involves the kinesin-dependent recruitment of new proteins to the synapse (Charalambous et al., 2012; Kondo et al., 2012; Maas et al., 2009; Puthanveettil et al., 2008; Wong et al., 2002). Several mechanisms exist to increase synaptic trafficking in response to neuronal activity. The most extensively studied of these is increased kinesin expression. The kinesin-2, Kif17 traffics NMDAR in rodent dendrites (Setou et al., 2000). Kif17 mRNA levels in cultured neurons increase in response to treatment with NMDAR agonists, which stimulate long-term potentiation (LTP) (Wong et al.,

2002; Yin et al., 2012). In *Aplysia,* application of serotonin to sensory and motor neurons increases transcript levels of Kinesin-1, which is a necessary component of LTP in these animals (Puthanveettil et al., 2008). Recently, the kinesin-3, Kif1A was shown to be necessary for enhanced learning in mice raised in an enriched environment (Kondo et al., 2012). Kif1A mRNA levels were higher in the brains of these mice than in mice raised in non-enriched environments (Kondo et al., 2012).

One mechanism of posttranscriptional regulation of protein expression is targeting of transcripts by microRNAs (miRNAs). miRNAs are endogenous small RNAs that bind to complementary sequences on target mRNAs to regulate translation (Bartel, 2009; Jan et al., 2011). The most common effect of miRNA binding is a decrease in target mRNA levels (Guo et al., 2010). miRNAs are important regulators of synaptic function as they have been shown to affect the levels of numerous synaptic proteins, including glutamate receptors (Ceman and Saugstad, 2011; Gao, 2010; Karr et al., 2009; Le et al., 2009; Le et al., 2009; Simon et al., 2008). In some cases miRNAs affect the trafficking of neuronal cargos by microtubule-based motors (Friggi-Grelin et al., 2008; Li et al., 2010). Expression of the *Drosophila* kinesin KHC-73, the orthologous motor to *C. elegans klp-4*, is negatively regulated by the *mir-310* miRNA family (Tsurudome et al., 2010). Loss of function mutations in the *mir-310* miRNA family result in increased KHC-73 protein levels and increase synaptic levels of the pre-synaptic organizing protein Bruchpilot (Brp), resulting in increased synaptic transmission (Tsurudome et al., 2010). Thus, regulation of the expression levels of kinesins by miRNAs can affect synaptic transmission.

We have shown that loss of function of KLP-4 results in a 40% decrease in GLR-1 abundance in the VNC of *C. elegans* and a significant decrease in anterograde trafficking of GLR-1 (Chapter 3 Figures 1, 5). KLP-4 plays a large role in GLR-1 trafficking, however a significant amount of GLR-1 trafficking to synapses occurs in the absence of functional KLP-

4. Clearly mechanisms for GLR-1 trafficking exist that do not require KLP-4.

It is likely that other microtubule based motors are involved in GLR-1 trafficking in the VNC. Multiple microtubule based motors are implicated in trafficking AMPA-type glutamate receptors (AMPAR) in mammals. The microtubule minus-end directed motor, cytoplasmic dynein contributes to AMPA receptor-mediated currents and to the trafficking of neuronal cargos along the mixed microtubule population of proximal dendrites (Kapitein et al., 2010; Kim and Lisman, 2001). Like dynein, Kinesin-1/KHC/Kif5 contributes to AMPAR mediated currents and can form a complex with AMPARs and the adaptor protein GRIP1 (GluR2-Interacting Protein) in dendrites (Kim and Lisman, 2001; Setou et al., 2002). Finally, the kinesin-3 Unc-104 forms a complex with AMPARs via the synaptic scaffolding protein Syd-2 (Shin et al., 2003; Wyszynski et al., 2002). In this chapter we examine potential mechanisms by which CDK-5 might regulate KLP-4 activity, determine whether KLP-4 is required for the *eat-4* loss of function–dependent increase in VNC GLR-1 and we identify novel regulators of GLR-1 abundance at synapses.

Results

CDK-5 is not required for KLP-4 regulation of GLR-1 abundance in the VNC

Overexpression of either *cdk-5* or *klp-4* in *glr-1* expressing neurons results in increased GLR-1 abundance in the VNC (Chapter 3; Figures 6, S5 and S8). Loss of function mutations in *klp-4* completely suppress these effects of *cdk-5* overexpression (Chapter 3; Figures 6 and S5). The latter result demonstrates that KLP-4 is required for the effects of *cdk-5* overexpression. We performed the converse experiment to determine whether CDK-5 is similarly required for the effects of *klp-4* over expression on GLR-1 abundance. We tested whether *cdk-5* loss of function completely suppresses the increased GLR-1 levels in the VNC of animals that overexpress *klp-4 [cdk-5;klp-4(xs)]*. Compared to

wild type animals, GLR-1::GFP puncta intensities were decreased by 25% ($p < 0.01$) in *cdk-5* mutants and increased by 25% ($p < 0.01$) in *klp-4(xs)* animals (Figure 4-1). Unlike in *cdk-5* mutants, GLR-1::GFP puncta intensities in *cdk-5;klp-4(xs)* animals are not decreased compared to those in wild type animals ($p = 0.5$) (Figure 4-1 A, D, E) and they are increased by 25% over those in *cdk-5* mutants ($p < 0.001$) (Figure 4-1 B, D, E). Puncta intensities in *cdk-5;klp-4(xs)* animals seem to trend towards an increase compared to wild type animals, however this difference was not statistically significant ($p = 0.5$) (Figure 4-1 A, D, E). Thus, while CDK-5 contributes to GLR-1 abundance in the VNC of *klp-4(xs)* animals, it is not absolutely required for the effects of *klp-4* over expression. Together with our previous results (Chapter 3; Figurea 6, S5), our data suggest that CDK-5 is necessary for the activity of endogenous KLP-4 in the anterograde trafficking of GLR-1. However at extremely high levels of *klp-4* expression, CDK-5 function is not required for KLP-4 to promote GLR-1 abundance in the VNC.

KLP-4 abundance increases in the VNC of *cdk-5* mutants

One possibility for how CDK-5 could contribute to GLR-1 trafficking is it could increase the movement of KLP-4 into the VNC. To determine whether CDK-5 acts to increase KLP-4 levels in the VNC we observed the effects of a loss of function of *cdk-5* on the abundance of GFP-tagged KLP-4 (KLP-4::GFP) in the VNC (Figure 4-3). If CDK-5 promotes KLP-4 trafficking to and/or abundance of KLP-4 in the VNC, we would expect that there would be less KLP-4::GFP in the VNC of *cdk-5* mutants than in wild type animals. Surprisingly, rather than decreased KLP-4::GFP abundance in *cdk-5* mutants, we observed a 28% increase ($p < 0.001$) in KLP-4::GFP puncta intensity and a 32% increase in puncta density ($p < 0.05$) in the VNC compared to wild type animals (Figure 4-3). These results suggest that the effects of CDK-5 on KLP-4 mediated GLR-1 abundance in the VNC cannot be explained simply by

CDK-5 acting to increase KLP-4 levels in the VNC.

Given these surprising results of KLP-4::GFP static imaging, we next wanted to determine if KLP-4 movement is affected in *cdk-5* mutants. Preliminary results suggest there is no obvious change in velocity or run length of KLP-4::GFP in *cdk-5* mutants compared to those in wild type animals. Further study is required to determine whether this result is statistically significant and to investigate any effects *cdk-5* may have on KLP-4 flux.

klp-4 **loss of function does not completely suppress increased GLR-1 abundance in animals with decreased presynaptic glutmate release**

Synaptic activity has been shown to regulate transport in several ways, including transcriptional regulation of kinesins (Guillaud et al., 2003; Kondo et al., 2012; Puthanveettil et al., 2008; Wong et al., 2002; Yin et al., 2011). To test whether synaptic activity could regulate *klp-4* we used animals with a loss of function mutation in the gene *eat-4 /* VGlut*,* which encodes a presynaptic vesicular glutamate transporter. In *eat-4* mutants, glutamate is not loaded into synaptic vesicles efficiently and presynaptic glutamate release is decreased (Berger et al., 1998; Lee et al., 1999). One result of this is increased abundance of GLR-1::GFP in the VNC (Grunwald et al., 2004). This post synaptic response is consistent with homeostatic synaptic scaling, in which chronically altered presynaptic release of neurotransmitter results in compensatory post synaptic changes (Grunwald et al., 2004; Turrigiano, 2008; Wang et al., 2012).

To determine whether KLP-4 could be involved in the post synaptic response to decreased glutamate release, we first examined the distribution of GLR-1::GFP in the VNC of *klp-4;eat-4* double mutants. If KLP-4 were completely necessary for increased GLR-1 levels in the VNC of *eat-4* mutants, then loss of function of *klp-4* should completely suppress this response. We found that compared to wild type controls, GLR-1::GFP puncta intensities

were increased by 35% in the posterior VNC of *eat-4* single mutants and puncta widths showed a small increase that was not statistically significant (Grunwald et al., 2004, Figure 4-2). Puncta intensity and width were significantly decreased in both *klp-4* single mutants and *klp-4;eat-4* double mutants compared to wild type controls (Figure 4-2). However, *klp-4* mutation did not completely suppress the GLR-1 increase in *eat-4* mutants because puncta intensity is higher in *eat-4;klp-4* double mutants than in *klp-4* single mutants. Thus, loss of function of *eat-4* partially suppressed the effects of the *klp-4* mutation. These results suggest that while KLP-4 is still required for trafficking in *eat-4* mutants, the homeostatic increase in GLR-1 abundance seen in *eat-4* mutants is not entirely dependent on KLP-4.

Because loss of function of KLP-4 reduces GLR-1 abundance in *eat-4* mutants, we next tested whether *klp-4* transcription might be upregulated in these animals. We conducted quantitative real time PCR experiments to measure *klp-4* transcript levels from a single sample each of *eat-4* mutants and wild type animals. Preliminary results show a small increase in *klp-4* mRNA levels (normalized to *act-1/*actin) in *eat-4* mutant animals compared to wild type controls (data not shown). Additional qPCR experiments with independent samples will have to be performed to determine whether this small increase is significant. Nevertheless, the possibility of increased *klp-4* expression in *eat-4* mutants suggests that synaptic activity may contribute to regulation of KLP-4.

The miRNA family *mir-75/mir-79* positively regulates GLR-1 abundance in the VNC

While synaptic activity is one potential regulator of KLP-4 expression, there are multiple other ways in which KLP-4 and its role in GLR-1 trafficking could be regulated. Posttranslational regulation of gene expression by microRNAs (miRNAs) is essential for many cellular processes (Bartel, 2009). Recently, expression of the *klp-4* ortholog in *Drosophila,* KHC-73 was shown to be regulated by miRNAs and this regulation led to

changes in trafficking of synaptic proteins and neurotransmission (Tsurudome et al., 2010). To identify miRNAs that could potentially target the *klp-4* transcript we used two available miRNA target prediction algorithms, Target Scan, (http://www.targetscan.org/worm_52/) (Jan et al., 2011) and the PicTar Web interface, (http://pictar.mdc-berlin.de/) (Lall et al., 2006). We chose the miRNAs *mir-75* and *mir-79,* which have identical consensus binding sites, due to their high predictive scores for targeting *klp-4* mRNA (see Methods and Figure 4-4 A). The *klp-4* 3'UTR contains two predicted target sites for *mir-75* and *mir-79,* one of which is conserved in the *klp-4* transcript of the nematode *C. briggsae.* We obtained deletion mutants for *mir-75(n4472)* and *mir-79(n4126)*, which are large deletions that completely delete the *mir-75* and *mir-79* genes, respectively. To determine whether loss of function of *mir-75* or *mir-79* affects the abundance of GLR-1 in the VNC, we examined the distribution of GLR-1::GFP in the VNC of wild type animals, *mir-75* mutants and *mir-79* mutants (Figure 4-4). If KLP-4 expression were down regulated by *mir-75* and *mir-79*, we would expect that loss of function of *mir-75* or *mir-79* would result in increased KLP-4 protein level and consequently, increased GLR-1 abundance in the VNC. We observed no significant difference in GLR-1::GFP abundance in the VNC of *mir-75* or *mir-79* single mutants when compared to wild type animals (Figure 4-4 B-F). However we did observe a significant difference in GLR-1::GFP puncta intensities and densities in the *mir-75;mir-79* double mutants compared to those in wild type animals (Figure 4-4 G-J). Surprisingly, rather than increased GLR-1::GFP abundance in the *mir-75;mir-79* double mutants, we observed a 21% decrease in GLR-1::GFP puncta intensities and an 11% decrease in puncta densities in these animals compared to wild type controls (Figure 4 G-J). The synthetic effect of *mir-75* and *mir-79* with respect to each other suggests that these two miRNAs may perform redundant functions to promote GLR-1 abundance in the VNC. The counterintuitive decrease in GLR-1 abundance in the *mir-75;mir-79* double mutant suggests that *klp-4*

transcript levels are not down regulated by the *mir-75/79* family. A few studies suggest that miRNAs can upregulate expression of their target transcripts, leaving open the possibility that *mir-75/79* may upregulate *klp-4* expression (Mortensen et al., 2011; Steitz and Vasudevan, 2009; Vasudevan et al., 2007).

Synaptobrevin abundance in the VNC is unchanged in *mir-75;mir-79* double mutants

One possible explanation for the surprising decrease in GLR-1 abundance in the VNC of *mir-75;mir-79* mutants is that loss of function of these two miRNAs results in synaptic development defects in *glr-1*-expressing neurons, resulting in a change in overall synapse number or size. To test for possible synaptic defects we examined the distribution of the synaptic vesicle protein, synaptobrevin tagged with GFP under the control of the *glr-1* promoter (SNB-1::GFP) in the VNC of wild type and *mir-75;mir-79* mutant animals (Figure 4-5). If *mir-75;mir-79* mutants experienced defects in synapse development, we would expect the distribution of synaptobrevin to be altered compared to that in wild type animals. Interestingly, we observed no difference in SNB-1::GFP puncta intensity ($p > 0.05$) or density ($p > 0.05$) in *mir-75;mir-79* double mutants when compared to wild type animals (Figure 4-5). These results suggest that the number of synapses and the trafficking of the synaptic protein, synaptobrevin, to synapses are unchanged in *mir-75;mir-79* double mutants.

The *mir-75/mir-79* miRNA family and KLP-4 act in the same genetic pathway to regulate GLR-1 in the VNC

Both *klp-4* mutants and *mir-75;mir-79* double mutants have decreased GLR-1 abundance in the VNC. To determine whether the target of *mir-75/79* that regulates its effects on GLR-1 abundance functions in the same genetic pathway as KLP-4, we tested

whether the *klp-4* mutation and the *mir-75;mir-79* mutations have additive effects on GLR-1::GFP. We would expect that if KLP-4 and the target of *mir-75/79* were to act in the same genetic pathway, then the decrease in GLR-1 abundance in *klp-4mir-75;mir-79* triple mutants would be no larger than that of *klp-4* single mutants. Conversely, if *mir-75/79* and KLP-4 were to act in separate genetic pathways, combining the three mutations would result in an additive decrease in GLR-1 abundance. We found that *klp-4mir-75;mir-79* triple mutants and *klp-4* single mutants showed similar decreases in GLR-1::GFP puncta intensity (40% and 34%, respectively) compared to wild type animals (Figure 4-6 A, C-F). There was no significant difference in puncta intensity ($p = 0.9$) or density ($p = 0.6$) between *klp-4mir-75;mir-79* triple mutants and *klp-4* single mutants (Figure 4-6 C-F). The lack of additive effects on GLR-1::GFP in *klp-4mir-75;mir-79* triple mutants suggest that *mir-75/79* and KLP-4 function in the same genetic pathway to positively regulate GLR-1 abundance in the VNC.

klp-4 **transcript levels are not increased in** ***mir-75;mir-79*** **mutants**

Given that the *klp-4* 3'UTR contains binding sites for *mir-75/79* and they function in the same pathway as KLP-4, it remains a possibility that the *klp-4* 3'UTR is the target of *mir-75/79* that is responsible for their effects on GLR-1. If this were the case, it would seem to require that *mir-75/79* function positively regulates KLP-4 levels, which would be an unconventional but not unprecedented function for miRNAs (Vasudevan, 2012). If *mir-75/79* were to upregulate KLP-4 protein levels, they could potentially do so by protecting *klp-4* transcript from degradation, thereby raising the level of *klp-4* transcript available for translation. If this were the case, one might expect *klp-4* transcript levels to be increased in *mir-75;mir-79* mutants compared to wild type animals. We have performed a single quantitative RT-PCR experiment comparing *klp-4* transcript levels (normalized to *act-1*/Actin) in wild type animals and *mir-75;mir-79* mutants (Figure 4-7). Our preliminary results

show no increase in *klp-4* transcript levels however these experiments will have to be repeated with independent samples to obtain reliable results. Future studies will be necessary to test directly whether *mir-75/79* regulate KLP-4 expression.

GLR-1 distribution is unaltered in the VNC of *dhc-1(js319)* mutants

We have shown that *klp-4* mutations cause large decreases in GLR-1 trafficking and abundance in the VNC. However in *klp-4* mutants GLR-1 movement, while reduced, still occurs and there is a significant amount of GLR-1 present at synapses in the VNC (Chapter 3 Figures 1, 5, S6). Thus, not all GLR-1 anterograde trafficking is dependent on KLP-4. Considering these results and the fact that multiple motors are involved in AMPA receptor trafficking in mammals, it very likely that other microtubule-based motors contribute to GLR-1 trafficking in *C. elegans* as well.

In mammalian neurons the minus-end directed motor dynein along with the kinesin-1 *unc-116/*Kif5, and the kinesin-3 *unc-104/*Kif1A have been implicated in trafficking AMPAR (Kapitein et al., 2010; Kim and Lisman, 2001; Setou et al., 2002; Shin et al., 2003; Wyszynski et al., 1999; Wyszynski et al., 2002). Loss of function of *unc-104* has previously been shown to have no effect on GLR-1 distribution in *C. elegans* (Rongo et al., 1998). To determine whether dynein or *unc-116* might regulate GLR-1 levels in the VNC we first examined the distribution of GLR-1::GFP in dynein heavy chain mutants *dhc-1(js319)*. We found that GLR-1::GFP abundance was not significantly affected in *dhc-1(js319)* mutants compared to wild type animals (Figure 4-8 A-B, E). CDK-5 has been proposed to exert its effects on polarized trafficking of neuronal cargo through inhibition of dynein-mediated trafficking in *C. elegans* motor neurons (Goodwin et al., 2012; Ou et al., 2010). We therefore tested the effects of the *dhc-1(js319)* mutation on GLR-1 in the VNC of *cdk-5* mutants. We found a 27 % decrease in GLR-1::GFP puncta intensity in *cdk-5* single

mutants (Figure 4-8; Juo et al., 2007). In *cdk5;dhc-1* double mutants, puncta intensity was reduced by 16% compared to wild type levels (Figure 4-8). Puncta intensity in *cdk-5;dhc-1* double mutants appeared to show a small increase compared to *cdk-5* single mutants although this difference did not reach statistical significance using the Tukey Kramer test ($p > 0.05$). These results suggest that regulation of dynein-mediated transport does not appear to be a significant mechanism by which CDK-5 regulates GLR-1 abundance.

UNC-116 affects GLR-1 abundance in the VNC

We next examined the distribution of GLR-1::GFP in the VNC of two separate *unc-116/* kinesin-1 mutants. *unc-116(rh24sb79)* and *unc-116(f130)* are reported to be loss of function alleles consisting of point mutations in the N-terminal motor domain (Patel et al., 1993; Su et al., 2006; Yang et al., 2005) (Figure 4-9A). We found that the *unc-116(rh24sb79)* and *unc-116(f130)* mutations have similar effects on GLR-1::GFP. Each of these two mutations results in a small decrease in GLR-1::GFP puncta intensity ($p < 0.05$) compared to wild type [*f130* = 17% decrease; *rh24sb79* = 16% decrease] (Figure 4-9 B-D, H). Neither *unc-116* mutation affected GLR-1::GFP puncta density (Figure 4-9 B-D, I). *klp-4* single mutants showed a 30% decrease in puncta intensity in this experiment (Figure 4-9 B, E, H) and we found that GLR-1::GFP puncta intensity is reduced by 42-43% in both *klp-4; unc116(f130)* double mutants and *klp-4; unc-116(rh24sb79)*. These values appear to trend towards a decrease from puncta intensities in *klp-4* single mutants, however neither difference reached statistical significance (Figure 4-9H). GLR-1::GFP puncta density in *klp-4* mutants was not affected by either the *(f130)* allele or the *(rh24sb79)* allele of *unc-116* (Figure 4-9 I). These results suggest that UNC-116 positively regulates GLR-1 abundance in the VNC of wild type animals and, may possibly contribute to GLR-1 abundance in *klp-4* mutants.

We also examined GLR-1::GFP distribution in a third independent *unc-116* mutant. The *unc-116(e2310)* mutation is caused by a transposon insertion that is predicted to shorten the C-terminal cargo binding tail of the protein by about 100 amino acids (Patel et al., 1993) (Figure 4-9 A). This mutation has been reported as a partial loss of function (Brown et al., 2009; Byrd et al., 2001; Patel et al., 1993; Sakamoto et al., 2005). We observed that GLR-1::GFP puncta intensity and density in *unc-116(e2310)* mutants were unchanged compared to wild type animals (Figure 4-10 A-B, H-I). However, the *unc-116(e2310)* allele had a synthetic effect on GLR-1::GFP puncta intensity and density when combined with the *klp-4* mutation. In *unc-116(e2310);klp-4* double mutants, GLR-1::GFP puncta density was reduced by 53% and puncta intensity was reduced by 45% compared to wild type animals (Figure 4-10 A, D, H-I). Puncta densities and intensities were significantly lower in *unc-116(e2310);klp-4* double mutants than in *klp-4* single mutants ($p < 0.001$ for density and $p < 0.05$ for intensity) (Figure 4-10 A-D, H-I). The synthetic effect of the *unc-116(e2310)* mutation in the absence of functional KLP-4 seems to suggest that this mutated protein product may act differently than the *unc-116(f130)* and *unc-116(rh24sb79)* loss of function mutants. While intriguing, these results are difficult to interpret because it is impossible to predict with certainty how the altered cargo binding tail of the *unc-116*(*e2310)* mutant (Figure 4-9 A) would affect the motor's ability to form a complex with GLR-1 (Patel et al., 1993). For example, the shorter cargo binding tail could theoretically increase, decrease or have no effect on the kinesin's affinity for the GLR-1 complex.

We next tested whether the *unc116(e2310)* mutation shows synthetic effects with the *cdk-5* mutation as well. Given CDK-5 and KLP-4 function in the same pathway to regulate GLR-1, we would expect that inhibiting this pathway with either *klp-4* or *cdk-5* mutations should have the same effect on *unc-116(e2310)* mutants. If this were true, then *cdk-5 unc-116(e2310)* double mutants should show the same synergistic decrease in GLR-1

abundance that is present in *klp-4;unc116(e2310)* mutants. Interestingly, we found *unc-116(e2310)* does not have the same synthetic effect with the *cdk-5* mutation as it does with the *klp-4* mutation. There is no significant decrease in puncta density or intensity in *cdk-5 unc116(e2310)* double mutants compared to *cdk-5* single mutants ($p > 0.05$) (Figure 4-10 A, E-F, H-I). In *cdk-5 unc-116(e2310);klp-4* triple mutants, puncta intensity and density are decreased to similar extents as those in *klp-4;unc116(e2310)* double mutants (Figure 4-10 A, D, G-I). These *klp-4* dependent effects of *unc-116(e2310)* on GLR-1 abundance demonstrate a potentially novel and interesting role for this *unc-116(e2310)* mutant allele.

UNC-104 effects on GLR-1 abundance in the VNC of *klp-4* mutants

Given the interesting results of combining the *unc-116(e2310)* mutation with the *klp-4* mutation, we were interested in testing the effects of *unc-104* loss of function in the VNC of *klp-4* mutants. Compared to wild type animals, the distribution of GLR-1::GFP in the VNC of *unc-104(e1265)* loss of function mutants is unchanged (Rongo et al., 1998; Figure 4-11 A-B, E-F). Loss of function of *klp-4* alone caused a 33% decrease in GLR-1::GFP puncta intensity and a 21% decrease in puncta density from wild type levels (Figure 4-11 A-F). In *unc-104;klp-4* double mutants, GLR-1::GFP density was reduced by 21% and puncta intensity was reduced by 48% compared to wild type. While puncta intensity of the *klp-4;unc-104* double mutant appeared to trend toward a decrease compared to that in *klp-4* single mutants, this difference did not reach statistical significance ($p = 0.13$) (Figure 4-11 C-F). Thus, *unc-104* does not appear to contribute to GLR-1 abundance in the VNC of *klp-4* mutants.

Discussion

CDK-5 Regulation of KLP-4 dependent trafficking of GLR-1

We have shown that CDK-5 and KLP-4 act in the same genetic pathway to regulate GLR-1 trafficking in the VNC (Chapter 3; Figure 4-6). While time-lapse and co-migration analyses of GLR-1 and KLP-4 strongly suggest that GLR-1 is a cargo of the KLP-4 motor (see Chapter 3 Figures 4-5 and Appendix Figure 4-1), the mechanism by which CDK-5 regulates KLP-4 dependent GLR-1 trafficking is unclear. One major aim of this chapter was to investigate further the role of CDK-5 in GLR-1 trafficking. We first asked whether CDK-5 is an essential component of the pathway in the presence of excess KLP-4 motor. We found that *cdk-5* loss of function does not completely suppress the increased GLR-1 levels in the VNC of animals that over express *klp-4* (Figure 4-1). We've previously shown that over expression of *cdk-5* in *klp-4* mutants has no effect on GLR-1 in the VNC (Chapter 3 Figure 4-6). Together these results suggest that, for the GLR-1 population that is trafficked by the CDK-5 / KLP-4 pathway, KLP-4 is absolutely required whereas CDK-5 is not; its absence can be overcome in the presence of sufficient KLP-4 motors. These results are consistent with a model in which CDK-5 functions upstream of KLP-4.

Interestingly, CDK-5 plays a similar facilitative role in the UNC-104 mediated trafficking of synaptic proteins to new synaptic sites during DD motor neuron remodeling (Park et al., 2012). In these neurons, *cdk-5* and *unc-104* single mutants show similar defects in synaptic protein transport whereas over expression of either gene increases transport. The *unc-104* mutation completely suppresses *cdk-5* over expression, however over expression of the *unc-104* motor increases transport in *cdk-5* mutants (Park et al., 2012). Thus in multiple cell types, CDK-5 seems to promote, but not be absolutely necessary for, the trafficking of certain motor/cargo complexes. One potential model for CDK-5 function that is consistent with these results is one in which different cargo

complexes compete for a limited amount of a given motor. If CDK-5 promoted binding of the motor to a particular cargo complex, thereby allocating the limited motor supply, CDK-5 could be rendered nonessential if motor levels were no longer limiting. This model would predict that CDK-5 would have an inhibitory effect on the trafficking of other cargo complexes that require KLP-4 for trafficking. This would be interesting to test once other KLP-4 cargos are identified.

While the exact mechanism of CDK-5 remains unknown our results argue against some potential mechanisms for CDK-5. Static imaging of KLP-4::GFP suggests that CDK-5 does not simply increase the level of KLP-4 in the VNC (Figure 4-2) and preliminary time-lapse imaging suggests that CDK-5 does not affect KLP-4 velocity or run length (data not shown). Further time-lapse imaging will be necessary to determine whether *cdk-5* mutations affect aspects of KLP-4 trafficking, such as the percent of movements that are anterograde vs. retrograde.

Additionally, unlike a previously demonstrated mechanism by which CDK-5 affects trafficking, CDK-5 does not seem to exert its effects through inhibition of dynein (Goodwin et al., 2012; Ou et al., 2010). In *C. elegans* some classes of motor neurons require CDK-5 for the polarized trafficking of synaptic vesicles and dense core vesicles to axons. In *cdk-5* mutants, these cargos are trafficked to dendrites, an effect that requires dynein heavy chain (*dhc-1*). A loss of function mutation in *dhc-1* suppresses the effects of the *cdk-5* mutation, suggesting that CDK-5 regulates trafficking of these cargos by inhibiting dynein-mediated trafficking to dendrites (Goodwin et al., 2012; Ou et al., 2010). Our results suggest that CDK-5 does not work primarily through dynein to promote GLR-1 trafficking because the GLR-1 phenotype of *cdk-5* mutants is only partially suppressed by the *dhc-1(js319)* loss of function mutation (Figure 4-3).

Interestingly, *dhc-1(js319)* alone does not have a significant effect on GLR-1 levels,

suggesting that dynein may not play a critical role in GLR-1 trafficking. This could be considered a surprising result based on previous work demonstrating the importance of dynein for AMPAR trafficking in mammals (Kapitein et al., 2010; Kim and Lisman, 2001). However, it is difficult to predict the expected contribution of dynein to synaptic cargo in *glr-1*-expressing interneurons because the microtubule orientation in these cells is not known. Also, it is important to note that while the *dhc-1(js319)* allele has been used as a loss of function allele for several different cargo (Goodwin et al., 2012; Koushika et al., 2004; Ou et al., 2010) it is a not a null mutation (Koushika et al., 2004). Therefore, its effects on any one particular cargo are difficult to predict. Additional mechanisms of dynein inhibition including other genetic mutants of dynein heavy chain or dynein light chain, (e.g, *dhc-1(js121), dhc-1(or195) dli-1(js351) dli-1(ku266)),* over expression of *dnc-2* (dynamitin) (Koushika et al., 2004) and RNAi will have to be tested to determine with confidence whether GLR-1 trafficking involves dynein.

Together, our results suggest that CDK-5 does not act to promote KLP-4 trafficking of GLR-1 primarily through increasing KLP-4 levels in the cord or inhibiting dynein mediated GLR-1 transport. Two informative tests to determine how CDK-5 might function would be to determine whether CDK-5 affects KLP-4/GLR-1 complex formation. To date our attempts to detect *in vivo* KLP-4/GLR-1 complex formation using an integrated FLAG-tagged KLP-4 and GLR-1::GFP have been unsuccessful. This is not surprising given the presumably tenuous association between motor and vesicular cargo. It is worth noting that to our knowledge, co-immunoprecipitation between kinesin and vesicular cargo has never been reported from *C. elegans.* Future experiments investigating KLP-4/GLR-1 complex formation in heterologous cells and the potential effects of CDK-5 on this association could represent an alternative method to pursuing this important question.

Another future line of research is the identity of the CDK-5 target in the CDK-5/KLP-4

pathway. It is well documented that kinesins are subject to regulation by phosphorylation (Avunie-Masala et al., 2011; Cahu et al., 2008; Espeut et al., 2008; Guillaud et al., 2008; Jang et al., 2009; Matthies et al., 1993; Mishima et al., 2004; Yamada et al., 2007; Yoshimura et al., 2010). It will be interesting to determine whether CDK-5 phosphorylates KLP-4 and whether this phosphorylation affects KLP-4 activity. Prediction of potential CDK-5 targets is difficult because the CDK-5 consensus sequence is weak. However, CDK-5 phosphorylates Ser and Thr residues that are upstream of Pro residues. While KLP-4 has many of these potential CDK-5 target sites, cross-species sequence alignment (Kalign program: msa.sbc.su.se/cgi-bin/msa.cgi) predicts that only three of these potential sites are conserved in the KLP-4 orthologs *Drosophila* KHC-73 and mammalian Kif13A (Figure 4-12). Genetic experiments using targeted mutagenesis of these residues will be valuable in determining their relevance for CDK-5 regulation of KLP-4 function.

mir-75/79 regulate GLR-1 abundance

The number of validated interactions between miRNAs and target transcripts continues to rise. We tested the hypothesis that *mir-75/79* miRNA family negatively regulates KLP-4 expression, expecting to see increased GLR-1 abundance in the VNC. Surprisingly, loss of function of *mir75/79* had the opposite result, decreased GLR-1 in the VNC. This result raises 2 possibilities: 1) The target of *mir-75/79* that affects GLR-1 abundance is something other than *klp-4,* or 2) The *mir-75/79* family targets *klp-4* transcripts and acts to increase KLP-4 expression. While the latter scenario would be an unconventional effect of a miRNA on a target transcript, miRNAs have been shown, on occasion to increase protein levels of their targets (Mortensen et al., 2011; Steitz and Vasudevan, 2009; Vasudevan et al., 2007).

Theoretically, a microRNA could increase protein level of its target by either

facilitating translation of the target transcript, (e.g., by changing the folding of the transcript to make it more accessible to translation machinery) or by increasing target transcript levels, (e.g, by protecting the transcript from degradation). Our preliminary quantitative real time PCR experiment suggests that *klp-4* transcript is not increased in *mir-75;mir-79* double mutants. While this result is preliminary, it would seem to suggest that, if *mir-75/79* increases KLP-4 protein level, it does so by facilitating translation, as opposed to increasing transcript levels.

It will be interesting to determine whether or not the effect of these miRNA on GLR-1 occur though *klp-4.* Future experiments determining the effect of the *mir-75;mir-79* double mutation on expression reporters with the *klp-4* 3' untranslated region, which is the site of the predicted targets of these miRNAs, will be helpful to this end. Additionally, if *klp-4* is not the target, the identification of the transcript that is regulated by these miRNAs will be an interesting new development in the study of the genes regulating GLR-1 in the VNC.

UNC-116 regulation of GLR-1 abundance

We found that the kinesin-1 *unc-116* can regulate GLR-1 levels in the VNC (Figures 4-9 to 4-10). Two loss of function *unc-116* alleles showed small individual effects on GLR-1 and potential additive effects with the *klp-4* mutation (Figure 4-9). The *unc-116 (e2310)* mutant had synergistic effects with the *klp-4* mutation (Figure 4-10). In all *unc-116; klp-4* double mutants, GLR-1::GFP puncta in the VNC are reduced to levels that appear lower than in *klp-4* single mutants. This effect is interesting in light of the weak effects that *unc-116(f130)* and the *unc-116(rh24sb79)* mutations have on GLR-1::GFP puncta individually. The potentially additive nature of these mutations with the *klp-4* mutations suggest that their function in GLR-1 trafficking is completely independent from that of KLP-4. The mechanism by which these *unc-116* loss of function mutations affect GLR-1 levels is an area for future

investigation.

In mammalian neurons, kinesin-1 has been shown to traffic numerous neuronal cargo including mRNA, mitochondria and various synaptic proteins and to contribute to the establishment of polarity (Amato et al., 2011; Hirokawa et al., 2010). In *C. elegans,* kinesin-1/UNC-116 contributes, together with UNC-104, to trafficking of synaptic vesicles (Byrd et al., 2001; Sakamoto et al., 2005). Given the numerous important roles for *unc-116* in neuronal development and function, it would not be surprising if its effects on GLR-1 abundance were secondary to developmental defects. Conditional loss of function and rescue experiments could start to address this possibility.

We found that the *unc-116(e2310)* mutation has an effect on GLR-1 distribution in *klp-4* mutants but not in animals with a functional KLP-4. This synthetic effect of *unc-116(e2310)* is particularly interesting because it is not seen in *unc-116(e2310);cdk-5* double mutants. As previously stated it is difficult to predict the effect on protein function of the *unc-116(e2310)* allele. *cdk-5;unc116* double mutant analysis will have to be performed with the other *unc-116* mutant alleles before results can be interpreted conclusively.

The simplest model that would explain the synthetic effects of *unc-116(e2310)* on GLR-1 is one in which, in a wild type animal, KLP-4 traffics GLR-1 to synapses with no contribution from UNC-104 or the mutated UNC-116 that is a product of *unc-116(e2310)*. However in the absence of functional KLP-4, UNC-104 and UNC-116 protein levels are upregulated, possibly to compensate for the residual cargo in some trafficking compartment. At increased levels, these motors could be able to perform some GLR-1 transport. Potentially this upregulation of UNC-116 could occur at the transcription, mRNA or protein level. Interestingly, there is some precedent for increased cargo levels and increased potential for cargo binding causing upregulation of motor protein level. UNC-104 protein level has been shown to be dependent on cargo binding in *C. elegans* mechanosensory

neurons (Kumar et al., 2010). UNC-104 can be degraded in a ubiquitin-dependent fashion when it can not bind to cargo, whereas UNC-104 levels are higher when the motor is able to bind cargo (Kumar et al., 2010).

Measurements of UNC-116 and UNC-104 expression including transcriptional reporter assays, qPCR experiments and western blots in *klp-4* mutants vs wild type animals could test this model. The identification of novel kinesin regulators of GLR-1 abundance is interesting and much work remains to characterize the roles that these, and possibly other motors, play in regulating glutamate receptors.

METHODS

Strains

The following strains were used in this study: *nuIs25* (P*glr-1*::GLR-1::GFP), *nuIs24* (P*glr-1*::GLR-1::GFP), *nuIs125* (P*glr-1*::SNB-1::GFP), *pzEx188* (P*glr-1*::KLP-4::GFP), *pzIs20* (*Pglr-1::klp-4*), *cdk-5(gm336),klp-4(tm2114), lin-10(e1439), mir-75(n4472)*, *mir-79(n4126*), *dhc-1(js319), unc-116(e2310)*, *unc-116(f130)*, *unc-116(rh24sb79), unc-104(e1264).* All strains have been described previously

Imaging

All quantitative imaging was performed as described in Chapter 2.

miRNA selection

The selection of *mir-75/79* family as one that might potentially target *klp-4* was made using cumulative results from two prediction websites. The Target Scan Worm function from

Targetscan.org (Whitehead Institute fo Biomedica Research). The *klp-4* 3' untranslated region (UTR) was predicted to have 8 nonconserved miRNA target sites for various miRNA families and a single conserved miRNA target site for miR-75/79

The PicTar web interface for nematodes (http://pictar.mdc-berlin.de/cgi-bin/new_PicTar_nematode.cgi?species=nematode) assigned *mir-75/79* the highest Pictar score for the *klp-4* 3' UTR (PicTar score = 0.7081). *klp-4* ranked 81st out of 180 genes as being likely targets of *mir-75/79.*

Real-Time Polymerase Chain Reaction (PCR)

Total RNA was isolated from mixed-stage wild-type *(nuIs24)* and *mir-75;mir-79* null [*nuIs24;mir-75(n4472); mir-79(n4126)*] animals. One RNA preparation for each genotype was used. RNA isolation, cDNA synthesis and quantitative rtPCR was performed as described in Chapter 2.

Figure 4-1.

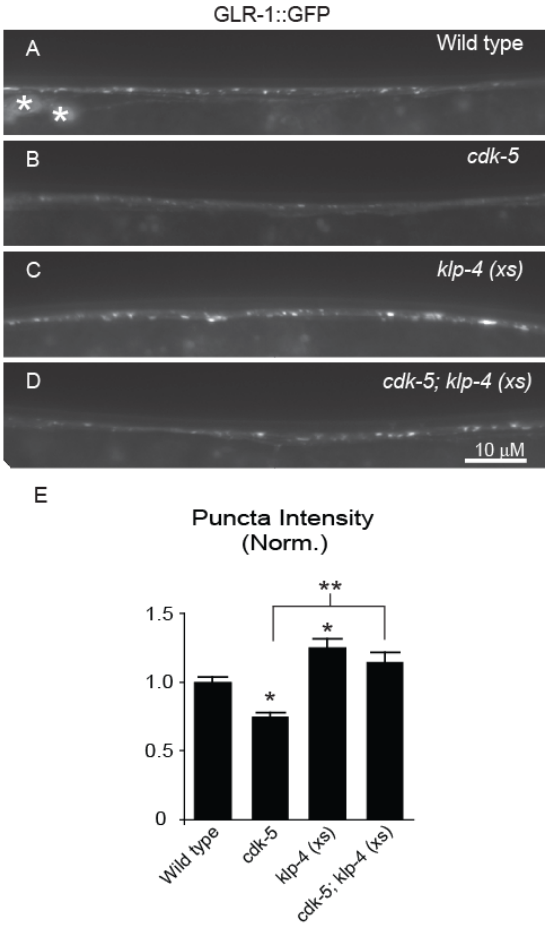

Figure 4-1. *klp-4(xs)* increases GLR-1 abundance in the VNC of *cdk-5* mutants (A-D) Representative images of the anterior VNC of L4 stage animals expressing GLR-1::GFP. Shown are wild type (A), *cdk-5-(gm336)* mutants (B), animals overexpressing *klp-4* under the control of the *glr-1* promoter [*klp-4(xs*)] (C), and *cdk-5(gm336)* mutants overexpressing *klp-4* [*cdk-5; klp-4(xs*)](D). For these and all subsequent VNC images, anterior is to the left and ventral is up. White asterisks mark neuronal cell bodies. (E) Quantification of GLR-1::GFP puncta intensities (normalized) for the strains pictured in A-D. Mean and SEM are shown for at least n = 20 animals in each group. Values that differ significantly from wild type are indicated above each bar, (#$p \leq 0.05$, **$p \leq 0.001$, Tukey-Kramer test).

Figure 4-2.

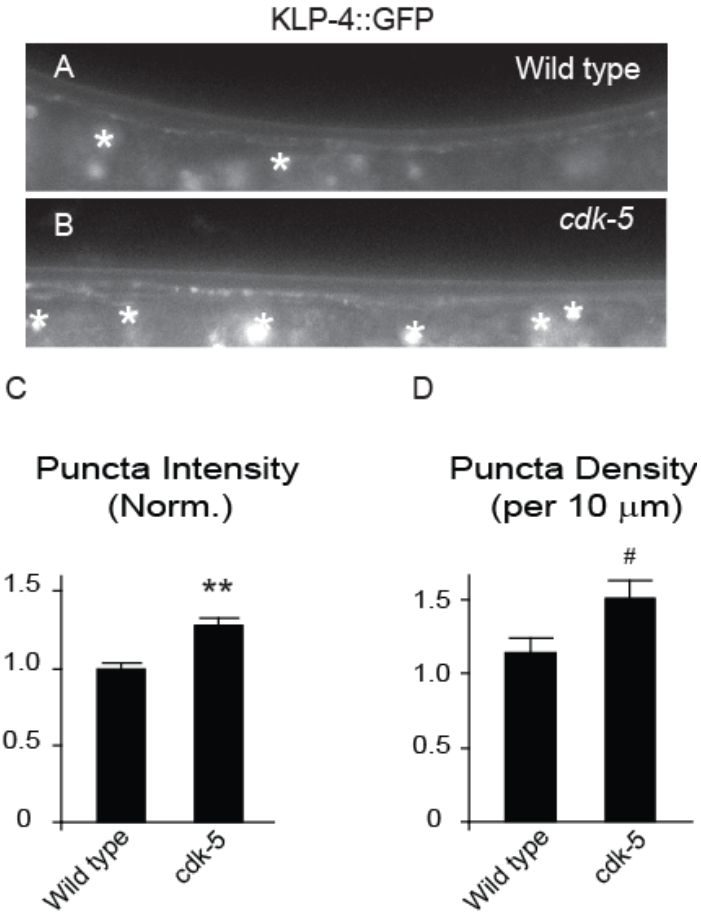

Figure 4-2. KLP-4 abundance increases in the VNC of *cdk-5* mutants

(A-B) Representative images of the anterior VNC of wild type (A), and *cdk-5 (gm336)* (B) L4 animals expressing KLP-4::GFP (*pzEx188*). White asterisks mark autofluorescent gut granules. (C-D) Quantification of KLP-4::GFP puncta intensities (normalized) (C) and densities (D) for the strains pictured. Mean and SEM are shown for at least n = 20 animals in each group. Values that differ significantly from wild type are indicated above each bar, (#$p \leq 0.05$,**$p \leq 0.001$, Tukey-Kramer test).

Figure 4-3.

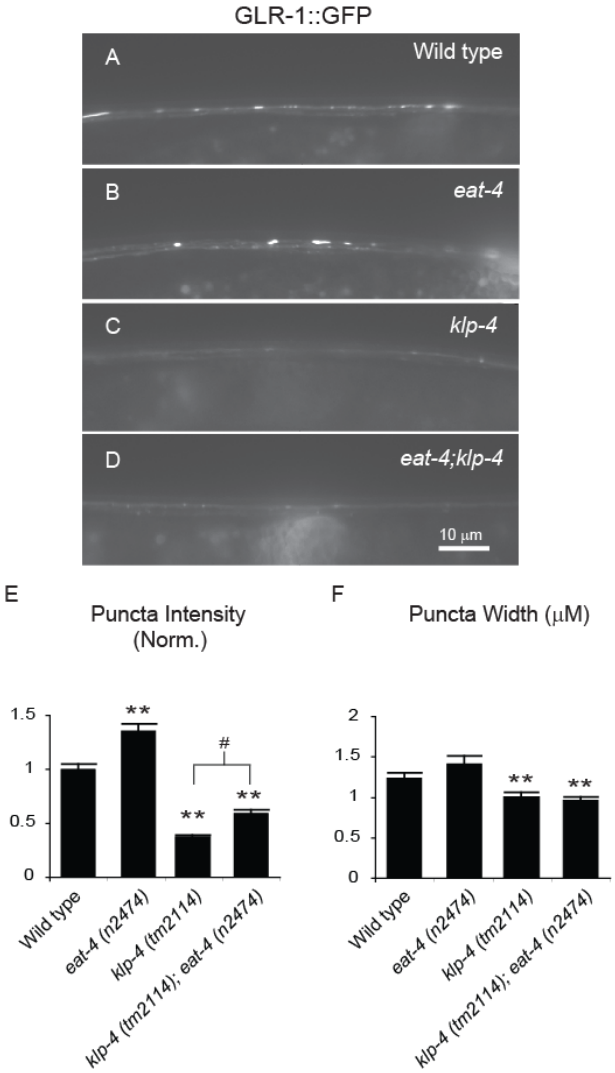

Figure 4-3. Loss of function of EAT-4 increases GLR-1 abundance in the VNC of *klp-4* mutants (A-D) Representative images of the posterior VNC of wild type (A), *eat-4(n2474)* (B), *klp-4(tm2114)* (C), and double mutant *klp-4(tm2114);eat-4(n2474)* (D), L4 animals expressing GLR-1::GFP. (E-F) Quantification of GLR-1::GFP puncta intensities (normalized) (E) and widths (F) for the strains pictured in A-D. Mean and SEM are shown for at least $n = 20$ animals in each group. Values that differ significantly from wild type are indicated above each bar, whereas other comparisons are marked by brackets (# $p \leq 0.05$, ** $p \leq 0.001$, Tukey-Kramer test).

Figure 4-4.

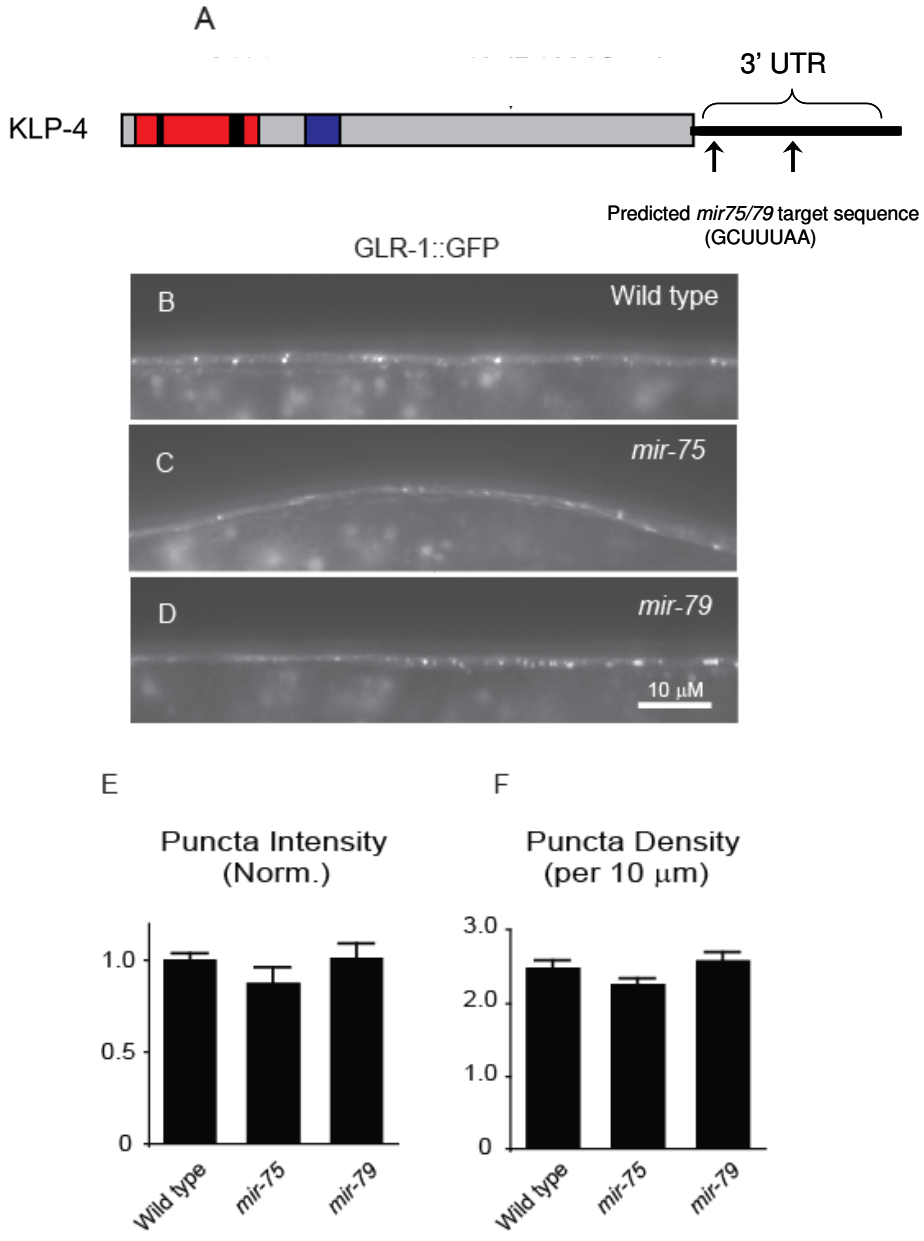
A
3' UTR
KLP-4
Predicted mir75/79 target sequence
(GCUUUAA)
GLR-1::GFP
B
Wild type
C
mir-75
D
mir-79
10 μM
E
Puncta Intensity
(Norm.)
1.0
0.5
0
Wild type
mir-75
mir-79
F
Puncta Density
(per 10 μm)
3.0
2.0
1.0
0
Wild type
mir-75
mir-79

Figure 4-4 (contd.).

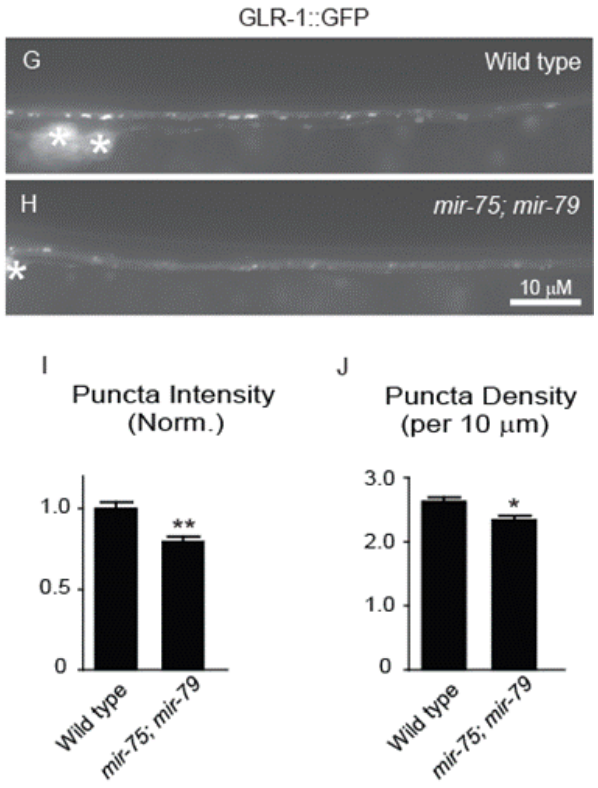

Figure 4-4. GLR-1 abundance in the VNC is decreased in *mir-75; mir-79* double mutants (A) mRNA of *klp-4* including predicted target sites for *mir-75/79*, indicated by arrows, in the 3' UTR. The N-terminal motor domain (red box) with the ATP-binding motif (thin black bar) and microtubule-binding regions (thick black bar), the cargo-binding domain (gray box) and the Forkhead-associated domain (FHA; purple box) are shown. (B-D, G-H) Representative images of the anterior VNC of wild type (B,G), *mir-75(n4472)* (C), *mir-79(n4126*) (D), and *mir-75(n4472)*; *mir-79(n4126*) double mutant (H) L4 animals expressing GLR-1::GFP. White asterisks mark neuronal cell bodies. (E-F, I-J) Quantification of GLR-1::GFP puncta intensities (normalized) (E, I) and densities (F, J) for the strains pictured. Mean and SEM are shown for at least $n = 15$ (E-F) or $n = 25$ (I-J) animals in each group. Values that differ significantly from wild type are indicated by asterisks above each bar ($*p \leq 0.01$,$**p \leq 0.001$, Tukey-Kramer test).

.**Figure 4-5.**

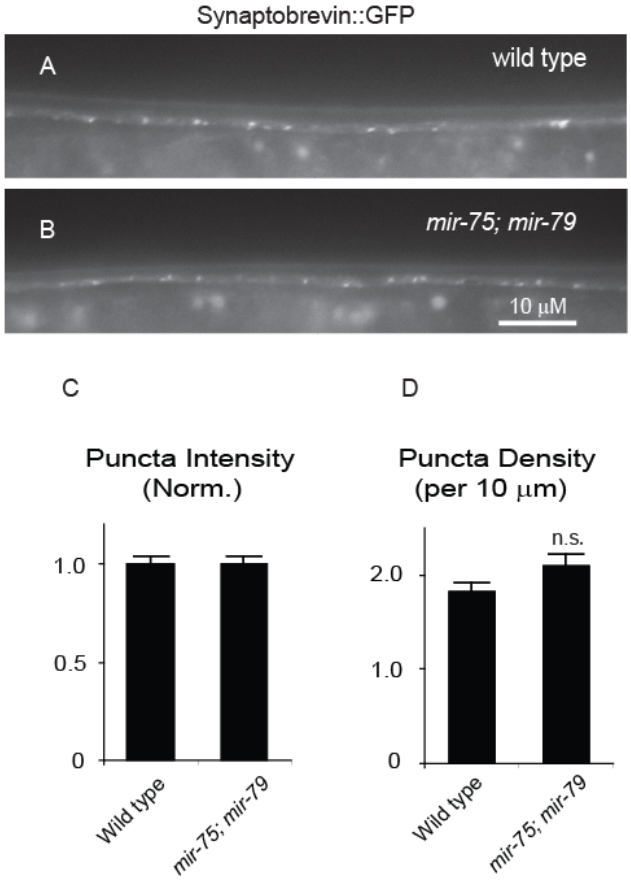

Figure 4-5. SNB-1 abundance in the VNC is unchanged in *mir-75; mir-79* double mutants (A-B) Representative images of the anterior VNC of L4 wild-type (A) and *mir-75(n4472); mir-79(n4126)* (B) animals expressing an integrated Synaptobrevin::GFP transgene under the control of the *glr-1* promoter. (C-D) Quantification of puncta intensities (normalized)(C) and densities (D) for the strains pictures. Mean and SEM are shown for at least $n = 18$ animals in each group. No significant difference was found between wild-type and *klp-4* mutant animals for puncta intensity or density ($p > 0.05$, Tukey-Kramer test).

Figure 4-6.

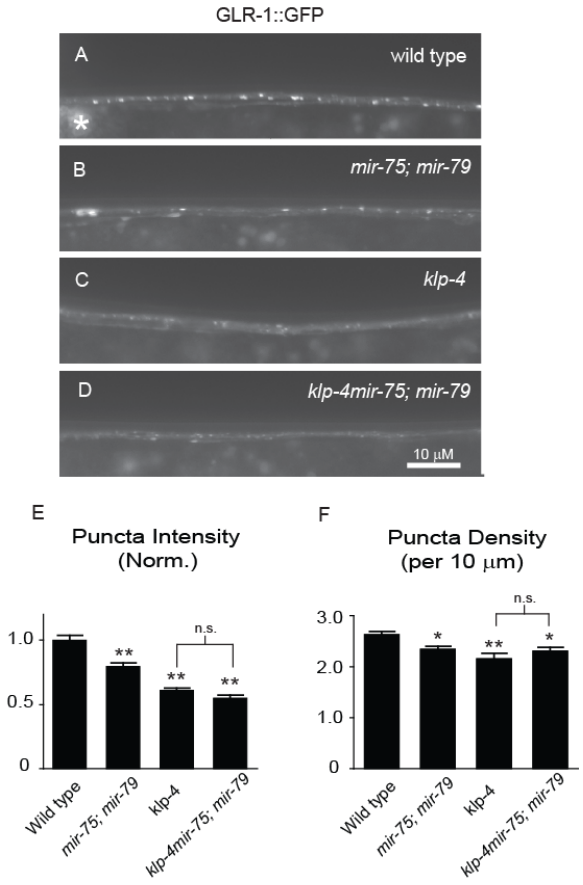

Figure 4-6. Mutations in *klp-4* and *mir-75; mir-79* have non-additive effects on GLR-1 abundance in the VNC. (A-D) Representative images of the anterior VNC of wild type (A), *mir-75(n4472); mir-79(n4126)* (B), *klp-4(tm2114)* (C), and *klp-4(tm2114)mir-75(n4472); mir-79(n4126)* (D) triple mutant L4 animals expressing GLR-1::GFP. White asterisks mark neuronal cell bodies. (E-F) Quantification of GLR-1::GFP puncta intensities (normalized) (E) and densities (F) for the strains pictured in A-D. Mean and SEM are shown for at least n = 25 animals in each group. Values that differ significantly from wild type are indicated by asterisks above each bar, whereas other comparisons are marked by brackets (*$p \leq 0.01$,**$p \leq 0.001$, Tukey-Kramer test). n.s. denotes no significant difference between the indicated strains ($p > 0.05$).

Figure 4-7.

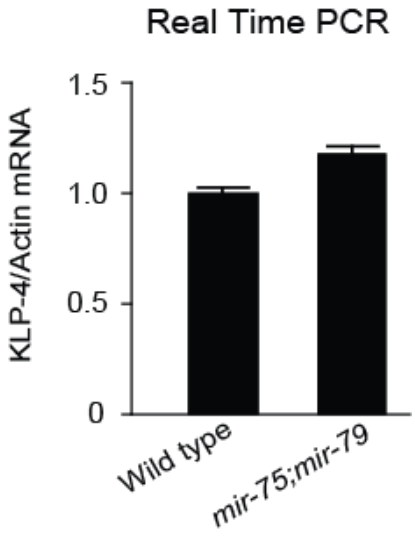

Figure 4-7. *klp-4* transcript levels are not increased in *mir-75;mir-79* mutants

Results of real-time quantitative PCR are shown. *klp-4* to actin mRNA ratios are shown for wild-type and *mir-75(n4472); mir-79(n4126)* double mutant animals integrated GLR-1::GFP (normalized to wild-type). For each genotype, $n = 6$ replicate measurements from a single preparation of GLR-1 mRNA level were normalized to the average of $n = 6$ replicate measurements of actin mRNA level. No significant difference in normalized *klp-4* transcript was detected Mean and SEM are shown. ($p > 0.05$ student's T-test).

Figure 4-8.

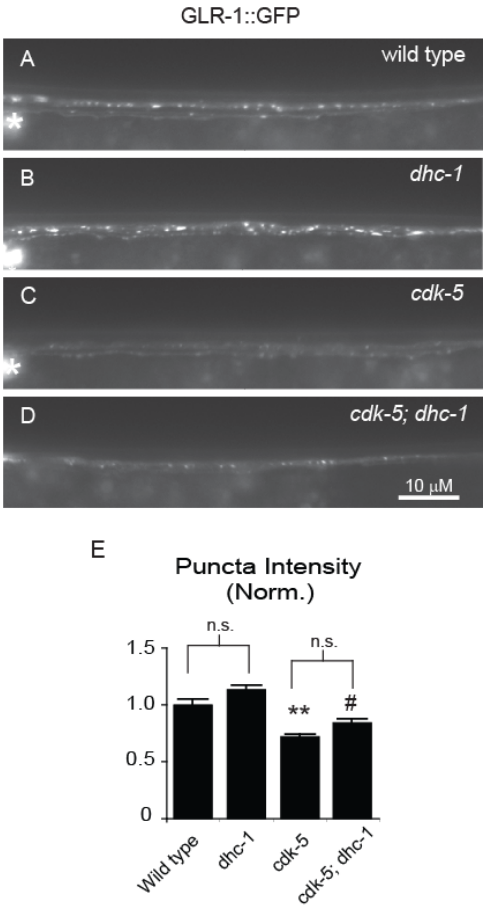

Figure 4-8. *dhc-1(js319)* partially suppress effects of *cdk-5* loss of function on GLR-1 in the VNC (A-D) Representative images of the anterior VNC of wild type (A), *dhc-1(js319)* (B), *cdk-5(gm336*), and double mutant *cdk-5(gm336); dhc-1(js319)* (D), L4 animals expressing GLR-1::GFP. White asterisks mark neuronal cell bodies. (E) Quantification of GLR-1::GFP puncta intensities (normalized) for the strains pictured in A-D. Mean and SEM are shown for at least $n = 30$ animals in each group. Values that differ significantly from wild type are indicated by asterisks above each bar, whereas other comparisons are marked by brackets (#$p \leq 0.05$,**$p \leq 0.001$, Tukey-Kramer test). n.s. denotes no significant difference between the indicated strains ($p > 0.05$).

Figure 4-9.

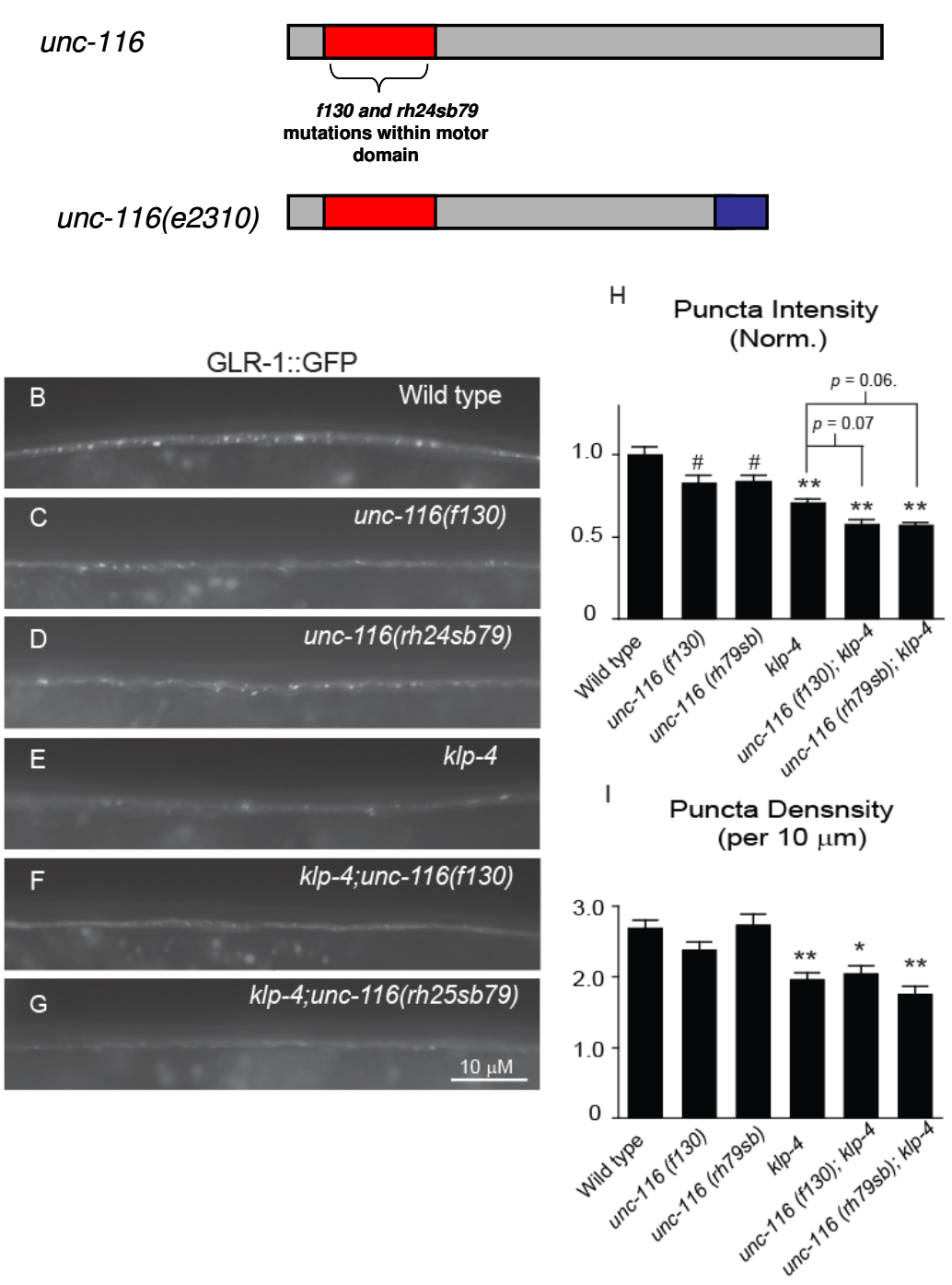
A
unc-116
f130 and rh24sb79 mutations within motor domain
unc-116(e2310)
GLR-1::GFP
B Wild type
C unc-116(f130)
D unc-116(rh24sb79)
E klp-4
F klp-4;unc-116(f130)
G klp-4;unc-116(rh25sb79)
10 μM
H
Puncta Intensity (Norm.)
p = 0.06.
p = 0.07
1.0
0.5
0
Wild type
unc-116 (f130)
unc-116 (rh79sb)
klp-4
unc-116 (f130); klp-4
unc-116 (rh79sb); klp-4
I
Puncta Densnsity (per 10 μm)
3.0
2.0
1.0
0

Figure 4-9. *unc-116* loss of function decreases GLR-1 abundance in the VNC

(A) Comparison of wild type *unc-116* and *unc-116(e2310).* Motor domains (red) and cargo binding tails (gray) are shown for both. The *e2310* mutation consists of a transposon insertion predicted to result in a truncated protein ending in 19 amino acids not present in the wild type protein (blue box) (B-G) Representative images of the anterior VNC of wild type (B), *unc-116(f130)* (C), *unc-116(rh24sb79)* (D) *klp-4(tm2114)* (E), *klp-4; unc-116(f130)* (F), and *klp-4; unc-116(rh24sb79)* (G), L4 animals expressing GLR-1::GFP. (H-I) Quantification of GLR-1::GFP puncta intensities (normalized) (H) and densities (I) for the strains pictured. Mean and SEM are shown for at least $n = 20$ animals in each group. Values that differ significantly from wild type are indicated above each bar, whereas other comparisons are marked by brackets (#$p \leq 0.05$, *$p \leq 0.01$, **$p \leq 0.001$, Tukey-Kramer test).

Figure 4-10.

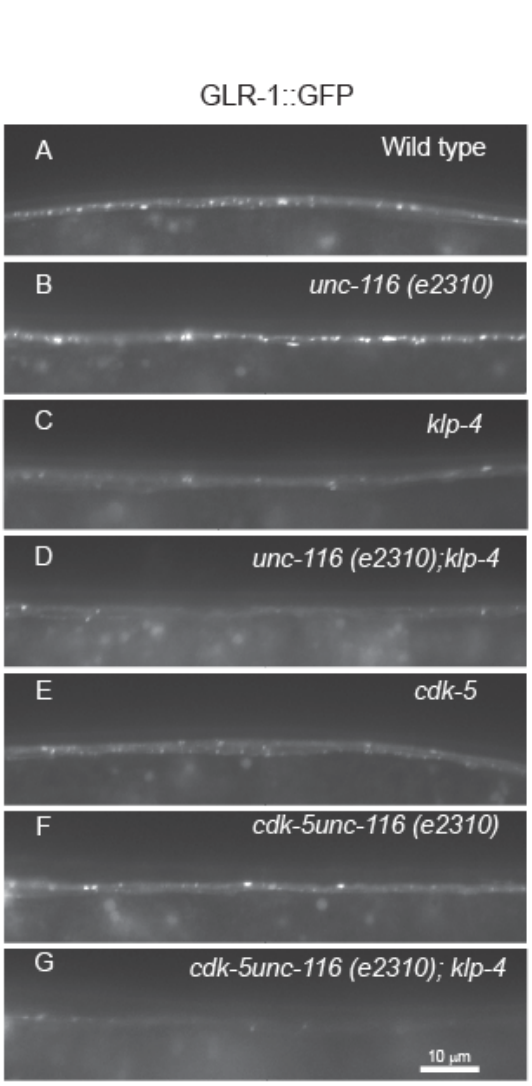
GLR-1::GFP
A
Wild type
B
unc-116 (e2310)
C
klp-4
D
unc-116 (e2310);klp-4
E
cdk-5
F
cdk-5unc-116 (e2310)
G
cdk-5unc-116 (e2310); klp-4
10 μm

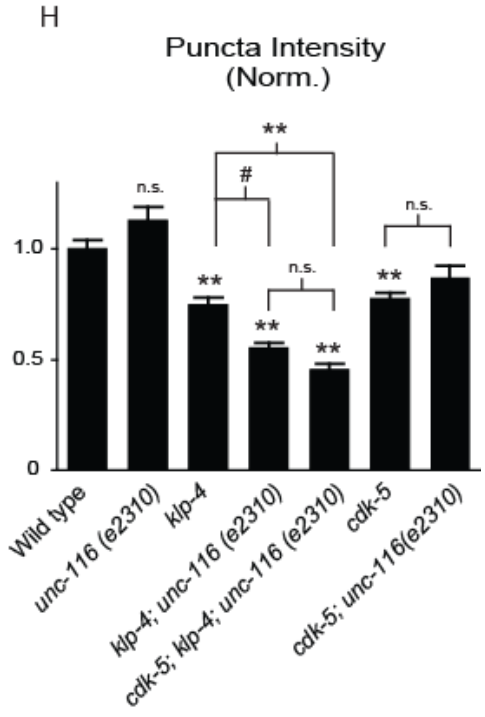
H
Puncta Intensity
(Norm.)
1.0
0.5
0
n.s.
#
**
Wild type
unc-116 (e2310)
klp-4
klp-4; unc-116 (e2310)
cdk-5; klp-4; unc-116 (e2310)
cdk-5
cdk-5; unc-116(e2310)

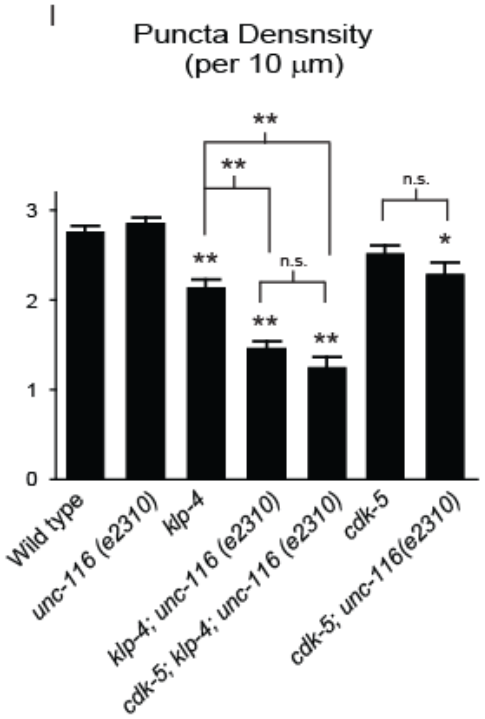
I
Puncta Densnsity
(per 10 μm)
3
2
1
0
n.s.
*
**
Wild type
unc-116 (e2310)
klp-4
klp-4; unc-116 (e2310)
cdk-5; klp-4; unc-116 (e2310)
cdk-5
cdk-5; unc-116(e2310)

Figure 4-10. *unc-116(e2310)* mutations decrease GLR-1 abundance in the VNC of *klp-4* mutants (A-D, G-L) Representative images of the anterior VNC of wild type (A, G), *unc-116(e2310)* (B, H), *klp-4(tm2114)* (C), *klp-4(tm2114); unc-116(e2310)* (D, K), *cdk-5(gm336)* (I),*cdk-5(gm336) unc-116(e2310)* (J), and *klp-4(tm2114);cdk-5(gm336) unc-116(e2310)* (L) triple mutant, L4 animals expressing GLR-1::GFP. (E-F, M-N) Quantification of GLR-1::GFP puncta intensities (normalized) (E, M) and densities (F, N) for the strains pictured. Mean and SEM are shown for at least $n = 20$ animals in each group. Values that differ significantly from wild type are indicated above each bar, whereas other comparisons are marked by brackets (#$p \leq 0.05$, *$p \leq 0.01$, **$p \leq 0.001$, Tukey-Kramer test). n.s. denotes no significant difference between the indicated strains ($p > 0.05$).

Figure 4-11.

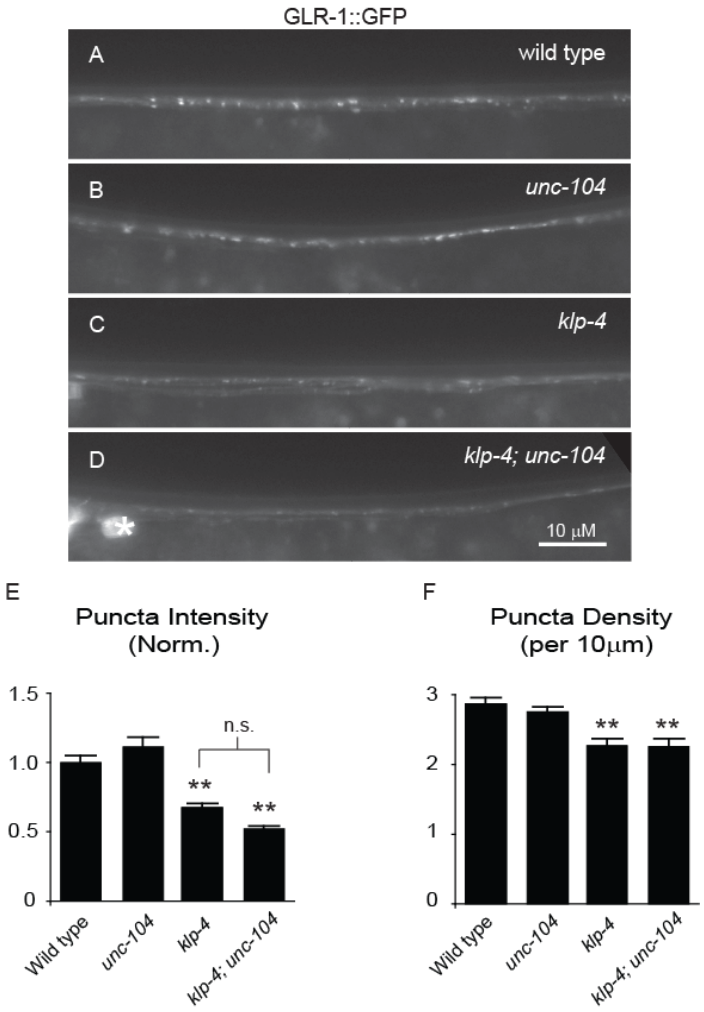

Figure 4-11. *unc-104(e1265)* mutations do not affect GLR-1 abundance in the VNC

Representative images of the anterior VNC of wild type (A), *unc-104(e1264)* (B), *klp-4(tm2114)* (C), *klp-4(tm2114); unc-104(e1265)* (D), double mutant, L4 animals expressing GLR-1::GFP. White asterisks mark neuronal cell bodies. (E-F) Quantification of GLR-1::GFP puncta intensities (normalized) (E) and densities (F) for the strains pictured. Mean and SEM are shown for at least $n = 25$ animals in each group. Values that differ significantly from wild type are indicated above each bar, whereas other comparisons are marked by brackets (**$p \leq 0.001$, Tukey-Kramer test). n.s. denotes no significant difference between the indicated strains ($p > 0.05$).

Figure 4-12.

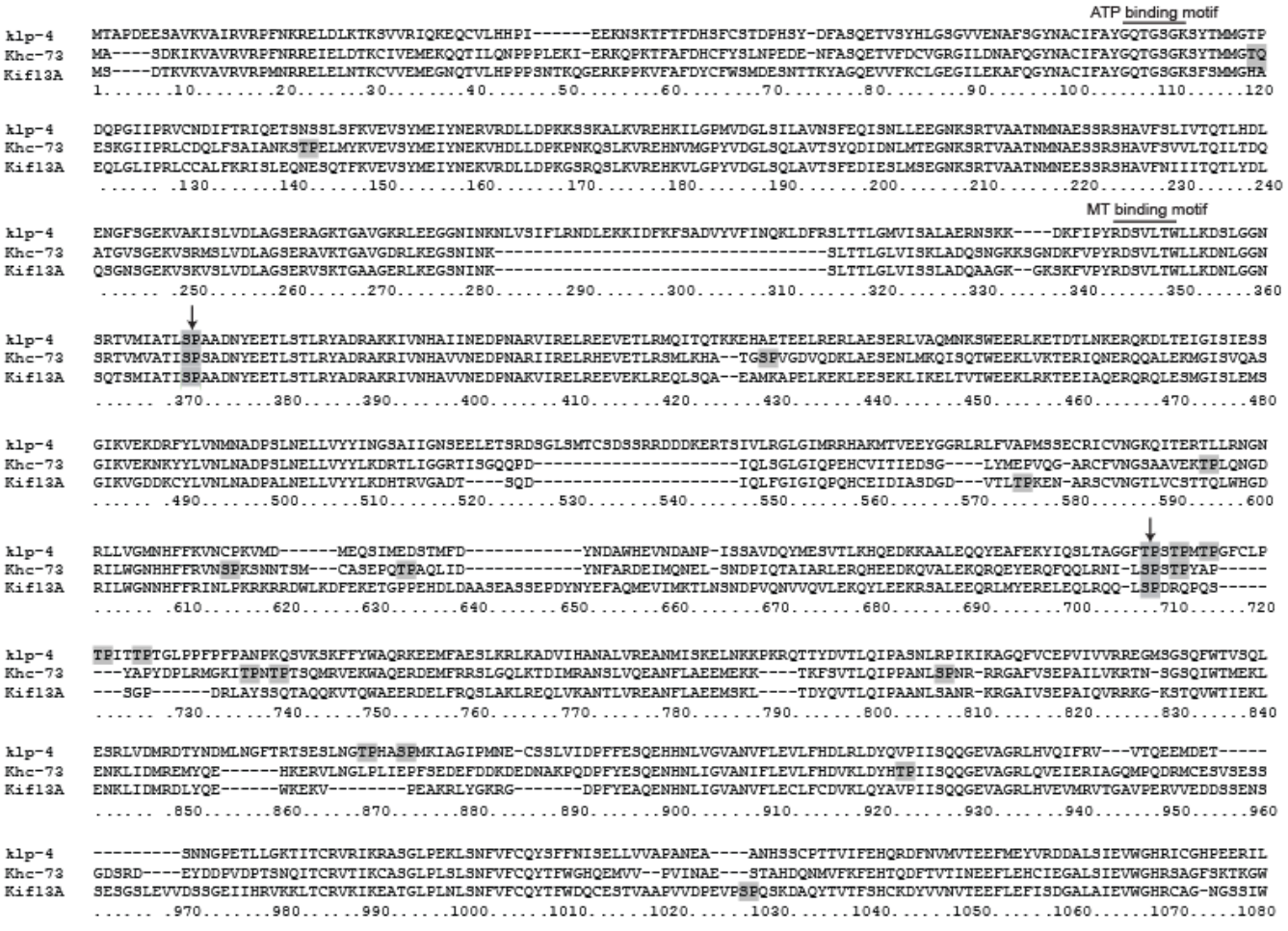

Figure 4-12. (contd.)

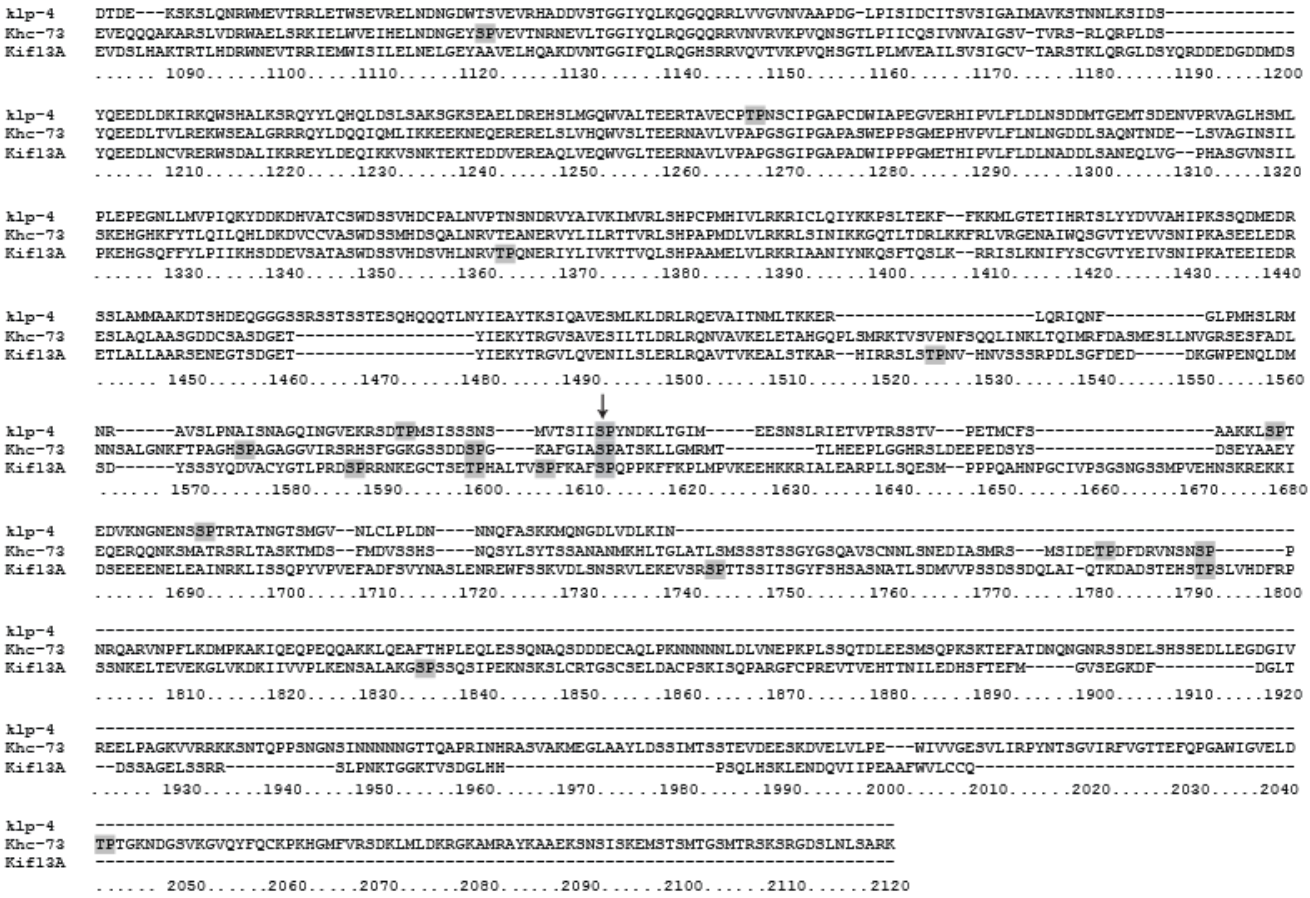

Figure 4-12. Potential CDK-5 phosphorylation sites in *klp-4* orthologs.

Kalign program multiple sequence alignment of amino acids in *C. elegans* KLP-4, *Drosophila* KHC-73 and mammalian Kif13A. S/T-P sequences are boxed and shaded in grey. The thin black line marks the ATP binding motif. Black arrows mark the three S/T-P sequences that are conserved across all three proteins.

Chapter 5

Discussion

Glutamate signaling has many important functions in the brain, such as its essential role in learning and memory. Deregulation of its signaling is a component of various neurological diseases (Bowie, 2008; Bredt and Nicoll, 2003; Kwak and Weiss, 2006). In order to understand conditions in which brain function is affected, it is vital to first understand the mechanisms that control glutamate signaling. The abundance of GluRs present in the synaptic membrane is an important factor in determining the strength of a synapse (Collingridge et al., 2004; Derkach et al., 2007). There are several steps in the process involved in regulating synaptic GluR abundance including assembly and loading into vesicles in the cell body, transport from the cell body to synapse and the insertion into and endocytosis from the synaptic membrane. Of these, transport from the cell body to the synapse is the least well understood. It is clear that long distance trafficking along microtubules is a tightly regulated process that requires the coordinated actions of many genes (Hammond et al., 2010; Verhey and Hammond, 2009). The identification of novel genes involved in this process will contribute to a greater understanding of GluR trafficking, which is fundamentally important to the health and function of the brain.

In this thesis, I present research that describes a function for the kinesin-3, *klp-4,* for the first time in *C. elegans* and identifies *klp-4* as a novel regulator of GLR-1 trafficking. We have performed a forward genetic screen to identify suppressors of the effects of *cdk-5* overexpression on GLR-1 abundance in the VNC. Identification of novel genes acting in the same pathway as CDK-5 to regulate GLR-1 will lead to a better understanding of how CDK-5 functions to regulate GLR-1 trafficking and, more broadly, will contribute to our knowledge of GluR trafficking (Chapter 2). We then showed that CDK-5 and KLP-4 function in a common pathway to promote the anterograde trafficking of GLR-1 and we demonstrated *in vivo* that KLP-4 is a fast, processive neuronal motor similar to other kinesin-3 family members, UNC-104, KHC-73, and Kif13A and Kif13B (Horiguchi et al., 2006; Huckaba et

al., 2011; Okada et al., 1995; Zhou et al., 2001). This work represents the first description of a motor that transports GLR-1. Additionally, this work could lead to the identification of a novel regulator of GluR transport in mammals as the mammalian homologs of *klp-4,* Kif13A and Kif13B have not been implicated in GluR trafficking. We also identified an interesting mechanism whereby GLR-1 is degraded in lysosomes in the cell bodies of *klp-4* mutants, which is in contrast to GLR-1 accumulation in the cell bodies of *cdk-5* mutants. This finding represents a significant contribution to the field because it suggests that not all trafficking defects affect a given cargo in the same manner. It also potentially reveals an important regulatory mechanism to avoid the aberrant accumulation of proteins when cellular levels of the motor are low (Chapter 3). In Chapter 4, we investigated the role of potential regulators of KLP-4 activity as well as the role of other microtubule motors in GLR-1 trafficking. We identified a novel example of miRNA regulation of GluRs that could potentially reveal an interesting and unusual method of miRNA regulation and we identified a role for a second kinesin motor, *unc-116,* in regulating GLR-1 levels (Chapter 4).

Isolation of *cdk-5(xs)* suppressor mutants

To identify novel regulators of GLR-1 trafficking and to better understand the mechanism by which CDK-5 regulates GLR-1 abundance in the VNC, we conducted a forward genetic *cdk-5(xs)* suppressor screen. GluR trafficking is a complex and poorly understood process. Therefore an unbiased approach to gene discovery for this pathway is likely to be informative. To date, we have isolated 43 suppressor mutants with decreased GLR-1 abundance in the VNC (Table 2-1). With the identification of one of these suppressor mutations, *klp-4(pz19),* we have begun to identify novel regulators of GLR-1 levels in the VNC that function in the same pathway as CDK-5. We have not yet determined whether KLP-4 is a direct substrate of CDK-5. The identification of the remaining

suppressor mutations should yield significant gains in understanding GluR trafficking and the role of CDK-5 in that process.

Characterization of KLP-4's role in GLR-1 trafficking

We identified *klp-4* as a novel regulator of GLR-1 in the VNC of *C. elegans.* Loss of function of *klp-4* results in decreased GLR-1 levels in the VNC, whereas overexpression of *klp*-4 increased abundance of GLR-1 (Figure 3-1, 3-S4 and Figure 4-1). Consistent with these effects, animals with decreased or increased levels of GLR-1::GFP in the VNC display decreased or increased GLR-1-dependent locomotion behavior, respectively. The identity of KLP-4 as a kinesin motor suggested that it may function in the microtubule-dependent anterograde trafficking of GLR-1 from the cell body to the synapse, a similar function to what has been previously been proposed for CDK-5 (Juo et al., 2007). We performed genetic analyses and time-lapse imaging of mobile GLR-1 puncta and found that KLP-4 functions upstream of endocytosis at the synapse and that both CDK-5 and KLP-4 promote the anterograde trafficking of GLR-1 in the VNC (Figure 3-3, 3-5 and 3-S7). KLP-4 is required for maintaining GLR-1 levels after early neuronal development because the decreased GLR-1 abundance in *klp-4* loss of function mutants can be completely rescued with the heat-shock induced expression of a *klp-4* rescue construct in L4 larval animals (Figure 3-2). Thus we propose that the kinesin-3 family motor KLP-4 promotes GLR-1 abundance at synapses in the VNC by positively regulating anterograde trafficking of GLR-1. KLP-4 is the first motor to be identified as contributing to GLR-1 transport. The identification of motors is an important step in gaining a better understanding of how synaptic receptor abundance is regulated. Our results suggest that multiple motors regulate GLR-1 trafficking. First, in *klp-4* mutants, time-lapse imaging indicates that GLR-1 transport still occurs, albeit at a reduced rate (Figures 3-5, 3-S6). Secondly, we have demonstrated that GLR-1 abundance is

reduced in the VNC of *unc-116 /* Kinesin-1 loss of function mutants, suggesting that UNC-116 is another motor involved in GLR-1 trafficking (Figure 4-9). Consistent with this, prior work in mammalian neurons has implicated multiple motors in AMPAR trafficking (Kapitein et al., 2010; Kim and Lisman, 2001; Setou et al., 2002; Shin et al., 2003; Wyszynski et al., 2002). The mammalian homologs of *klp-4,* Kif13A and Kif13B have not been implicated in trafficking of neurotransmitter receptors or postsynaptic proteins in mammals. Interestingly, however, two recent studies have implicated KIF13A and Kif13B in dendritic trafficking in mammalian neurons (Huang and Banker, 2011; Jenkins et al., 2012). In the first, constitutively active motor domains of all kinesins were expressed in cultured hippocampal neurons. All but four of the motor domains accumulated exclusively in axon tips. Kif13A and Kif13B, however, accumulated in dendrites as well as axons (Huang and Banker, 2011), suggesting that these motors may normally transport cargoes into dendrites. Subsequent work studying preferential association of kinesin cargo binding tails with either dendritically or axonally-trafficked vesicles in hippocampal neurons demonstrated that the cargo binding tails of Kif13A and Kif13B are capable of associating with and transporting dendritic vesicles (Jenkins et al., 2012). Together this work demonstrates that the *klp-4* homologs Kif13A and Kif13B have an inherent preference for trafficking dendritic vesicles into dendrites and it suggests that they may have an as yet undiscovered role in transporting dendritic cargo in mammalian neurons.

In addition to regulating GLR-1 abundance in wild type animals, we demonstrated that KLP-4 is required for the increased GLR-1 abundance in *cdk-5(xs)* animals. Moreover, *cdk-5;klp-4* double mutants display no further decrease in GLR-1 abundance than either *klp-4* or *cdk-5* single mutants (Figure 3-6 and 3-S7). Together these results demonstrate that KLP-4, which we identified based on its ability to suppress the effects of *cdk-5(xs)*, indeed functions in the same genetic pathway as CDK-5 to regulate GLR-1 trafficking. We

identified a novel regulatory mechanism for GLR-1 whereby in *klp-4* mutants, GLR-1 undergoes lysosomal degradation in the cell body (Figure 3-7). This was particularly interesting given the previous finding that GLR-1 accumulated in the cell bodies of *cdk-5* mutants (Juo et al., 2007) and it suggests that inefficient anterograde trafficking of GLR-1 is not sufficient to trigger its degradation. Instead, the lack of the motor itself appears to be necessary to initiate this degradation pathway (Figure 3-7). This is consistent with previous results demonstrating that changes in the expression of a motor result in correlated changes in the expression of its cargo proteins (Guillaud et al., 2003; Dhar et al., 2011; Yin et al., 2011; Wong et al., 2002; Puthanveettil et al., 2008).

Previous examples of this phenomenon have occurred when changes in neuronal activity affect transcription of a motor and cargo similarly, as is the case for the kinesin-2 family motor Kif17 and one of its cargoes, the NMDAR subunit NR2B (Guillaud et al., 2003; Dhar et al., 2011; Yin et al. 2011, Wong et al., 2002). In rodent neurons, reduction of Kif17 protein levels by RNAi results in decreased NR2B levels (Guillaud et al., 2003; Yin et al., 2011). This co-regulation occurs through a common synaptic-activity induced signaling pathway. Changes in neuronal activity affect the expression of NRF-1, a transcription factor that, in turn controls expression of both Kif17 and NR2B (Dhar and Wong-Riley, 2011; Yin et al., 2011). Protein levels of a separate NMDAR subunit, NR2A is also down regulated in Kif17 RNAi-treated neurons. However, transcript levels of NR2A in these cells are unaffected and down regulation of protein levels occurs through increased ubiquitin-mediated degradation (Yin et al., 2011). The mechanism for this co-regulation is not well understood. This latter co-regulation is more similar to the effect we observed on GLR-1 in *klp-4* mutants. GLR-1 protein appears to be degraded in the lysosome in the absence of KLP-4 (Figure 3-7). It would be very interesting in the future to investigate the mechanism by which this particular co-regulation occurs, specifically, the identity of the protein that

senses the lack of the kinesin and triggers the degradation response. Our finding that non-ubiquitinatable GLR-1, GLR-1(4KR)::GFP, accumulates in cell bodies of *klp-4* mutants demonstrates that GLR-1 degradation in the cell body of *klp4* mutants likely requires GLR-1 ubiquitination. Therefore it would be interesting to examine the activity of proteins that affect GLR-1 ubiquitination in *klp-4* mutants. The E3 ubiquitin ligase that targets GLR-1 for degradation has not yet been identified. However, the deubiquitinating enzyme *usp-46* was recently shown to deubiquitinate GLR-1 and loss of function of *usp-46* results in decreased GLR-1 abundance in the VNC and cell body (Kowalski et al., 2011). It might be interesting to investigate whether the GLR-1 degradation pathway in the cell body of *klp-4* mutants is separate from the canonical *usp-46* pathway. For example, is increased GLR-1 degradation in *klp-4* mutants a result of decreased *usp-46* or *usp-46* activator protein expression?

The mechanism by which the degradation of cargo in the absence of motor is induced could have important implications for neurological disease. Dysfunctional transport and aberrant protein accumulation is implicated in diseases, including Alzheimer's disease, Huntington's disease, Spinal and bulbar muscular atrophy and amyotrophic lateral sclerosis (Chevalier-Larsen and Holzbaur, 2006; Salinas et al., 2008). Perhaps a greater understanding of the cell biology behind coupling cargo degradation to decreased kinesin levels could inform the quest to understand the pathology of complex neuronal diseases.

Is KLP-4 a potential CDK-5 substrate?

One objective of the *cdk-5(xs)* suppressor screen was to find a CDK-5 substrate that mediates its effects on GLR-1 trafficking. Our results demonstrating that KLP-4 acts in the same genetic pathway as CDK-5 to promote GLR-1 abundance in the VNC raise the question of whether or not KLP-4 is a direct substrate of CDK-5. Predicting potential CDK-5 target sites within a protein is difficult because there is no known, well-defined CDK-5

consensus site. However, CDK-5 only phosphorylates Ser and Thr residues with a Pro residue in the +1 position. Therefore, we searched for S/T-P sites in KLP-4 that are conserved in the *klp-4* orthologs, *Drosophila* KHC-73 and mammalian Kif13A. We identified three conserved S/T-P sites that are potential CDK-5 targets (Figure 4-12). It will be interesting to determine whether one or more of these sites are important for KLP-4 and CDK-5-dependent GLR-1 trafficking. Site-directed mutagenesis could be used to create phospho-mutant versions of KLP-4. For example, if phosphorylation of these residues were important for KLP-4 function, then replacing the Ser or Thr residue with an Ala, should mimic the loss of function of CDK-5 and result in decreased GLR-1 in the VNC. Conversely, replacing a the Ser or Thr residue with a phosphor-mimic Glu or Asp residue should mimc the effects of CDK-5 overexpression. Additionally *in vitro* kinase assays could be performed with CDK-5 and wild type and phospho-mutant versions of KLP-4 to test directly whether CDK-5 can phosphorylate KLP-4 at these particular sites.

Which step of GLR-1 trafficking does CDK-5 regulate?

In addition to identifying a direct substrate for CDK-5, the characterization of mutants identified in the *cdk-5(xs)* suppressor screen should shed light on which step CDK-5 regulates in the GLR-1 trafficking pathway. The identification of KLP-4 functioning in the same pathway as CDK-5 to promote GLR-1 anterograde trafficking provided the opportunity to test for specific functions of CDK-5. In chapter 4 we tested whether CDK-5 might increase the amount of KLP-4 in the VNC. Instead, we found the opposite result. KLP-4 abundance in the VNC increases in *cdk-5* loss of function mutants, demonstrating that CDK-5 does not promote KLP-4 abundance in the VNC (Figure 4-2). Our preliminary time-lapse imaging of mobile KLP-4 puncta in *cdk-5* mutants suggests that CDK-5 does not dramatically alter the velocity or run length of KLP-4 in the VNC (data not shown).

Another potential function of CDK-5 could be to increase KLP-4 expression. If CDK-5 increased *klp-4* transcription, we should be able to detect decreased *klp-4* transcript levels in *cdk-5* loss of function mutants. To address this question, we will perform real time qPCR experiments measuring *klp-4* mRNA levels in wild type animals and *cdk-5* mutants. Theoretically, CDK-5 regulation of KLP-4 expression could occur posttranslationally as well. If this were true we would expect that we would be able to detect an increase or decrease in KLP protein levels in *cdk-5(xs)* and *cdk-5* loss of function mutants, respectively. We will perform western blots of tagged-KLP-4 in *cdk-5* mutants and wild type controls to test this directly. Although we cannot answer this question definitively until we have measured total KLP-4 protein levels in *cdk-5* mutants, two results suggest that the effects of CDK-5 on GLR-1 trafficking are not limited to increasing KLP-4 protein levels. First, the abundance of KLP-4::GFP is increased in the VNC of *cdk-5* mutants compared to wild type animals (Figure 4-2). While this experiment does not provide information on total protein level of KLP-4 because abundance of KLP-4::GFP in the cell body was not measured, it suggests that KLP-4 protein levels are not decreased in *cdk-5* mutants. Second, the effect of *cdk-5* loss of function on GLR-1 in the cell body differs with the effect of *klp-4* loss of function (Figure 3-7). GLR-1 accumulates in the cell bodies of *cdk-5* mutants whereas it is degraded in the cell bodies of *klp-4* mutants. If CDK-5 acted solely to increase KLP-4 levels, then loss of function mutations in either gene should have the same effect on GLR-1 in the cell body.

Another possible mechanism by which CDK-5 could regulate GLR-1 trafficking is promoting GLR-1/KLP-4 complex formation. There is ample evidence that loading of cargo onto motors can be regulated by phosphorylation of a member of the trafficking complex, such as the motor, adaptor protein or cargo (Ikeda et al., 2008; Morfini et al., 2002; Vagnoni et al., 2011). One way to test if CDK-5 could act in this capacity for KLP-4-mediated GLR-1 trafficking would be to determine whether CDK-5 affects co-immunoprecipitation (co-IP)

between GLR-1 and KLP-4. We attempted to perform *in vivo* co-immunoprecipitation experiments between an integrated FLAG-tagged KLP-4 construct, and GLR-1::GFP but we have been unsuccessful so far. This is not surprising for the following reasons. First, to our knowledge, co-IP between a kinesin and a vesicular cargo has never been demonstrated in *C. elegans* likely due to the difficulty of preserving these potentially fragile interactions during the membrane solubilization and purification process. Second, the vast majority of GLR-1 at any one time is stationary, either in the VNC or in the cell body. Thus, only a very small percentage should be in a trafficking complex with KLP-4. Likewise, most kinesins transport many different cargos and therefore, it is likely that only a small percent of KLP-4 would be in complex with GLR-1 at any given time. We predict this would render biochemical detection of this interaction very challenging. Examples of co-IP between GLR-1 and various proteins have been demonstrated in heterologous cells (Walker et al., 2006; Zheng et al., 2006). Therefore, one future experiment to test for potential effects of CDK-5 on KLP-4/GLR-1 complex formation will be to co-express KLP-4 and GLR-1 in a mammalian cell culture system in the presence and absence of CDK-5 co-expression. We would predict that CDK-5 might increase formation of the KLP-4/GLR-1 trafficking complex however, it is important to consider the possibility that the putative KLP-4/GLR-1 complex may require one or more linker proteins which may or may not be present in the heterologous cell culture. This would have to be considered if attempts to detect any co-IP between KLP-4 and GLR-1 were unsuccessful.

In chapter 3 we demonstrated co-migration between GLR-1 and KLP-4 in the cell body (Appendix 1). Another approach to ask how CDK-5 contributes to GLR-1 trafficking will be to determine what effects, if any, CDK-5 has on GLR-1/KLP-4 co-migration. We demonstrated in Chapter 3 that loss of function of CDK-5 results in decreased anterograde flux and run length of GLR-1 (Figures 3-5 and 3-S6). Our preliminary results from time-

lapse imaging of fluorescently tagged KLP-4 (KLP-4::GFP) in *cdk-5* null mutants suggest that neither run length nor flux of KLP-4::GFP are affected in *cdk-5* mutants (data not shown). However it is difficult to compare trafficking of KLP-4::GFP to trafficking of GLR-1::GFP when both are imaged separately because there is no way to predict what percent of mobile KLP-4::GFP puncta are transporting GLR-1. Therefore, it will be necessary to determine the effects of CDK-5 on puncta that are red and green in animals that co-express GLR-1::GFP and KLP-4::mCherry. This experiment should yield information on CDK-5's potential effects on several measures of GLR-1 / KP-4 trafficking including, complex formation, run length and velocity.

An interesting model for how CDK-5 could indirectly affect loading of GLR-1 onto KLP-4 is through β-Catenin signaling and the actions of glycogen synthase kinase 3 (GSK3) (Dreier et al., 2005; Morfini et al., 2002; Morfini et al., 2004; Ratner et al., 1998). In squid axoplasm, CDK-5 regulates the anterograde trafficking of neuronal vesicles by regulating the activity of GSK3 (Morfini et al., 2002; Morfini et al., 2004). GSK3 phosphorylates kinesin light chain (KLC) and decrease its affinity for vesicular cargo resulting in decreased vesicular trafficking (Morfini et al., 2002; Morfini et al., 2004). GSK3 is activated by protein phosphatase 1 (PP1), which dephosphorylates an inhibitory phospho-Tyrosine residue on GSK3 (Morfini et al., 2004). CDK-5 activity indirectly inhibits PP1 through an unknown mechanism. Thus, by inhibiting the activity of a negative regulator of trafficking, CDK-5 promotes anterograde trafficking of vesicular cargo in neurons. Interestingly, GSK3 activity has been shown to negatively regulate GLR-1 abundance in the VNC of *C. elegans* (Dreier et al., 2005). In the VNC of *gsk-3* loss of function mutants, GLR-1::GFP puncta intensity and width are increased compared to wild type animals (Dreier et al., 2005). These effects are likely due, at least in part to the role of GSK3 in regulating Wnt signaling (Dreier et al., 2005), However it would be interesting to determine whether increased GLR-1 abundance in

the VNC of *gsk-3* mutants could be partially explained by the loss of GSK-3-mediated GLR-1/KLP-4 complex disassociation.

How does KLP-4 regulate anterograde trafficking?

We identified KLP-4 as a positive regulator of the anterograde trafficking of GLR-1. Given that KLP-4 is a kinesin, the simplest model to explain the mechanism by which KLP-4 regulates GLR-1 trafficking is one in which GLR-1 is a KLP-4 cargo and KLP-4 transports GLR-1 along microtubules from the cell body to the VNC. Indeed we observed co-migration between KLP-4 and GLR-1 within the cell body, which strongly suggests GLR-1 is in fact a cargo of KLP-4. To date we have not observed co-migration between KLP-4 and GLR-1 in the VNC. It is possible that this could be due to less than optimal imaging parameters, which will be addressed in the future. However it is also possible that we did not see co-migration between KLP-4 and GLR-1 in the VNC because KLP-4 does not transport GLR-1 in the VNC.

One possible model for how KLP-4 might function in the cell body to regulate GLR-1 trafficking is demonstrated by the mammalian kinesin-3 family member, Kif16B. Kif16B is most homologous to Kif1A (Hoepfner et al., 2005). Kif16B was originally identified based on the presence of a phosphoinositide-3 phosphate (PI3P) binding domain (PX domain) near its C-terminus. *unc-104*/Kif1A is the only other kinesin with a conserved phosphoinositide binding domain in its cargo-binding tail.

Kif16B was shown to mediate the trafficking of Rab-5-containing early endosomes in a PI3P-dependent manner (Hoepfner et al., 2005). Overexpression of Kif16B resulted in the redistribution of early endosomes to the cell periphery, whereas Kif16B loss of function caused Rab-5-containing early endosomes to collapse into perinuclear clusters (Hoepfner et al., 2005). These changes in trafficking had a striking effect on the epithelial growth factor

receptor (EGFR) that was transported in early endosomes. Treatment with epithelial growth factor (EGF) causes internalization of EGFR into the endo-lysosomal trafficking pathway, leading to degradation of EGFR. In cells that had been treated with KIF16B RNAi, perinuclear clustering of early endosomes was coupled with accelerated degradation of EGFR (Hoepfner et al., 2005). This is similar to the effect we observed on GLR-1 in *klp-4* of loss of function mutants (Figure 3-7). In a subsequent study in mouse embryonic fibroblasts (MEFs) from Kif16B$^{-/-}$ knockout mice, a similar effect was seen on another Kif16B cargo protein, fibroblast growth factor receptor (FGFR) (Ueno et al., 2011). However, vesicles containing FGFR were identified as recycling endosomes being transported from the Golgi to the plasma membrane by the presence of Rab-14 and absence of Rab-5. The loss of Kif16B resulted in perinuclear clustering of FGFR-containing recycling endosomes and Kif16B co-immunoprecipitated with FGFR in wild type cells (Ueno et al., 2011). Thus, Kif16B can regulate the trafficking of early endosomes and recycling endosomes containing transmembrane receptors. Moreover, in one example, its role in trafficking can regulate the balance between recycling and lysosomal degradation of its receptor cargo (Hoepfner et al., 2005; Ueno et al., 2011). Some of our results describing *klp-4* could be consistent with the role described for Kif16B. First, KLP-4 and GLR-1 co-migrate in the cell body, suggesting that KLP-4 is transporting GLR-1-containing vesicles (Appendix 1). Second, GLR-1 undergoes lysosomal degradation in the cell bodies of *klp-4* mutants (Figure 3-7). Interestingly, there is no direct homolog for Kif16B in *C. elegans* so *unc-104* and *klp-4* are the most closely related genes by sequence. This raises the interesting possibility that KLP-4 could be performing a function in *C. elegans*, similar to the one performed by Kif16B in mammalian cells. To explore this possibility, we tested whether *klp-4* loss of function alters the distribution of Rab-5-containing vesicles in *glr-1*-expressing interneurons using a fluorescently tagged Rab-5 under the control of the *glr-1* promoter. Rab-5 distribution was

not obviously different in *klp-4* mutants compared to wild type controls (data not shown). In wild type and *klp-4* animals, Rab-5 appeared to be distributed in a punctate pattern in the cell body. Neither the pattern of distribution nor the total amounts of Rab-5 appeared to change in *klp-4* mutants. Rab-5 puncta in the VNC were faint but visible in both wild type and *klp-4* mutants. To date we have only examined the distribution of Rab-5-containing early endosomes. To investigate a potential role for KLP-4 in endosomal trafficking more fully, we will have to examine the distribution of other endosomal markers in *klp-4* mutants.

Multiple motors regulate GLR-1 abundance

Whether KLP-4 functions only in the cell body or in the cell body and the VNC, it is clear that it is not the only motor that contributes to GLR-1 transport. *unc-116* / kinesin-1 is perhaps the most obvious candidate for this role as we know that it does regulate GLR-1 abundance in the VNC. We found that *unc-116* loss of function resulted in decreased GLR-1 levels in the VNC (Figure 4-9). Moreover, the mammalian homolog of *unc-116*, Kif-5/Kinesin-1 traffics AMPARs in mammalian neurons (Kim et al., 2001; 2002) and it would seem logical that this function might have been conserved through evolution. It is not entirely clear from our results whether *klp-4* and *unc-116* function in the same or parallel pathways to regulate GLR-1. GLR-1 abundance in the VNC of *klp-4;unc116* double mutants appears lower than in the *klp-4* single mutants but this difference failed to reach statistical significance (Figure 4-9). More imaging will be required to determine if this lack of statistical significance is simply a result of an insufficient number of animals used to quantify results. Given the apparent magnitude of the decrease in GLR-1 abundance in *klp-4;unc-116* double mutants compared to *klp-4* single mutants, we suspect that a larger *n* of imaged animals will, in fact, result in a statistically significant difference. If this were the case, it would suggest that *klp-4* and *unc-116* function in separate genetic pathways to regulate GLR-1 abundance in the VNC. It is important to note that *unc-116* has been shown to traffic multiple cargoes in

neurons and these animals have synaptic development defects,(Byrd et al., 2001; Patel et al., 1993; Sakamoto et al., 2005; Tsuboi et al., 2005)). This raises the possibility that some or all of the effects of *unc-116* loss of function on GLR-1 could be secondary to developmental defects. Conditional rescue of the GLR-1 decrease in *unc-116* mutants performed in animals after neuronal development, similar to the heat-shock rescue of *klp-4* mutants we performed (Figure 3-2), may be necessary to determine whether *unc-116* has effects on GLR-1 abundance independent of any developmental defects in these animals. It will be interesting to determine whether UNC-116, like KLP-4, affects GLR-1 trafficking directly and to characterize the way that multiple motors contribute to GLR-1 trafficking.

Concluding remarks

In this thesis I used the genetic model organism *C. elegans* to discover novel genes that regulate GLR-1 glutamate receptor abundance at synapses in the VNC. The abundance of GluRs at synapses is an important regulator of synaptic transmission in the human brain. Changes in the strength of glutamatergic synapses are widely believed to underlie the cellular mechanism of learning and memory. We had previously demonstrated that overexpression of CDK-5 resulted in increased GLR-1 abundance at synapses (Juo et al., 2007). We performed a forward genetic suppressor screen of *cdk-5(xs)* animals and isolated 46 mutants with decreased GLR-1 abundance in the VNC. Two of these mutants have been identified, *ire-1(pz11)* and *klp-4(pz19),* and the rest remain unknown. The identification of the remaining unidentified mutants holds great promise for elucidating the mechanism by which CDK-5 regulates GLR-1 abundance, and the regulation of GluR abundance in general.

We characterized the role of the kinesin-3 family motor KLP-4 in trafficking GLR-1. Microtubule-based motors play an important role in spatially regulating their cargo, particularly in neurons, which are especially dependent on kinesins and dynein for the

polarized long-distance trafficking of cellular cargo (Hirokawa et al., 2010; Verhey and Hammond, 2009). Our work represents the first description of KLP-4 motor properties. We demonstrate that KLP-4 is a fast processive neuronal motor that functions in the same cellular pathway as CDK-5 to promote the anterograde trafficking of GLR-1. We made the surprising discovery that, while *cdk-5* null mutations result in accumulation of GLR-1 in the cell body, KLP-4 loss of function results in lysosomal degradation of GLR-1. This is consistent with previous studies that have shown that the expression levels of motors and cargoes can be co-regulated (Dhar and Wong-Riley, 2011; Guillaud et al., 2003; Yin et al., 2011; Yin et al., 2012). The fact that this co-regulation is conserved from *C. elegans* to mammals and that it can occur by more than one mechanism, suggests that it may be a fundamental aspect of cell biology for preserving the health and function of the cell.

Finally we identified two additional novel regulators of GLR-1 levels in the VNC, the microRNA family *mir-75/79* and the motor *unc-116 /* kinesin-1. *mir-75* and *mir-79* have predicted target sites in the 3' UTR of *klp-4*, suggesting that they might down regulate *klp-4* translation and that in their absence, *klp-4* protein level would increase. We show the surprising result that GLR-1 abundance is decreased in the absence of *mir-75/79*, and that *mir-75/79* function in the same pathway as KLP-4 to promote synaptic GLR-1 abundance. We have yet to determine the relevant target transcript for *mir-75/79* and it remains a possibility that they directly target *klp-4.* This would represent an unusual function of miRNAs and lead to the interesting question of what determines whether a miRNA promotes or inhibits target transcript translation (Vasudevan, 2012).

We also described the effects of *unc-116 /* kinesin-1 loss of function on GLR-1 abundance in the VNC, suggesting it is a potential regulator of GLR-1 trafficking. This offers the opportunity to look at two functionally important kinesin motors in an *in vivo* system to examine how they contribute, individually and together to deliver cargo. The question of

how kinesins interact with each other is an open and important one in cell biology. It is becoming clear that trafficking of cargo requires the interaction of multiple motors. This process is a fundamental issue in cell biology and it holds great potential for a better understanding of an untold number of cellular processes. In conclusion, I have identified several new genes that are involved in GluR trafficking in *C. elegans* and fully characterized the mechanism by which one, *klp-4* contributes to GluR trafficking.

Appendix 1.

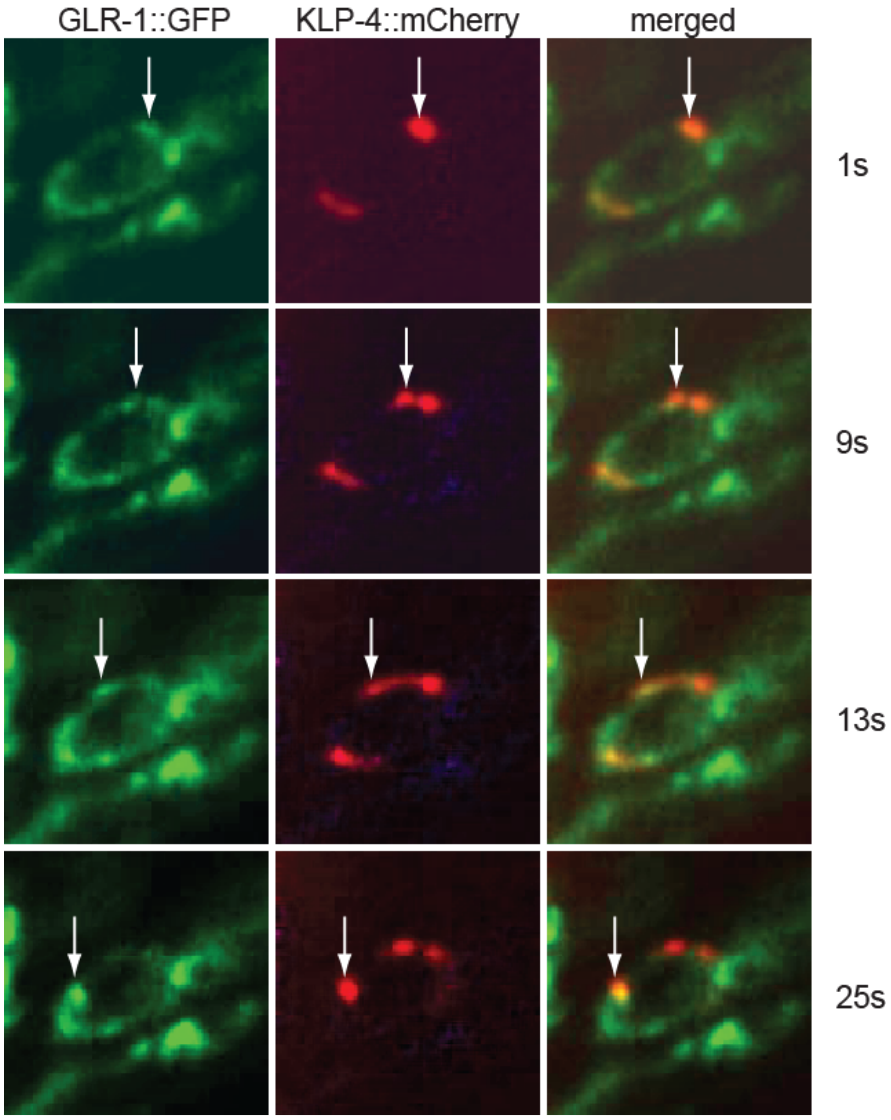

Appendix 1. KLP-4::mCherry co-migrates with GLR-1::GFP in the cell body. KLP-4::mCherry punctum migrating with a GLR-1::GFP punctum (a white arrow marks the relevant puncta) in an interneuron cell body in the head of animals expressing an extrachromosomal array of KLP-4::mCherry under the control of the glr-1 promoter (pzEx234) and integrated GLR-1::GFP (nuIs25). Time (seconds) of each image is indicated to the right of each merged image.

Bibliography

Akhmanova, A., & Hammer, J. A.,3rd. (2010). Linking molecular motors to membrane cargo. *Current Opinion in Cell Biology, 22*(4), 479-487.

Amato, S., Liu, X., Zheng, B., Cantley, L., Rakic, P., & Man, H. Y. (2011). AMP-activated protein kinase regulates neuronal polarization by interfering with PI 3-kinase localization. *Science, 332*(6026), 247-251.

Avunie-Masala, R., Movshovich, N., Nissenkorn, Y., Gerson-Gurwitz, A., Fridman, V., Koivomagi, M., . . . Gheber, L. (2011). Phospho-regulation of kinesin-5 during anaphase spindle elongation. *Journal of Cell Science, 124*(Pt 6), 873-878.

Baas, P. W., Deitch, J. S., Black, M. M., & Banker, G. A. (1988). Polarity orientation of microtubules in hippocampal neurons: Uniformity in the axon and nonuniformity in the dendrite. *Proceedings of the National Academy of Sciences of the United States of America, 85*(21), 8335-8339.

Babst, M., Katzmann, D. J., Snyder, W. B., Wendland, B., & Emr, S. D. (2002). Endosome-associated complex, ESCRT-II, recruits transport machinery for protein sorting at the multivesicular body. *Dev Cell, 3*(2), 283-9.

Barkus, R. V., Klyachko, O., Horiuchi, D., Dickson, B. J., & Saxton, W. M. (2008). Identification of an axonal kinesin-3 motor for fast anterograde vesicle transport that facilitates retrograde transport of neuropeptides. *Mol Biol Cell, 19*(1), 274-83.

Barria, A., Muller, D., Derkach, V., Griffith, L. C., & Soderling, T. R. (1997). Regulatory phosphorylation of AMPA-type glutamate receptors by CaM-KII during long-term potentiation. *Science, 276*(5321), 2042-2045.

Bartel, D. P. (2009). MicroRNAs: Target recognition and regulatory functions. *Cell, 136*(2), 215-233.

Benke, T. A., Luthi, A., Isaac, J. T., & Collingridge, G. L. (1998). Modulation of AMPA receptor unitary conductance by synaptic activity. *Nature, 393*(6687), 793-797.

Berger, A. J., Hart, A. C., & Kaplan, J. M. (1998). G alphas-induced neurodegeneration in caenorhabditis elegans. *J Neurosci, 18*(8), 2871-80.

Blasius, T. L., Cai, D., Jih, G. T., Toret, C. P., & Verhey, K. J. (2007). Two binding partners cooperate to activate the molecular motor kinesin-1. *The Journal of Cell Biology, 176*(1), 11-17.

Bliss, T. V., & Lomo, T. (1970). Plasticity in a monosynaptic cortical pathway. *The Journal of Physiology, 207*(2), 61P.

Bliss, T. V., & Lomo, T. (1973). Long-lasting potentiation of synaptic transmission in the dentate area of the anaesthetized rabbit following stimulation of the perforant path. *The Journal of Physiology, 232*(2), 331-356.

Bowie, D. (2008). Ionotropic glutamate receptors & CNS disorders. *CNS Neurol.Disord.Drug Targets, 7*(2), 129-143.

Bredt, D. S., & Nicoll, R. A. (2003). AMPA receptor trafficking at excitatory synapses. *Neuron, 40*(2), 361-379.

Brenner, S. (1974). The genetics of caenorhabditis elegans. *Genetics, 77*(1), 71-94.

Brockie, P. J., Madsen, D. M., Zheng, Y., Mellem, J., & Maricq, A. V. (2001). Differential expression of glutamate receptor subunits in the nervous system of caenorhabditis elegans and their regulation by the homeodomain protein UNC-42. *The Journal of Neuroscience : The Official Journal of the Society for Neuroscience, 21*(5), 1510-1522.

Brown, H. M., Van Epps, H. A., Goncharov, A., Grant, B. D., & Jin, Y. (2009). The JIP3 scaffold protein UNC-16 regulates RAB-5 dependent membrane trafficking at C. elegans synapses. *Dev.Neurobiol., 69*(2-3), 174-190.

Burbea, M., Dreier, L., Dittman, J. S., Grunwald, M. E., & Kaplan, J. M. (2002). Ubiquitin and AP180 regulate the abundance of GLR-1 glutamate receptors at postsynaptic elements in C. elegans. *Neuron, 35*(1), 107-20.

Byrd, D. T., Kawasaki, M., Walcoff, M., Hisamoto, N., Matsumoto, K., & Jin, Y. (2001). UNC-16, a JNK-signaling scaffold protein, regulates vesicle transport in C. elegans. *Neuron, 32*(5), 787-800.

Cahu, J., Olichon, A., Hentrich, C., Schek, H., Drinjakovic, J., Zhang, C., . . . Surrey, T. (2008). Phosphorylation by Cdk1 increases the binding of Eg5 to microtubules in vitro and in xenopus egg extract spindles. *PLoS ONE, 3*(12), .

Carroll, R. C., Beattie, E. C., Xia, H., Luscher, C., Altschuler, Y., Nicoll, R. A., . . . von Zastrow, M. (1999). Dynamin-dependent endocytosis of ionotropic glutamate receptors. *Proc Natl Acad Sci U S A, 96*(24), 14112-7.

Case, R.B., Pierce, D.W., Hom-Booher, N., Hart, C.L., and Vale, R.D. (1997). The directional preference of kinesin motors is specified by an element outside of the motor catalytic domain. Cell *90*, 959-966.

Ceman, S., & Saugstad, J. (2011). MicroRNAs: Meta-controllers of gene expression in synaptic activity emerge as genetic and diagnostic markers of human disease. *Pharmacology & Therapeutics, 130*(1), 26-37.

Chao, M.Y., Komatsu, H., Fukuto, H.S., Dionne, H.M., and Hart, A.C. (2004). Feeding status and serotonin rapidly and reversibly modulate a Caenorhabditis elegans chemosensory circuit. Proc Natl Acad Sci U S A *101*, 15512-15517.

Charalambous, D. C., Pasciuto, E., Mercaldo, V., Pilo Boyl, P., Munck, S., Bagni, C., & Santama, N. (2012). KIF1Bbeta transports dendritically localized mRNPs in neurons and is recruited to synapses in an activity-dependent manner. *Cellular and Molecular Life Sciences : CMLS,*

Chen, L., Chetkovich, D. M., Petralia, R. S., Sweeney, N. T., Kawasaki, Y., Wenthold, R. J., . . . Nicoll, R. A. (2000). Stargazin regulates synaptic targeting of AMPA receptors by two distinct mechanisms. *Nature, 408*(6815), 936-943.

Cheung, Z. H., Fu, A. K., & Ip, N. Y. (2006). Synaptic roles of Cdk5: Implications in higher cognitive functions and neurodegenerative diseases. *Neuron, 50*(1), 13-18.

Chevalier-Larsen, E., & Holzbaur, E. L. (2006). Axonal transport and neurodegenerative disease. *Biochimica Et Biophysica Acta, 1762*(11-12), 1094-1108.

Chudakov, D.M., Lukyanov, S., and Lukyanov, K.A. (2007). Tracking intracellular protein movements using photoswitchable fluorescent proteins PS-CFP2 and Dendra2. Nat Protoc *2*, 2024-2032.

Chun, D. K., McEwen, J. M., Burbea, M., & Kaplan, J. M. (2008). UNC-108/Rab2 regulates postendocytic trafficking in caenorhabditis elegans. *Molecular Biology of the Cell, 19*(7), 2682-2695.

Coleman, S. K., Moykkynen, T., Cai, C., von Ossowski, L., Kuismanen, E., Korpi, E. R., & Keinanen, K. (2006). Isoform-specific early trafficking of AMPA receptor flip and flop variants. *The Journal of Neuroscience : The Official Journal of the Society for Neuroscience, 26*(43), 11220-11229.

Coleman, S. K., Moykkynen, T., Hinkkuri, S., Vaahtera, L., Korpi, E. R., Pentikainen, O. T., & Keinanen, K. (2010). Ligand-binding domain determines endoplasmic reticulum exit of AMPA receptors. *Journal of Biological Chemistry, 285*(46), 36032-36039.

Collingridge, G. L., Isaac, J. T., & Wang, Y. T. (2004). Receptor trafficking and synaptic plasticity. *Nature Reviews. Neuroscience, 5*(12), 952-962.

Collins, C. A., Wairkar, Y. P., Johnson, S. L., & DiAntonio, A. (2006). Highwire restrains synaptic growth by attenuating a MAP kinase signal. *Neuron, 51*(1), 57-69.

Conde, C., & Caceres, A. (2009). Microtubule assembly, organization and dynamics in axons and dendrites. *Nature Reviews. Neuroscience, 10*(5), 319-332.

Coy, D. L., Hancock, W. O., Wagenbach, M., & Howard, J. (1999). Kinesin's tail domain is an inhibitory regulator of the motor domain. *Nature Cell Biology, 1*(5), 288-292.

Cruz, J. C., & Tsai, L. H. (2004). Cdk5 deregulation in the pathogenesis of alzheimer's disease. *Trends in Molecular Medicine, 10*(9), 452-458.

De Vos, K. J., Grierson, A. J., Ackerley, S., & Miller, C. C. (2008). Role of axonal transport in neurodegenerative diseases. *Annual Review of Neuroscience, 31*, 151-173.

Deacon, S. W., Nascimento, A., Serpinskaya, A. S., & Gelfand, V. I. (2005). Regulation of bidirectional melanosome transport by organelle bound MAP kinase. *Current Biology : CB, 15*(5), 459-463.

Delevoye, C., Hurbain, I., Tenza, D., Sibarita, J. B., Uzan-Gafsou, S., Ohno, H., . . . Raposo, G. (2009). AP-1 and KIF13A coordinate endosomal sorting and positioning during melanosome biogenesis. *The Journal of Cell Biology, 187*(2), 247-264.

Derkach, V. A., Oh, M. C., Guire, E. S., & Soderling, T. R. (2007). Regulatory mechanisms of AMPA receptors in synaptic plasticity. *Nature Reviews. Neuroscience, 8*(2), 101-113.

Dhar, S. S., & Wong-Riley, M. T. (2011). The kinesin superfamily protein KIF17 is regulated by the same transcription factor (NRF-1) as its cargo NR2B in neurons. *Biochimica Et Biophysica Acta, 1813*(3), 403-411.

Dhariwala, F. A., & Rajadhyaksha, M. S. (2008). An unusual member of the cdk family: Cdk5. *Cellular and Molecular Neurobiology, 28*(3), 351-369.

Dhavan, R., & Tsai, L. H. (2001). A decade of CDK5. *Nature Reviews. Molecular Cell Biology, 2*(10), 749-759.

Dong, H., O'Brien, R. J., Fung, E. T., Lanahan, A. A., Worley, P. F., & Huganir, R. L. (1997). GRIP: A synaptic PDZ domain-containing protein that interacts with AMPA receptors. *Nature, 386*(6622), 279-284.

Dreier, L., Burbea, M., & Kaplan, J. M. (2005). LIN-23-mediated degradation of beta-catenin regulates the abundance of GLR-1 glutamate receptors in the ventral nerve cord of C. elegans. *Neuron, 46*(1), 51-64.

Duncan, J. E., & Goldstein, L. S. (2006). The genetics of axonal transport and axonal transport disorders. *PLoS Genetics, 2*(9), e124.

Dunwiddie, T., & Lynch, G. (1978). Long-term potentiation and depression of synaptic responses in the rat hippocampus: Localization and frequency dependency. *The Journal of Physiology, 276*, 353-367.

Durand, G. M., Kovalchuk, Y., & Konnerth, A. (1996). Long-term potentiation and functional synapse induction in developing hippocampus. *Nature, 381*(6577), 71-75.

Ehlers, M.D. (2000). Reinsertion or degradation of AMPA receptors determined by activity-dependent endocytic sorting. Neuron *28*, 511-525.

Emtage, L., Chang, H., Tiver, R., and Rongo, C. (2009). MAGI-1 modulates AMPA receptor synaptic localization and behavioral plasticity in response to prior experience. PLoS One *4*, e4613.

Espeut, J., Gaussen, A., Bieling, P., Morin, V., Prieto, S., Fesquet, D., . . . Abrieu, A. (2008). Phosphorylation relieves autoinhibition of the kinetochore motor cenp-E. *Molecular Cell, 29*(5), 637-643.

Ferreira, A., Niclas, J., Vale, R.D., Banker, G., and Kosik, K.S. (1992). Suppression of kinesin expression in cultured hippocampal neurons using antisense oligonucleotides. J Cell Biol *117*, 595-606.

Fleck, M. W., Cornell, E., & Mah, S. J. (2003). Amino-acid residues involved in glutamate receptor 6 kainate receptor gating and desensitization. *The Journal of Neuroscience : The Official Journal of the Society for Neuroscience, 23*(4), 1219-1227.

Friggi-Grelin, F., Lavenant-Staccini, L., & Therond, P. (2008). Control of antagonistic components of the hedgehog signaling pathway by microRNAs in drosophila. *Genetics, 179*(1), 429-439.

Gao, F. B. (2010). Context-dependent functions of specific microRNAs in neuronal development. *Neural Dev., 5*, 25. doi: 1749-8104-5-25 [pii]; 10.1186/1749-8104-5-25 [doi]

Gengyo-Ando, K., & Mitani, S. (2000). Characterization of mutations induced by ethyl methanesulfonate, UV, and trimethylpsoralen in the nematode caenorhabditis elegans. *Biochemical and Biophysical Research Communications, 269*(1), 64-69.

Gill, M. B., Vivithanaporn, P., & Swanson, G. T. (2009). Glutamate binding and conformational flexibility of ligand-binding domains are critical early determinants of efficient kainate receptor biogenesis. *Journal of Biological Chemistry, 284*(21), 14503-14512. doi: M900510200 [pii];

Goldstein, A.Y., Wang, X., and Schwarz, T.L. (2008). Axonal transport and the delivery of pre-synaptic components. Curr Opin Neurobiol *18*, 495-503.

Goodwin, P. R., Sasaki, J. M., & Juo, P. (2012). CDK-5 regulates the polarized trafficking of neuropeptide-containing dense-core vesicles in C. elegans motor neurons.

Greger, I. H., Khatri, L., & Ziff, E. B. (2002). RNA editing at arg607 controls AMPA receptor exit from the endoplasmic reticulum. *Neuron, 34*(5), 759-772. doi: S0896627302006931 [pii]

Grunwald, M. E., & Kaplan, J. M. (2003). Mutations in the ligand-binding and pore domains control exit of glutamate receptors from the endoplasmic reticulum in C. elegans. *Neuropharmacology, 45*(6), 768-76.

Grunwald, M. E., Mellem, J. E., Strutz, N., Maricq, A. V., & Kaplan, J. M. (2004). Clathrin-mediated endocytosis is required for compensatory regulation of GLR-1 glutamate receptors after activity blockade. *Proc Natl Acad Sci U S A, 101*(9), 3190-5.

Guillaud, L., Setou, M., & Hirokawa, N. (2003). KIF17 dynamics and regulation of NR2B trafficking in hippocampal neurons. *The Journal of Neuroscience : The Official Journal of the Society for Neuroscience, 23*(1), 131-140.

Guillaud, L., Wong, R., & Hirokawa, N. (2008). Disruption of KIF17-Mint1 interaction by CaMKII-dependent phosphorylation: A molecular model of kinesin-cargo release. *Nature Cell Biology, 10*(1), 19-29.

Guo, H., Ingolia, N. T., Weissman, J. S., & Bartel, D. P. (2010). Mammalian microRNAs predominantly act to decrease target mRNA levels. *Nature, 466*(7308), 835-840.

Gurskaya, N.G., Verkhusha, V.V., Shcheglov, A.S., Staroverov, D.B., Chepurnykh, T.V., Fradkov, A.F., Lukyanov, S., and Lukyanov, K.A. (2006). Engineering of a monomeric green-to-red photoactivatable fluorescent protein induced by blue light. Nat Biotechnol *24*, 461-465

Guzik, B.W., and Goldstein, L.S. (2004). Microtubule-dependent transport in neurons: steps towards an understanding of regulation, function and dysfunction. Curr Opin Cell Biol *16*, 443-450.

Hackney, D. D., Levitt, J. D., & Suhan, J. (1992). Kinesin undergoes a 9 S to 6 S conformational transition. *Journal of Biological Chemistry, 267*(12), 8696-8701.

Hackney, D. D., Levitt, J. D., & Wagner, D. D. (1991). Characterization of alpha 2 beta 2 and alpha 2 forms of kinesin. *Biochemical and Biophysical Research Communications, 174*(2), 810-815.

Hafezparast, M., Klocke, R., Ruhrberg, C., Marquardt, A., Ahmad-Annuar, A., Bowen, S., . . . Fisher, E. M. (2003). Mutations in dynein link motor neuron degeneration to defects in retrograde transport. *Science, 300*(5620), 808-812.

Hall, D. H., & Hedgecock, E. M. (1991). Kinesin-related gene unc-104 is required for axonal transport of synaptic vesicles in C. elegans. *Cell, 65*(5), 837-847.

Hammond, J. W., Blasius, T. L., Soppina, V., Cai, D., & Verhey, K. J. (2010). Autoinhibition of the kinesin-2 motor KIF17 via dual intramolecular mechanisms. *The Journal of Cell Biology, 189*(6), 1013-1025.

Hammond, J. W., Cai, D., Blasius, T. L., Li, Z., Jiang, Y., Jih, G. T., . . . Verhey, K. J. (2009). Mammalian kinesin-3 motors are dimeric in vivo and move by processive motility upon release of autoinhibition. *PLoS Biology, 7*(3), e72.

Hammond, J. W., Huang, C. F., Kaech, S., Jacobson, C., Banker, G., & Verhey, K. J. (2010). Posttranslational modifications of tubulin and the polarized transport of kinesin-1 in neurons. *Molecular Biology of the Cell, 21*(4), 572-583.

Hanada, T., Lin, L., Tibaldi, E. V., Reinherz, E. L., & Chishti, A. H. (2000). GAKIN, a novel kinesin-like protein associates with the human homologue of the drosophila discs large tumor suppressor in T lymphocytes. *Journal of Biological Chemistry, 275*(37), 28774-28784.

Hart, A. C., Sims, S., & Kaplan, J. M. (1995). Synaptic code for sensory modalities revealed by C. elegans GLR-1 glutamate receptor. *Nature, 378*(6552), 82-5.

Hart, A.C., Kass, J., Shapiro, J.E., and Kaplan, J.M. (1999). Distinct signaling pathways mediate touch and osmosensory responses in a polymodal sensory neuron. J Neurosci *19*, 1952-1958.

Hawasli, A. H., Benavides, D. R., Nguyen, C., Kansy, J. W., Hayashi, K., Chambon, P., . . . Bibb, J. A. (2007). Cyclin-dependent kinase 5 governs learning and synaptic plasticity via control of NMDAR degradation. *Nature Neuroscience, 10*(7), 880-886.

Helliwell, S.B., Losko, S., and Kaiser, C.A. (2001). Components of a ubiquitin ligase complex specify polyubiquitination and intracellular trafficking of the general amino acid permease. J Cell Biol *153*, 649-662.

Hillier, L. W., Marth, G. T., Quinlan, A. R., Dooling, D., Fewell, G., Barnett, D., . . . Mardis, E. R. (2008). Whole-genome sequencing and variant discovery in C. elegans. *Nat.Methods, 5*(2), 183-188.

Hirokawa, N., Nitta, R., & Okada, Y. (2009). The mechanisms of kinesin motor motility: Lessons from the monomeric motor KIF1A. *Nature Reviews.Molecular Cell Biology, 10*(12), 877-884. doi: 10.1038/nrm2807

Hirokawa, N., Niwa, S., & Tanaka, Y. (2010). Molecular motors in neurons: Transport mechanisms and roles in brain function, development, and disease. *Neuron, 68*(4), 610-638.

Hirokawa, N., Noda, Y., Tanaka, Y., & Niwa, S. (2009). Kinesin superfamily motor proteins and intracellular transport. *Nature Reviews.Molecular Cell Biology, 10*(10), 682-696.

Hirokawa, N., & Takemura, R. (2004). Molecular motors in neuronal development, intracellular transport and diseases. *Current Opinion in Neurobiology, 14*(5), 564-573.

Hobert, O. (2010). The impact of whole genome sequencing on model system genetics: Get ready for the ride. *Genetics, 184*(2), 317-319.

Hodgkin, J. (2005). Genetic suppression. *WormBook,* , 1-13. doi: 10.1895/wormbook.1.59.1 [doi]

Hoepfner, S., Severin, F., Cabezas, A., Habermann, B., Runge, A., Gillooly, D., . . . Zerial, M. (2005). Modulation of receptor recycling and degradation by the endosomal kinesin KIF16B. *Cell, 121*(3), 437-50.

Hoerndli, F. J., Walser, M., Frohli Hoier, E., de Quervain, D., Papassotiropoulos, A., & Hajnal, A. (2009). A conserved function of C. elegans CASY-1 calsyntenin in associative learning. *PLoS One, 4*(3), e4880.

Horiguchi, K., Hanada, T., Fukui, Y., & Chishti, A. H. (2006). Transport of PIP3 by GAKIN, a kinesin-3 family protein, regulates neuronal cell polarity. *The Journal of Cell Biology, 174*(3), 425-436.

Horiuchi, D., Barkus, R. V., Pilling, A. D., Gassman, A., & Saxton, W. M. (2005). APLIP1, a kinesin binding JIP-1/JNK scaffold protein, influences the axonal transport of both vesicles and mitochondria in drosophila. *Current Biology : CB, 15*(23), 2137-2141.

Horiuchi, D., Collins, C. A., Bhat, P., Barkus, R. V., Diantonio, A., & Saxton, W. M. (2007). Control of a kinesin-cargo linkage mechanism by JNK pathway kinases. *Current Biology : CB, 17*(15), 1313-1317.

Huang, C. F., & Banker, G. (2011). The translocation selectivity of the kinesins that mediate neuronal organelle transport. *Traffic (Copenhagen, Denmark),*

Huckaba, T. M., Gennerich, A., Wilhelm, J. E., Chishti, A. H., & Vale, R. D. (2011). Kinesin-73 is a processive motor that localizes to Rab5-containing organelles. *The Journal of Biological Chemistry, 286*(9), 7457-7467.

Hunt-Newbury, R., et al. (2007). High-throughput in vivo analysis of gene expression in Caenorhabditis elegans. PLoS Biol *5*, e237.

Ikeda, D. D., Duan, Y., Matsuki, M., Kunitomo, H., Hutter, H., Hedgecock, E. M., & Iino, Y. (2008). CASY-1, an ortholog of calsyntenins/alcadeins, is essential for learning in caenorhabditis elegans. *Proceedings of the National Academy of Sciences of the United States of America, 105*(13), 5260-5265.

Isaac, J. T., Nicoll, R. A., & Malenka, R. C. (1995). Evidence for silent synapses: Implications for the expression of LTP. *Neuron, 15*(2), 427-434.

Jacob, T. C., & Kaplan, J. M. (2003). The EGL-21 carboxypeptidase E facilitates acetylcholine release at caenorhabditis elegans neuromuscular junctions. *The Journal of Neuroscience : The Official Journal of the Society for Neuroscience, 23*(6), 2122-2130.

Jan, C. H., Friedman, R. C., Ruby, J. G., & Bartel, D. P. (2011). Formation, regulation and evolution of caenorhabditis elegans 3'UTRs. *Nature, 469*(7328), 97-101. doi: nature09616 [pii]; 10.1038/nature09616 [doi]

Jang, C. Y., Coppinger, J. A., Seki, A., Yates, J. R., & Fang, G. (2009). Plk1 and aurora A regulate the depolymerase activity and the cellular localization of Kif2a. *Journal of Cell Science, 122*(9), 1334-1341.

Jenkins, B., Decker, H., Bentley, M., Luisi, J., & Banker, G. (2012). A novel split kinesin assay identifies motor proteins that interact with distinct vesicle populations. *The Journal of Cell Biology, 198*(4), 749-761.

Jin, M., Fujita, M., Culley, B. M., Apolinario, E., Yamamoto, M., Maundrell, K., & Hoffman, C. S. (1995). sck1, a high copy number suppressor of defects in the cAMP-dependent protein kinase pathway in fission yeast, encodes a protein homologous to the saccharomyces cerevisiae SCH9 kinase. *Genetics, 140*(2), 457-467.

Jorgensen, E. M., & Mango, S. E. (2002). The art and design of genetic screens: Caenorhabditis elegans. *Nature Reviews. Genetics, 3*(5), 356-369.

Juo, P., Harbaugh, T., Garriga, G., & Kaplan, J. M. (2007). CDK-5 regulates the abundance of GLR-1 glutamate receptors in the ventral cord of caenorhabditis elegans. *Mol Biol Cell, 18*(10), 3883-93.

Juo, P., & Kaplan, J. M. (2004). The anaphase-promoting complex regulates the abundance of GLR-1 glutamate receptors in the ventral nerve cord of C. elegans. *Curr Biol, 14*(22), 2057-62.

Kanaan, N. M., Morfini, G. A., LaPointe, N. E., Pigino, G. F., Patterson, K. R., Song, Y., . . . Binder, L. I. (2011). Pathogenic forms of tau inhibit kinesin-dependent axonal transport through a mechanism involving activation of axonal phosphotransferases. *The Journal of Neuroscience : The Official Journal of the Society for Neuroscience, 31*(27), 9858-9868.

Kapitein, L. C., Schlager, M. A., Kuijpers, M., Wulf, P. S., van Spronsen, M., MacKintosh, F. C., & Hoogenraad, C. C. (2010). Mixed microtubules steer dynein-driven cargo transport into dendrites. *Current Biology : CB, 20*(4), 290-299.

Kapitein, L. C., Schlager, M. A., van der Zwan, W. A., Wulf, P. S., Keijzer, N., & Hoogenraad, C. C. (2010). Probing intracellular motor protein activity using an inducible cargo trafficking assay. *Biophysical Journal, 99*(7), 2143-2152.

Kardon, J. R., & Vale, R. D. (2009). Regulators of the cytoplasmic dynein motor. *Nature Reviews. Molecular Cell Biology, 10*(12), 854-865.

Karr, J., Vagin, V., Chen, K., Ganesan, S., Olenkina, O., Gvozdev, V., & Featherstone, D. E. (2009). Regulation of glutamate receptor subunit availability by microRNAs. *The Journal of Cell Biology, 185*(4), 685-697.

Katzmann, D. J., Odorizzi, G., & Emr, S. D. (2002). Receptor downregulation and multivesicular-body sorting. *Nat Rev Mol Cell Biol, 3*(12), 893-905.

Kessels, H.W., and Malinow, R. (2009). Synaptic AMPA receptor plasticity and behavior. Neuron *61*, 340-350.

Kim, C. H., & Lisman, J. E. (2001). A labile component of AMPA receptor-mediated synaptic transmission is dependent on microtubule motors, actin, and N-ethylmaleimide-sensitive factor. *The Journal of Neuroscience : The Official Journal of the Society for Neuroscience, 21*(12), 4188-4194.

Kim, J. H., Park, K. C., Chung, S. S., Bang, O., & Chung, C. H. (2003). Deubiquitinating enzymes as cellular regulators. *J Biochem, 134*(1), 9-18.

Kondo, M., Takei, Y., & Hirokawa, N. (2012). Motor protein KIF1A is essential for hippocampal synaptogenesis and learning enhancement in an enriched environment. *Neuron, 73*(4), 743-757.

Koushika, S. P., Schaefer, A. M., Vincent, R., Willis, J. H., Bowerman, B., & Nonet, M. L. (2004). Mutations in caenorhabditis elegans cytoplasmic dynein components reveal specificity of neuronal retrograde cargo. *The Journal of Neuroscience : The Official Journal of the Society for Neuroscience, 24*(16), 3907-3916.

Kowalski, J. R., Dahlberg, C. L., & Juo, P. (2011). The deubiquitinating enzyme USP-46 negatively regulates the degradation of glutamate receptors to control their abundance in the ventral nerve cord of caenorhabditis elegans. *J Neurosci, 31*(4), 1341-54.

Kumar, J., Choudhary, B. C., Metpally, R., Zheng, Q., Nonet, M. L., Ramanathan, S., . . . Koushika, S. P. (2010). The caenorhabditis elegans kinesin-3 motor UNC-104/KIF1A is degraded upon loss of specific binding to cargo. *PLoS Genet., 6*(11), e1001200.

Kwak, S., & Weiss, J. H. (2006). Calcium-permeable AMPA channels in neurodegenerative disease and ischemia. *Current Opinion in Neurobiology, 16*(3), 281-287.

Lai, K. O., & Ip, N. Y. (2009). Recent advances in understanding the roles of Cdk5 in synaptic plasticity. *Biochimica Et Biophysica Acta, 1792*(8), 741-745.

Lall, S., Grun, D., Krek, A., Chen, K., Wang, Y. L., Dewey, C. N., . . . Rajewsky, N. (2006). A genome-wide map of conserved microRNA targets in C. elegans. *Current Biology : CB, 16*(5), 460-471.

Le, M. T., Xie, H., Zhou, B., Chia, P. H., Rizk, P., Um, M., . . . Lodish, H. F. (2009). MicroRNA-125b promotes neuronal differentiation in human cells by repressing multiple targets. *Molecular and Cellular Biology, 29*(19), 5290-5305.

Lee, L. A., Elfring, L. K., Bosco, G., & Orr-Weaver, T. L. (2001). A genetic screen for suppressors and enhancers of the drosophila PAN GU cell cycle kinase identifies cyclin B as a target. *Genetics, 158*(4), 1545-1556.

Lee, R. Y., Sawin, E. R., Chalfie, M., Horvitz, H. R., & Avery, L. (1999). EAT-4, a homolog of a mammalian sodium-dependent inorganic phosphate cotransporter, is necessary for glutamatergic neurotransmission in caenorhabditis elegans. *J Neurosci, 19*(1), 159-67.

Li, G., Luna, C., Qiu, J., Epstein, D. L., & Gonzalez, P. (2010). Targeting of integrin beta1 and kinesin 2alpha by microRNA 183. *The Journal of Biological Chemistry, 285*(8), 5461-5471.

Liao, D., Hessler, N. A., & Malinow, R. (1995). Activation of postsynaptically silent synapses during pairing-induced LTP in CA1 region of hippocampal slice. *Nature, 375*(6530), 400-404.

Lin, A., Hou, Q., Jarzylo, L., Amato, S., Gilbert, J., Shang, F., & Man, H. Y. (2011). Nedd4-mediated AMPA receptor ubiquitination regulates receptor turnover and trafficking. *Journal of Neurochemistry, 119*(1), 27-39.

Lin, J. W., Ju, W., Foster, K., Lee, S. H., Ahmadian, G., Wyszynski, M., . . . Sheng, M. (2000). Distinct molecular mechanisms and divergent endocytotic pathways of AMPA receptor internalization. *Nat Neurosci, 3*(12), 1282-90.

Lo, K. Y., Kuzmin, A., Unger, S. M., Petersen, J. D., & Silverman, M. A. (2011). KIF1A is the primary anterograde motor protein required for the axonal transport of dense-core vesicles in cultured hippocampal neurons. *Neuroscience Letters, 491*(3), 168-173.

Lussier, M. P., Nasu-Nishimura, Y., & Roche, K. W. (2011). Activity-dependent ubiquitination of the AMPA receptor subunit GluA2. *The Journal of Neuroscience : The Official Journal of the Society for Neuroscience, 31*(8), 3077-3081.

Maas, C., Belgardt, D., Lee, H. K., Heisler, F. F., Lappe-Siefke, C., Magiera, M. M., . . . Kneussel, M. (2009). Synaptic activation modifies microtubules underlying transport of postsynaptic cargo. *Proceedings of the National Academy of Sciences of the United States of America, 106*(21), 8731-8736.

Mabb, A. M., & Ehlers, M. D. (2010). Ubiquitination in postsynaptic function and plasticity. *Annual Review of Cell and Developmental Biology, 26*, 179-210.

Mah, S. J., Cornell, E., Mitchell, N. A., & Fleck, M. W. (2005). Glutamate receptor trafficking: Endoplasmic reticulum quality control involves ligand binding and receptor function. *The Journal of Neuroscience : The Official Journal of the Society for Neuroscience, 25*(9), 2215-2225.

Mandal, M., Wei, J., Zhong, P., Cheng, J., Duffney, L. J., Liu, W., . . . Yan, Z. (2011). Impaired alpha-amino-3-hydroxy-5-methyl-4-isoxazolepropionic acid (AMPA) receptor trafficking and function by mutant huntingtin. *Journal of Biological Chemistry, 286*(39), 33719-33728.

Maricq, A. V., Peckol, E., Driscoll, M., & Bargmann, C. I. (1995). Mechanosensory signalling in C. elegans mediated by the GLR-1 glutamate receptor. *Nature, 378*(6552), 78-81.

Martin, M., Iyadurai, S.J., Gassman, A., Gindhart, J.G., Jr., Hays, T.S., and Saxton, W.M. (1999). Cytoplasmic dynein, the dynactin complex, and kinesin are interdependent and essential for fast axonal transport. Mol Biol Cell *10*, 3717-3728.

Martin, S. J., Grimwood, P. D., & Morris, R. G. (2000). Synaptic plasticity and memory: An evaluation of the hypothesis. *Annual Review of Neuroscience, 23*, 649-711.

Matsuda, S., Miura, E., Matsuda, K., Kakegawa, W., Kohda, K., Watanabe, M., & Yuzaki, M. (2008). Accumulation of AMPA receptors in autophagosomes in neuronal axons lacking adaptor protein AP-4. *Neuron, 57*(5), 730-745.

Matthies, H. J., Miller, R. J., & Palfrey, H. C. (1993). Calmodulin binding to and cAMP-dependent phosphorylation of kinesin light chains modulate kinesin ATPase activity. *The Journal of Biological Chemistry, 268*(15), 11176-11187.

McKay, S.J., et al. (2003). Gene expression profiling of cells, tissues, and developmental stages of the nematode C. elegans. Cold Spring Harb Symp Quant Biol *68*, 159-169.

Mellem, J. E., Brockie, P. J., Zheng, Y., Madsen, D. M., & Maricq, A. V. (2002). Decoding of polymodal sensory stimuli by postsynaptic glutamate receptors in C. elegans. *Neuron, 36*(5), 933-44.

Mennella, V., Tan, D. Y., Buster, D. W., Asenjo, A. B., Rath, U., Ma, A., . . . Sharp, D. J. (2009). Motor domain phosphorylation and regulation of the drosophila kinesin 13, KLP10A. *The Journal of Cell Biology, 186*(4), 481-490.

Mishima, M., Pavicic, V., Gruneberg, U., Nigg, E. A., & Glotzer, M. (2004). Cell cycle regulation of central spindle assembly. *Nature, 430*(7002), 908-913.

Morfini, G., Pigino, G., Beffert, U., Busciglio, J., & Brady, S. T. (2002). Fast axonal transport misregulation and alzheimer's disease. *Neuromolecular Medicine, 2*(2), 89-99.

Morfini, G., Pigino, G., Szebenyi, G., You, Y., Pollema, S., & Brady, S. T. (2006). JNK mediates pathogenic effects of polyglutamine-expanded androgen receptor on fast axonal transport. *Nature Neuroscience, 9*(7), 907-916.

Morfini, G., Szebenyi, G., Brown, H., Pant, H. C., Pigino, G., DeBoer, S., . . . Brady, S. T. (2004). A novel CDK5-dependent pathway for regulating GSK3 activity and kinesin-driven motility in neurons. *The EMBO Journal, 23*(11), 2235-2245.

Morfini, G., Szebenyi, G., Elluru, R., Ratner, N., & Brady, S. T. (2002). Glycogen synthase kinase 3 phosphorylates kinesin light chains and negatively regulates kinesin-based motility. *The EMBO Journal, 21*(3), 281-293. doi: 10.1093/emboj/21.3.281

Morrison, G. E., & van der Kooy, D. (2001). A mutation in the AMPA-type glutamate receptor, glr-1, blocks olfactory associative and nonassociative learning in caenorhabditis elegans. *Behav Neurosci, 115*(3), 640-9.

Morsci, N. S., & Barr, M. M. (2011). Kinesin-3 KLP-6 regulates intraflagellar transport in male-specific cilia of caenorhabditis elegans. *Current Biology : CB, 21*(14), 1239-1244.

Mortensen, R. D., Serra, M., Steitz, J. A., & Vasudevan, S. (2011). Posttranscriptional activation of gene expression in xenopus laevis oocytes by microRNA-protein complexes (microRNPs). *Proceedings of the National Academy of Sciences of the United States of America, 108*(20), 8281-8286.

Mu, Y., Otsuka, T., Horton, A. C., Scott, D. B., & Ehlers, M. D. (2003). Activity-dependent mRNA splicing controls ER export and synaptic delivery of NMDA receptors. *Neuron, 40*(3), 581-94.

Nakagawa, T., Setou, M., Seog, D., Ogasawara, K., Dohmae, N., Takio, K., & Hirokawa, N. (2000). A novel motor, KIF13A, transports mannose-6-phosphate receptor to plasma membrane through direct interaction with AP-1 complex. *Cell, 103*(4), 569-581.

Nakata, K., Abrams, B., Grill, B., Goncharov, A., Huang, X., Chisholm, A. D., & Jin, Y. (2005). Regulation of a DLK-1 and p38 MAP kinase pathway by the ubiquitin ligase RPM-1 is required for presynaptic development. *Cell, 120*(3), 407-420.

Nonet, M.L., Holgado, A.M., Brewer, F., Serpe, C.J., Norbeck, B.A., Holleran, J., Wei, L., Hartwieg, E., Jorgensen, E.M., and Alfonso, A. (1999). UNC-11, a Caenorhabditis elegans AP180 homologue, regulates the size and protein composition of synaptic vesicles. Mol Biol Cell *10*, 2343-2360.

Nurrish, S. J. (2002). An overview of C. elegans trafficking mutants. *Traffic (Copenhagen, Denmark), 3*(1), 2-10.

Ohshima, T., Gilmore, E. C., Longenecker, G., Jacobowitz, D. M., Brady, R. O., Herrup, K., & Kulkarni, A. B. (1999). Migration defects of cdk5(-/-) neurons in the developing cerebellum is cell autonomous. *J Neurosci, 19*(14), 6017-26.

Ohshima, T., Ward, J. M., Huh, C. G., Longenecker, G., Veeranna, Pant, H. C., . . . Kulkarni, A. B. (1996). Targeted disruption of the cyclin-dependent kinase 5 gene results in abnormal corticogenesis, neuronal pathology and perinatal death. *Proc Natl Acad Sci U S A, 93*(20), 11173-8.

Okada, Y., Yamazaki, H., Sekine-Aizawa, Y., & Hirokawa, N. (1995). The neuron-specific kinesin superfamily protein KIF1A is a unique monomeric motor for anterograde axonal transport of synaptic vesicle precursors. *Cell, 81*(5), 769-780.

Ou, C. Y., Poon, V. Y., Maeder, C. I., Watanabe, S., Lehrman, E. K., Fu, A. K., . . . Shen, K. (2010). Two cyclin-dependent kinase pathways are essential for polarized trafficking of presynaptic components. *Cell, 141*(5), 846-858.

Ou, C. Y., Poon, V. Y., Maeder, C. I., Watanabe, S., Lehrman, E. K., Fu, A. K., . . . Shen, K. (2010b). Two cyclin-dependent kinase pathways are essential for polarized trafficking of presynaptic components. *Cell, 141*(5), 846-58.

Pack-Chung, E., Kurshan, P.T., Dickman, D.K., and Schwarz, T.L. (2007). A Drosophila kinesin required for synaptic bouton formation and synaptic vesicle transport. Nat Neurosci *10*, 980-989.

Park, E. C., Ghose, P., Shao, Z., Ye, Q., Kang, L., Xu, X. Z., . . . Rongo, C. (2012). Hypoxia regulates glutamate receptor trafficking through an HIF-independent mechanism. *The EMBO Journal, 31*(6), 1379-1393.

Park, E. C., Glodowski, D. R., & Rongo, C. (2009). The ubiquitin ligase RPM-1 and the p38 MAPK PMK-3 regulate AMPA receptor trafficking. *PLoS One, 4*(1), e4284.

Park, M., Penick, E. C., Edwards, J. G., Kauer, J. A., & Ehlers, M. D. (2004). Recycling endosomes supply AMPA receptors for LTP. *Science, 305*(5692), 1972-1975.

Park, M., Salgado, J. M., Ostroff, L., Helton, T. D., Robinson, C. G., Harris, K. M., & Ehlers, M. D. (2006). Plasticity-induced growth of dendritic spines by exocytic trafficking from recycling endosomes. *Neuron, 52*(5), 817-830.

Park, M., Watanabe, S., Poon, V. Y., Ou, C. Y., Jorgensen, E. M., & Shen, K. (2011). CYY-1/cyclin Y and CDK-5 differentially regulate synapse elimination and formation for rewiring neural circuits. *Neuron, 70*(4), 742-757.

Patel, N., Thierry-Mieg, D., & Mancillas, J. R. (1993). Cloning by insertional mutagenesis of a cDNA encoding caenorhabditis elegans kinesin heavy chain. *Proceedings of the National Academy of Sciences of the United States of America, 90*(19), 9181-9185.

Patzke, H., & Tsai, L. H. (2002). Cdk5 sinks into ALS. *Trends in Neurosciences, 25*(1), 8-10.

Peden, E. M., & Barr, M. M. (2005). The KLP-6 kinesin is required for male mating behaviors and polycystin localization in caenorhabditis elegans. *Curr Biol, 15*(5), 394-404.

Penn, A. C., Williams, S. R., & Greger, I. H. (2008). Gating motions underlie AMPA receptor secretion from the endoplasmic reticulum. *The EMBO Journal, 27*(22), 3056-3068.

Pfaffl, M.W. (2001). A new mathematical model for relative quantification in real-time RT-PCR. Nucleic Acids Res *29*, e45.

Puthanveettil, S. V., Monje, F. J., Miniaci, M. C., Choi, Y. B., Karl, K. A., Khandros, E., . . . Kandel, E. R. (2008). A new component in synaptic plasticity: Upregulation of kinesin in the neurons of the gill-withdrawal reflex. *Cell, 135*(5), 960-973.

Ratner, N., Bloom, G. S., & Brady, S. T. (1998). A role for cyclin-dependent kinase(s) in the modulation of fast anterograde axonal transport: Effects defined by olomoucine and the APC tumor suppressor protein. *The Journal of Neuroscience : The Official Journal of the Society for Neuroscience, 18*(19), 7717-7726.

Risinger, A.L., and Kaiser, C.A. (2008). Different ubiquitin signals act at the Golgi and plasma membrane to direct GAP1 trafficking. Mol Biol Cell *19*, 2962-2972.

Rongo, C., & Kaplan, J. M. (1999). CaMKII regulates the density of central glutamatergic synapses in vivo. *Nature, 402*(6758), 195-199.

Rongo, C., Whitfield, C. W., Rodal, A., Kim, S. K., & Kaplan, J. M. (1998). LIN-10 is a shared component of the polarized protein localization pathways in neurons and epithelia. *Cell, 94*(6), 751-9.

Rose, J. K., Kaun, K. R., Chen, S. H., & Rankin, C. H. (2003). GLR-1, a non-NMDA glutamate receptor homolog, is critical for long-term memory in caenorhabditis elegans. *The Journal of Neuroscience : The Official Journal of the Society for Neuroscience, 23*(29), 9595-9599.

Sagona, A. P., Nezis, I. P., Pedersen, N. M., Liestol, K., Poulton, J., Rusten, T. E., . . . Stenmark, H. (2010). PtdIns(3)P controls cytokinesis through KIF13A-mediated recruitment of FYVE-CENT to the midbody. *Nature Cell Biology, 12*(4), 362-371.

Sakamoto, R., Byrd, D. T., Brown, H. M., Hisamoto, N., Matsumoto, K., & Jin, Y. (2005). The caenorhabditis elegans UNC-14 RUN domain protein binds to the kinesin-1 and UNC-16

complex and regulates synaptic vesicle localization. *Molecular Biology of the Cell, 16*(2), 483-496.

Salinas, S., Bilsland, L. G., & Schiavo, G. (2008). Molecular landmarks along the axonal route: Axonal transport in health and disease. *Current Opinion in Cell Biology, 20*(4), 445-453.

Sarin, S., Prabhu, S., O'Meara, M. M., Pe'er, I., & Hobert, O. (2008). Caenorhabditis elegans mutant allele identification by whole-genome sequencing. *Nat.Methods, 5*(10), 865-867.

Sato-Yoshitake, R., Yorifuji, H., Inagaki, M., & Hirokawa, N. (1992). The phosphorylation of kinesin regulates its binding to synaptic vesicles. *The Journal of Biological Chemistry, 267*(33), 23930-23936.

Scannevin, R. H., & Huganir, R. L. (2000). Postsynaptic organization and regulation of excitatory synapses. *Nature Reviews. Neuroscience, 1*(2), 133-141.

Schaefer, H., & Rongo, C. (2006). KEL-8 is a substrate receptor for CUL3-dependent ubiquitin ligase that regulates synaptic glutamate receptor turnover. *Molecular Biology of the Cell, 17*(3), 1250-1260.

Schwarz, L. A., Hall, B. J., & Patrick, G. N. (2010). Activity-dependent ubiquitination of GluA1 mediates a distinct AMPA receptor endocytosis and sorting pathway. *The Journal of Neuroscience : The Official Journal of the Society for Neuroscience, 30*(49), 16718-16729.

Scott, D. B., Blanpied, T. A., & Ehlers, M. D. (2003). Coordinated PKA and PKC phosphorylation suppresses RXR-mediated ER retention and regulates the surface delivery of NMDA receptors. *Neuropharmacology, 45*(6), 755-767.

Scott, D. B., Blanpied, T. A., Swanson, G. T., Zhang, C., & Ehlers, M. D. (2001). An NMDA receptor ER retention signal regulated by phosphorylation and alternative splicing. *The Journal of Neuroscience : The Official Journal of the Society for Neuroscience, 21*(9), 3063-3072.

Setou, M., Nakagawa, T., Seog, D. H., & Hirokawa, N. (2000). Kinesin superfamily motor protein KIF17 and mLin-10 in NMDA receptor-containing vesicle transport. *Science (New York, N.Y.), 288*(5472), 1796-1802.

Setou, M., Seog, D. H., Tanaka, Y., Kanai, Y., Takei, Y., Kawagishi, M., & Hirokawa, N. (2002). Glutamate-receptor-interacting protein GRIP1 directly steers kinesin to dendrites. *Nature, 417*(6884), 83-87.

Shepherd, J. D., & Huganir, R. L. (2007). The cell biology of synaptic plasticity: AMPA receptor trafficking. *Annual Review of Cell and Developmental Biology, 23*, 613-643.

Shi, S. H., Hayashi, Y., Petralia, R. S., Zaman, S. H., Wenthold, R. J., Svoboda, K., & Malinow, R. (1999). Rapid spine delivery and redistribution of AMPA receptors after synaptic NMDA receptor activation. *Science, 284*(5421), 1811-1816.

Shim, J., Umemura, T., Nothstein, E., & Rongo, C. (2004). The unfolded protein response regulates glutamate receptor export from the endoplasmic reticulum. *Molecular Biology of the Cell, 15*(11), 4818-4828.

Shin, H., Wyszynski, M., Huh, K. H., Valtschanoff, J. G., Lee, J. R., Ko, J., . . . Kim, E. (2003). Association of the kinesin motor KIF1A with the multimodular protein liprin-alpha. *The Journal of Biological Chemistry, 278*(13), 11393-11401.

Sieburth, D., Ch'ng, Q., Dybbs, M., Tavazoie, M., Kennedy, S., Wang, D., . . . Kaplan, J. M. (2005). Systematic analysis of genes required for synapse structure and function. *Nature, 436*(7050), 510-517.

Siegrist, S. E., & Doe, C. Q. (2005). Microtubule-induced Pins/Galphai cortical polarity in drosophila neuroblasts. *Cell, 123*(7), 1323-1335.

Simon, D. J., Madison, J. M., Conery, A. L., Thompson-Peer, K. L., Soskis, M., Ruvkun, G. B., . . . Kim, J. K. (2008). The microRNA miR-1 regulates a MEF-2-dependent retrograde signal at neuromuscular junctions. *Cell, 133*(5), 903-915.

Stagi, M., Gorlovoy, P., Larionov, S., Takahashi, K., & Neumann, H. (2006). Unloading kinesin transported cargoes from the tubulin track via the inflammatory c-jun N-terminal kinase pathway. *FASEB Journal : Official Publication of the Federation of American Societies for Experimental Biology, 20*(14), 2573-2575.

Steitz, J. A., & Vasudevan, S. (2009). miRNPs: Versatile regulators of gene expression in vertebrate cells. *Biochemical Society Transactions, 37*(Pt 5), 931-935.

Stepanova, T., Slemmer, J., Hoogenraad, C. C., Lansbergen, G., Dortland, B., De Zeeuw, C. I., . . . Galjart, N. (2003). Visualization of microtubule growth in cultured neurons via the use of EB3-GFP (end-binding protein 3-green fluorescent protein). *The Journal of Neuroscience : The Official Journal of the Society for Neuroscience, 23*(7), 2655-2664.

Su, C. W., Tharin, S., Jin, Y., Wightman, B., Spector, M., Meili, D., . . . Hengartner, M. O. (2006). The short coiled-coil domain-containing protein UNC-69 cooperates with UNC-76 to regulate axonal outgrowth and normal presynaptic organization in caenorhabditis elegans. *J.Biol., 5*(4), 9.

Su, S. C., & Tsai, L. H. (2011). Cyclin-dependent kinases in brain development and disease. *Annual Review of Cell and Developmental Biology, 27*, 465-491.

Sun, F., Zhu, C., Dixit, R., & Cavalli, V. (2011). Sunday Driver/JIP3 binds kinesin heavy chain directly and enhances its motility. *The EMBO Journal, 30*(16), 3416-3429.

Tanaka, K., Sugiura, Y., Ichishita, R., Mihara, K., & Oka, T. (2011). KLP6: A newly identified kinesin that regulates the morphology and transport of mitochondria in neuronal cells. *Journal of Cell Science, 124*(Pt 14), 2457-2465.

Tanaka, T., Veeranna, Ohshima, T., Rajan, P., Amin, N. D., Cho, A., . . . Kulkarni, A. B. (2001). Neuronal cyclin-dependent kinase 5 activity is critical for survival. *The Journal of Neuroscience : The Official Journal of the Society for Neuroscience, 21*(2), 550-558.

Therrien, M., Morrison, D. K., Wong, A. M., & Rubin, G. M. (2000). A genetic screen for modifiers of a kinase suppressor of ras-dependent rough eye phenotype in drosophila. *Genetics, 156*(3), 1231-1242.

Tien, N. W., Wu, G. H., Hsu, C. C., Chang, C. Y., & Wagner, O. I. (2011). Tau/PTL-1 associates with kinesin-3 KIF1A/UNC-104 and affects the motor's motility characteristics in C. elegans neurons. *Neurobiology of Disease, 43*(2), 495-506.

Toda, H., Mochizuki, H., Flores, R.,3rd, Josowitz, R., Krasieva, T. B., Lamorte, V. J., . . . Tomoda, T. (2008). UNC-51/ATG1 kinase regulates axonal transport by mediating motor-cargo assembly. *Genes & Development, 22*(23), 3292-3307.

Tsuboi, D., Hikita, T., Qadota, H., Amano, M., & Kaibuchi, K. (2005). Regulatory machinery of UNC-33 ce-CRMP localization in neurites during neuronal development in caenorhabditis elegans. *Journal of Neurochemistry, 95*(6), 1629-1641.

Tsurudome, K., Tsang, K., Liao, E. H., Ball, R., Penney, J., Yang, J. S., . . . Haghighi, A. P. (2010). The drosophila miR-310 cluster negatively regulates synaptic strength at the neuromuscular junction. *Neuron, 68*(5), 879-893.

Turrigiano, G. G. (2008). The self-tuning neuron: Synaptic scaling of excitatory synapses. *Cell, 135*(3), 422-435.

Twelvetrees, A. E., Yuen, E. Y., Arancibia-Carcamo, I. L., MacAskill, A. F., Rostaing, P., Lumb, M. J., . . . Kittler, J. T. (2010). Delivery of GABAARs to synapses is mediated by HAP1-KIF5 and disrupted by mutant huntingtin. *Neuron, 65*(1), 53-65.

Ueno, H., Huang, X., Tanaka, Y., & Hirokawa, N. (2011). KIF16B/Rab14 molecular motor complex is critical for early embryonic development by transporting FGF receptor. *Dev.Cell., 20*(1), 60-71.

Unno, K., Hanada, T., & Chishti, A. H. (2008). Functional involvement of human discs large tumor suppressor in cytokinesis. *Experimental Cell Research, 314*(17), 3118-3129.

Vacher, H., Yang, J. W., Cerda, O., Autillo-Touati, A., Dargent, B., & Trimmer, J. S. (2011). Cdk-mediated phosphorylation of the Kvbeta2 auxiliary subunit regulates Kv1 channel axonal targeting. *The Journal of Cell Biology, 192*(5), 813-824.

van der Sluijs, P., and Hoogenraad, C.C. (2011). New insights in endosomal dynamics and AMPA receptor trafficking. Semin Cell Dev Biol *22*, 499-505.

Venkateswarlu, K., Hanada, T., and Chishti, A.H. (2005). Centaurin-alpha1 interacts directly with kinesin motor protein KIF13B. J Cell Sci *118*, 2471-2484.

Vagnoni, A., Rodriguez, L., Manser, C., De Vos, K. J., & Miller, C. C. (2011). Phosphorylation of kinesin light chain 1 at serine 460 modulates binding and trafficking of calsyntenin-1. *Journal of Cell Science, 124*(Pt 7), 1032-1042.

Vale, R. D. (2003). The molecular motor toolbox for intracellular transport. *Cell, 112*(4), 467-480.

Van Den Bosch, L., Van Damme, P., Bogaert, E., & Robberecht, W. (2006). The role of excitotoxicity in the pathogenesis of amyotrophic lateral sclerosis. *Biochimica Et Biophysica Acta, 1762*(11-12), 1068-1082.

Van Epps, H., Dai, Y., Qi, Y., Goncharov, A., & Jin, Y. (2010). Nuclear pre-mRNA 3'-end processing regulates synapse and axon development in C. elegans. *Development (Cambridge, England), 137*(13), 2237-2250.

Vandenberghe, W., & Bredt, D. S. (2004). Early events in glutamate receptor trafficking. *Current Opinion in Cell Biology, 16*(2), 134-139.

Vandenberghe, W., Nicoll, R. A., & Bredt, D. S. (2005). Interaction with the unfolded protein response reveals a role for stargazin in biosynthetic AMPA receptor transport. *J Neurosci, 25*(5), 1095-102.

Vasudevan, S. (2012). Posttranscriptional upregulation by microRNAs. *Wiley Interdiscip.Rev.RNA, 3*(3), 311-330.

Vasudevan, S., Tong, Y., & Steitz, J. A. (2007). Switching from repression to activation: MicroRNAs can up-regulate translation. *Science, 318*(5858), 1931-1934.

Verhey, K. J., & Hammond, J. W. (2009). Traffic control: Regulation of kinesin motors. *Nature Reviews.Molecular Cell Biology, 10*(11), 765-777.

Verhey, K. J., Kaul, N., & Soppina, V. (2011). Kinesin assembly and movement in cells. *Annual Review of Biophysics, 40*, 267-288.

Verhey, K. J., Meyer, D., Deehan, R., Blenis, J., Schnapp, B. J., Rapoport, T. A., & Margolis, B. (2001). Cargo of kinesin identified as JIP scaffolding proteins and associated signaling molecules. *The Journal of Cell Biology, 152*(5), 959-970.

Walker, C. S., Francis, M. M., Brockie, P. J., Madsen, D. M., Zheng, Y., & Maricq, A. V. (2006). Conserved SOL-1 proteins regulate ionotropic glutamate receptor desensitization. *Proceedings of the National Academy of Sciences of the United States of America, 103*(28), 10787-10792.

Wan, H. I., DiAntonio, A., Fetter, R. D., Bergstrom, K., Strauss, R., & Goodman, C. S. (2000). Highwire regulates synaptic growth in drosophila. *Neuron, 26*(2), 313-329.

Wang, G., Gilbert, J., & Man, H. Y. (2012). AMPA receptor trafficking in homeostatic synaptic plasticity: Functional molecules and signaling cascades. *Neural Plasticity, 2012*, 825364.

Wang, G. J., Kang, L., Kim, J. E., Maro, G. S., Xu, X. Z., & Shen, K. (2010). GRLD-1 regulates cell-wide abundance of glutamate receptor through post-transcriptional regulation. *Nature Neuroscience, 13*(12), 1489-1495.]

Wang, R., Walker, C. S., Brockie, P. J., Francis, M. M., Mellem, J. E., Madsen, D. M., & Maricq, A. V. (2008). Evolutionary conserved role for TARPs in the gating of glutamate receptors and tuning of synaptic function. *Neuron, 59*(6), 997-1008.

White, J. G., Southgate, E., Thomson, J. N., & Brenner, S. (1976). The structure of the ventral nerve cord of caenorhabditis elegans. *Philosophical Transactions of the Royal Society of London. Series B: Biological Sciences, 275*(938), 327-348.

Wiese, M., Antebi, A., & Zheng, H. (2010). Intracellular trafficking and synaptic function of APL-1 in caenorhabditis elegans. *PloS One, 5*(9), e12790.

Wong, R. W., Setou, M., Teng, J., Takei, Y., & Hirokawa, N. (2002). Overexpression of motor protein KIF17 enhances spatial and working memory in transgenic mice. *Proceedings of the National Academy of Sciences of the United States of America, 99*(22), 14500-14505.

Wyszynski, M., Kim, E., Dunah, A. W., Passafaro, M., Valtschanoff, J. G., Serra-Pages, C., . . . Sheng, M. (2002). Interaction between GRIP and liprin-alpha/SYD2 is required for AMPA receptor targeting. *Neuron, 34*(1), 39-52.

Wyszynski, M., Valtschanoff, J. G., Naisbitt, S., Dunah, A. W., Kim, E., Standaert, D. G., . . . Sheng, M. (1999). Association of AMPA receptors with a subset of glutamate receptor-interacting protein in vivo. *The Journal of Neuroscience : The Official Journal of the Society for Neuroscience, 19*(15), 6528-6537.

Xia, H., Hornby, Z. D., & Malenka, R. C. (2001). An ER retention signal explains differences in surface expression of NMDA and AMPA receptor subunits. *Neuropharmacology, 41*(6), 714-23.

Yamada, K. H., Hanada, T., & Chishti, A. H. (2007). The effector domain of human dlg tumor suppressor acts as a switch that relieves autoinhibition of kinesin-3 motor GAKIN/KIF13B. *Biochemistry, 46*(35), 10039-10045.

Yang, H. Y., Mains, P. E., & McNally, F. J. (2005). Kinesin-1 mediates translocation of the meiotic spindle to the oocyte cortex through KCA-1, a novel cargo adapter. *The Journal of Cell Biology, 169*(3), 447-457.

Yin, X., Feng, X., Takei, Y., & Hirokawa, N. (2012). Regulation of NMDA receptor transport: A KIF17-cargo Binding/Releasing underlies synaptic plasticity and memory in vivo. *The Journal of Neuroscience : The Official Journal of the Society for Neuroscience, 32*(16), 5486-5499.

Yin, X., Takei, Y., Kido, M. A., & Hirokawa, N. (2011). Molecular motor KIF17 is fundamental for memory and learning via differential support of synaptic NR2A/2B levels. *Neuron, 70*(2), 310-325.

Yonekawa, Y., Harada, A., Okada, Y., Funakoshi, T., Kanai, Y., Takei, Y., Terada, S., Noda, T., and Hirokawa, N. (1998). Defect in synaptic vesicle precursor transport and neuronal cell death in KIF1A motor protein-deficient mice. J Cell Biol *141*, 431-441.

Yoshimura, Y., Terabayashi, T., & Miki, H. (2010). Par1b/MARK2 phosphorylates kinesin-like motor protein GAKIN/KIF13B to regulate axon formation. *Molecular and Cellular Biology, 30*(9), 2206-2219.

Zhang, B., Koh, Y.H., Beckstead, R.B., Budnik, V., Ganetzky, B., and Bellen, H.J. (1998). Synaptic vesicle size and number are regulated by a clathrin adaptor protein required for endocytosis. Neuron *21*, 1465-1475.

Zhang, D., Isack, N. R., Glodowski, D. R., Liu, J., Chen, C. C., Xu, X. Z., . . . Rongo, C. (2012). RAB-6.2 and the retromer regulate glutamate receptor recycling through a retrograde pathway. *The Journal of Cell Biology, 196*(1), 85-101.

Zhen, M., Huang, X., Bamber, B., & Jin, Y. (2000). Regulation of presynaptic terminal organization by C. elegans RPM-1, a putative guanine nucleotide exchanger with a RING-H2 finger domain. *Neuron, 26*(2), 331-343.

Zheng, Y., Brockie, P. J., Mellem, J. E., Madsen, D. M., & Maricq, A. V. (1999). Neuronal control of locomotion in C. elegans is modified by a dominant mutation in the GLR-1 ionotropic glutamate receptor. *Neuron, 24*(2), 347-361.

Zheng, Y., Brockie, P. J., Mellem, J. E., Madsen, D. M., Walker, C. S., Francis, M. M., & Maricq, A. V. (2006). SOL-1 is an auxiliary subunit that modulates the gating of GLR-1 glutamate receptors in caenorhabditis elegans. *Proceedings of the National Academy of Sciences of the United States of America, 103*(4), 1100-1105.

Zheng, Y., Mellem, J. E., Brockie, P. J., Madsen, D. M., & Maricq, A. V. (2004). SOL-1 is a CUB-domain protein required for GLR-1 glutamate receptor function in C. elegans. *Nature, 427*(6973), 451-7.

Zhou, H. M., Brust-Mascher, I., & Scholey, J. M. (2001). Direct visualization of the movement of the monomeric axonal transport motor UNC-104 along neuronal processes in living caenorhabditis elegans. *J Neurosci, 21*(11), 3749-55.